RESPONSE OF UNBOUND PAVEMENT MATERIAL TO STRESS

By

Tafari Tarfa Isho

A thesis submitted to the school of graduate studies of Addis Ababa Science and Technology University in partial fulfillment of the requirements for the degree of Master of Science in Civil Engineering (Road and Transportation Engineering)

Addis Ababa Science and Technology University

Advisor: Dr. Melaku Sisay

September 2017

Declaration of Authorship

I hereby declare that all information in this document has been obtained and presented in accordance with academic rules and ethical conduct. I also declare that, as required by these rules and conduct, I have fully cited and referenced all material and results that are not original to this work. This research work is original and has not been submitted for the award of any other Master Degree, either in this or any other.

Tafari Tarfa Isho

RESPONSE OF UNBOUND PAVEMENT MATERIAL TO STRESS

By Tafari Tarfa Isho

Approved by the Examining Board

Dr. Melaku Sisay	_____	_____
Advisor	Signature	Date
Dr. Bikila Teklu	_____	_____
External Examiner	Signature	Date
Dr. Fitsum Tesfaye.	_____	_____
Internal Examiner	Signature	Date
_____	_____	_____
Dean of College	Signature	Date
_____	_____	_____
Head, Department	Signature	Date

Abstract

This thesis presented response of unbound pavement material to stress for gravel road subgrade material. Type of design method significant to analysis responses of pavement material to stress articulated in first part of this study. Permanent deformation of pavement layers indicated as main problems of this investigation. The main objective of this research was to explore responses of unbound pavement material to stress in pavement layer. Different research materials have been reviewed to conduct this research. Pavement design analysis and pavement response modeling vastly reviewed in literature section. Disturbed sampling method used for sampling subgrade material from existing borrow pit of gravel road project; triaxial sample of thirty eight millmeter in diameter with height of seventy six millmeter prepared in standard compaction method and tested in triaxial test with three confininng stress at one hundered,two hundred and three hundred kilopascals, in applying vertical dynamic load in laboratory as designated in methodology to attain the inputs of mechanistc model. This mechanstic model is layered elastic model utilized for determination of pavement responses to stress. Subgrade material test and modeling results represented in figures and tables of this reseasch. These results discussed and analyzed layered elastic model. Minimum stiffness of subgrade soil and pavement wearing material used for pavement model, required as inputs of layered elastic model determined from correlation of calfornian bearing ratio to stiffness.The following findings obtained from results and discussion of this research: Stiffness and Shear strength of material increased as cell stresses increased. The output of Layered elastic model indicated pavement maximum deflection; pavement critical strain and maximum shear stress found at wheel contact area on pavement surface. Pavement maximum shear strain was located at sides of wheel contact area on pavement surface. Pavement layers deflection,strain and shear diminished away from the wheel contact area in horizontal and vertical direction. And maximum damage of pavement layers was taken as pavement cumulative damage. In conclusion, layered elastic model explored responses of unbound pavement material to stress in form of pavement layers deflection, stress and strain, shears and estimating pavement layers cumulative damages. Consequently investigating response of unbound subbase and base material to moving load in Discrete Element Modeling recommended for future research.

Key Words: *Layered Elastic Model; Mechanistic Pavement Design; Pavement Layer Responses; Triaxial Test; and Unbound Pavement Material.*

Acknowledgments

I wish to express sincere gratitude for my thesis advisor, Dr. Melaku Sisay for his guidance, advice, patience and encouragement in preparation of this research. With his passionate contribution the validation of thesis could have been successfully conducted. And I would like to express especial gratitude for Dr. Bikila Teklu for his valuable guidance of this research.

I would like to express gratitude for support and assistance provided during my study, especially for: Ethiopian Roads Authority (ERA) who had sponsored this research. And Ethiopian Construction Design and Supervision Work Corporation who provided me accelerated subgrade material test data.

I would like to thank Mr. Abera Eshetu, Dean for College, for his generous support; comments and his loving encouragement during this thesis work. And also my appreciation goes to Mr. Samson Birhanu, Project Manager for his coordination during sampling of this research material.

Finally, I must express my especial gratitude to my parents and friends for providing me with reliable support and continuous encouragement throughout my years of study and during the process of researching and writing this thesis.

Dedication

This thesis is dedicated to my father, Kabada Fufa. His motivation, helpful and fun thought was a continuous form of encouragement to try best but still have fun along the way.

Table of Content

List of Tables

List of Figures

Notations

α Material Constant

β Material Constant

ε Strain

ε_{EI} Resilient Strain

ε_{P} Permanent Strain

ε_{P1} Permanent Vertical Strain

$\varepsilon_{P1\,N}$ Permanent Vertical Strain at N Load Cycles

ε_{R} Horizontal Strain

ε_{Z} Vertical Strain

ϕ Angle Of Internal Friction

μ Poisson Ratio

σ Stress

σ_{1} Principal Failure Stress

$\sigma_{3,}$ Minor Principal Failure Stress

σ_{C} Confining Pressure

σ_{D} Deviatoric Stress

σ_{1} Max Peak Axial Stress, $(\sigma_{D} + \sigma_{C})$

σ_{R} Horizontal Stress

σ_{Z} Vertical Stress

τ Shear Stress

Abbreviations

AASHO	American Association of State Highway Officials
AASHTO	American Association of State Highway and Transportation Officials
AC	Asphalt Concrete
ALF	Accelerated Loading Facility
ATS	Automated Testing System
CBR	California Bearing Ratio
CCP	Constant Confining Pressure
CDF	Cumulative damaging Factor
D	Material Layer Thickness
DEM	Distinct Element Method
DOC	Degree of Compaction
E	Modulus of Elasticity
ERA	Ethiopian Road Authority
ECDSWC	Ethiopian Construction Design and Supervision Work Corporation
FE	Finite Element
FWD	Falling Weight Deflectometer
G15	Subgrade material CBRvalue greater than 15
G7	Subgrade material CBRvalue greater than 7
HVS	Heavy Vehicle Simulator
LL	Liquid Limit
LVDT	Linear Variable Differential Transformer
MDD	Maximum Dry Density
N	Number of Load Cycles
NAASRA	National Association of Australian State Road Authorities

NCHRP	National Cooperative Highway Research Program
OMC	Optimum Moisture Content
PD	Permanent Deformation
PI	Plasticity Index
PL	Plastic Limit
RLT	Repeated Load Triaxial
SMA	Stone Mastic Asphalt
SS	Single Stage
ST	Static Triaxial
UGL	Unbound Granular Layer
UGM	Unbound Granular Material
VCP	Variable Confining Pressure

1. Introduction

Trend pavement (NCHRP 1-37A) designed against subgrade shear failure in providing pavement layers to increase subgrade bearing capacity. Thickness of trend pavement design was determined depend on experience of previously constructed projects. This trend pavement design had gap to consider growth of traffic volume, pavement performance evaluation and pavement thickness determination. These gaps considered to upgrade trend pavement design method to AASHTO track test experiments.

Track test experiments developed Empirical Pavement Design, namely AASHTO Pavement Design Guide. This method works for present pavement design. Currently, empirical pavement design method entirely relying on experimental data for in-service pavement performance and full scale road test. This method has also gap to determine pavement responses and estimate pavement cumulative damage to traffic load based on layered elastic theory.

ERA pavement design guide needs response based pavement design method that used to determine pavement responses and estimate pavement cumulative damage to traffic load using mechanistic models. Additionally, it needs to embrace specification that used to test unbound pavement material mechanical properties namely shear strength and stiffness.

In last three decades, researcher's coming with mechanistic pavement design method that used to explore pavement responses subjected to traffic load. This pavement design method mostly depending on mechanical property of pavement materials under contact stress. These mechanical properties are stiffness and shear strength of material. This unbound pavement material has Elasto -plastic behaviour. Consequently, Pavement had two types of deformational responses when subjected to traffic loads (Werkmeister, 2003), namely elastic and stable strain response. Pavement elastic strain response is significant for load carrying capacity while permanent strain response is used to characterize long term pavement performance. The significance of investigation of pavement responses is to predict pavement critical damage, critical strain and stress and critical deflection. Additionally, researchers developed a layered elastic model for modeling pavement responses under contact stress.

This mechanistic model required mathematical models to analysis pavement responses to surface loadings. Although, there are different functional models utilized for pavement structural

modeling. These function models are layered elastic model (Gerrard, 1969) and finite elements model (FEM) typically used in pavement structural analysis and design. These models can easily be run on personal computers and required data that easily obtainable. A layered elastic model used to analysis engineering problems, namely stresses, strains and deflections at any point in a pavement structure resulting from application of a circular load. This model was basically developed for pavement structural modeling. The origin of layered elastic theory is credited to V.J. Boussinesq who published his classic work in 1885. Layered Elastic Model used for this research to analysis responses unbound pavement material to stress. This layered elastic model is CIRCLY used for more than thirty years in Austroads mechanistic pavement design guide.

CIRCLY (Austroads 2004) developed based on layered elastic model and used to explore different circular load on pavement surface. It works based on integral transform technique and input data for this program is much easier than the essential finite element programs. CIRCLY was used to calculate the load-induced stresses, strains and displacements at any selected points in the layered system. Layered elastic models assume that each pavement structural layer is isotropic and anisotropic properties. Subgrade material and subgrade soil have anisotropic material properties, asphalt and cemented materials comprise isotropic properties. The interface between layers can be considered as fully continuous or rough.

1.1. Research Problem

The main problem of this research was permanent deformation or rutting. Pavement surface loading is the contact stress. This contact stress formed two significant strain components in pavement; the maximum vertical compressive strain caused surface rutting and the maximum horizontal tensile strain caused fatigue cracking. The distress mode of gravel road was roughness usually caused by traffic action combined with low stiffness layer resulted from poor material quality, poor compaction and excessive moisture in pavement structure. This roughness formed a wave or corrugation across pavement surface. The factors led to such damage are material types, nature of subgrade soil and environment pavement existed. Permanent deformation and fatigue cracking formed by contact stress are main deterioration modes in pavement structure.

1.2. General Objective

The main object of this research is to explore responses of unbound pavement material to stress in pavement structures.

1.3. Specific Objectives

This research has the following specific objectives;

1. Used to find out the maximum pavement deflection, critical strain and shear strain, maximum stress and shear stress locations on pavement layer during loading time.
2. Help to demonstrate pavement layers deflection, strain and intensity of stress depend on distance and depth from wheel contact area at loading time.
3. And help to predict maximum damage of pavement layers during design of the pavement.

1.4. Significance of the Research

The outcomes of this research underline the following key significances;

1. Enhance to have a deep understanding of pavement responses to contact stress for highway pavement researchers, engineers and planners.
2. Promote to use mechanistic pavement design method for road industries more than empirical pavement design method.
3. Promote layered elastic model software for researchers, engineers and planners to use in highway designs and researches.
4. Enhance to embrace mechanical property test equipments for unbound pavement materials to highway industries pavement design specification.

1.5. Limitation of the Research

Stiffness test of subgrade material in laboratory was a limitation of this research in exploring response of unbound pavement material to stress particularly for unbound pavement material retained above 4.75mm sieve size used for subgrade, subbase and base of pavement structures.

2. Literature Review

2.1. Pavement Structure

The bearing capacity of subgrade soil to support traffic loads without providing protective layer is unattainable. This protective layer is multilayer and known as pavement as indicated in figure 2.1. The main function of the pavement is to distribute the traffic load over the top of subgrade soil at much wider than the contact area between the wheel tyre and pavement surface. This technique used to reduce the maximum stress induced in subgrade soil and prevent the excessive deformation in pavement design period. Sufficient stiffness and thickness is provided for a pavement to protect excessive permanent deformation during the pavement design life while the pavement designed for twenty and more years (Thom, 2008).

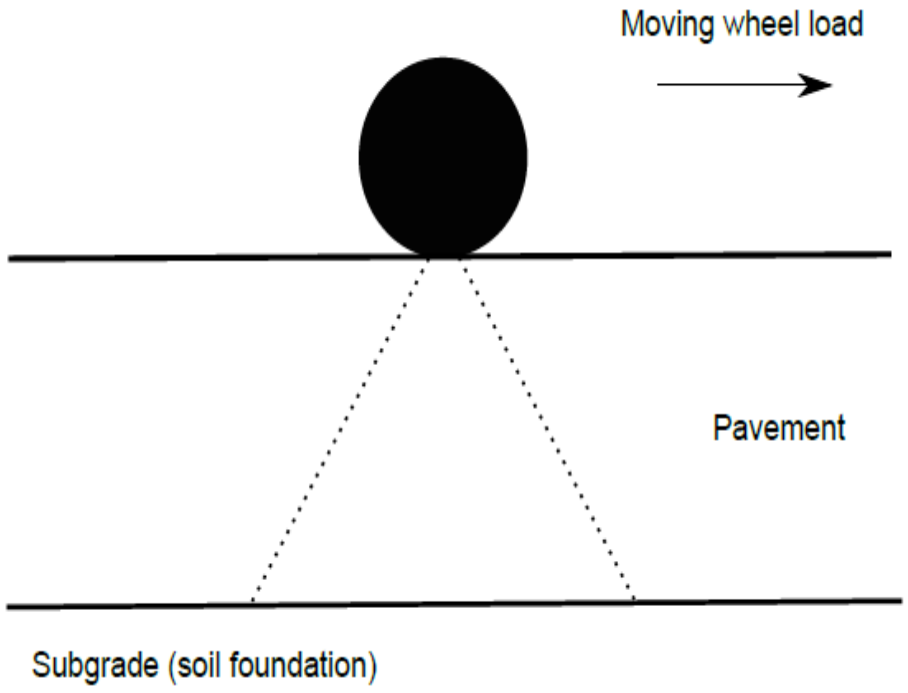

Figure 2.1: Wheel Load Distribution through Pavement Structure (Thom, 2008)

2.1.1. Flexible Pavement Structures

Currently, flexible pavements have three main layers: bituminous surface course, roadbase and subbase. The soil foundation for flexible pavements is known as subgrade. The components of flexible pavements are shown in figure 2.2.

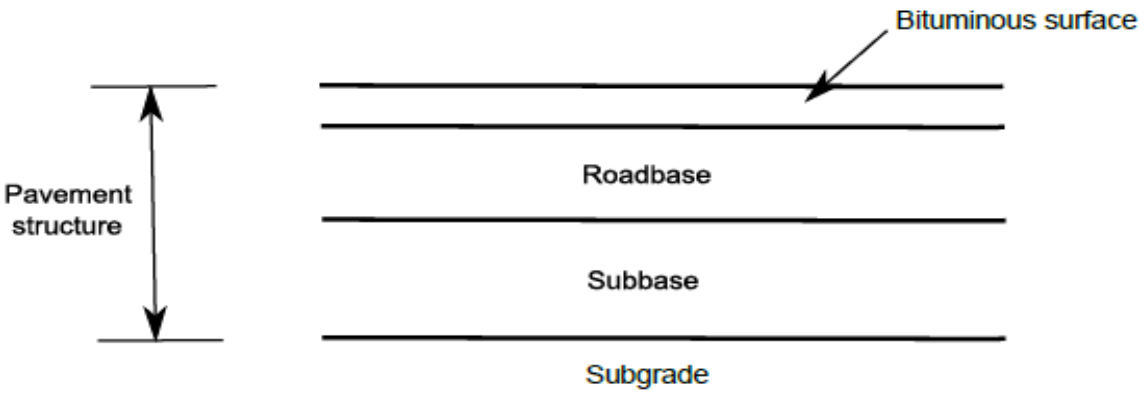

Figure 2.2: The Components of Flexible Pavements (Shiau, 2001)

Ninety percent of paved highways contain a bituminous surface layer (Thom, 2008). The main importance of this surface is to provide a safe and smooth riding for Vehicular Traffic. Bitumen is a binder, like Portland cement and other hydraulic binding agents. But, they have quite different properties. Hydraulic binding agents used for a rigid pavement layer, which have not deformable under repeated traffic load, bitumen has the ability to flow since it remains viscous liquid at in- service temperatures. The main mechanical characteristics of a bitumen-bound layer are the shear strength development induced by particle interlock and cohesion, as well as significant tensile strength. The properties are temperature sensitive. The normal distress modes of pavements are the fracture induced by fatigue and overloading, as well as the permanent deformation. The critical property required for pavement design, stiffness, the resistance to permanent deformation under repeated traffic load and fatigue.

The pavement structural layers lying below the bitumen bound layers and used to distribute the moving wheel load to the top of subgrade or pavement foundation. They are constructed from materials: stone fragments, granular materials or selected materials like crushed stone in natural or by crusher plant. Behavioral description of base and subbase are shear strength development through particles interlock and has lack of tensile strength. The generally failure type of base and subbase layers are deformation induced through shear, densification and disintegration of

particles. The key parameters of base and subbase are stiffness and resistance to accumulated deformation under repeated loads (Shiau, 2001).

The function of subgrade is to support pavement structure and moving loads during its design life (Brown and Selig, 1991). The soil type and characteristics are varies along the route of study or construction with the terrain type, whereas the soil are very sensitive to moisture contents (Thom, 2008). The behavioral characteristics of subgrade layer are stiffness under transient load and resistance to the accumulated deformation under repeated traffic loads.

2.1.2. Contact Area and Pressure Distribution

The pavement layers support the wheel load transferred to the subgrade soil. The depth of the pavement layers are used to reduce the wheel load stress. The behaviour of the pavement structures is affected by the contact form between wheel tyre and pavement surface. The shape of the contact depends on the ratio of applied load to the maximum recommended tyre pressure (Croney, 1977). If the ratio is small, the circular contact observed. When the ratio increased, the contact area becomes elongated.

The contact stress between the wheel tyre and pavement surface is classified into three; vertical, longitudinal and transversal stresses. As shown in figure 2.3, the vertical stress is perpendicular to the contact surface; the longitudinal stress is parallel to central plane and the transversal stress perpendicular to central plane. In generally, the tyre pressure is usually assumed to the normal contact pressure for a small car 250kpa and for large truck 600kpa. The typical axle load for highway Traffic design is 80KN or 100KN, 80KN is currently being used in UK (Thom, 2008).

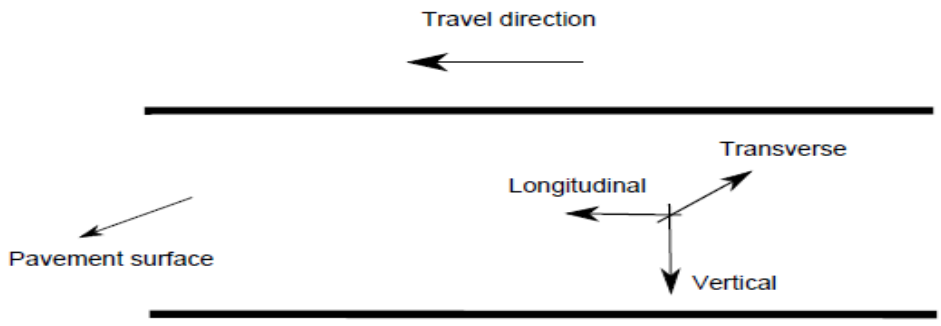

Figure 2.3: The direction of contact stresses on pavement surface (De Beer et at., 1997)

According to (De Beer at.al, 1997), the maximum vertical contact stress is found under the two sides of tyre than the center; the transversal stress is zero at the center of the tyre; the longitudinal stress distribution is sensitive to load and inflation pressure as shown in figure 2.4. In theory or simulation research the traffic contact pressure is considered as Hertz or Trapezoidal distribution under plan strain condition (Yu, 2005; Yu and Hossain, 1998), while in three dimensions, a hertz distribution acting on elliptical contact area used to describe the contact pressure (Ponter et al., 1985; Yu, 2005). In practice, a uniform pressure distribution is normal assumed (Thom, 2008).

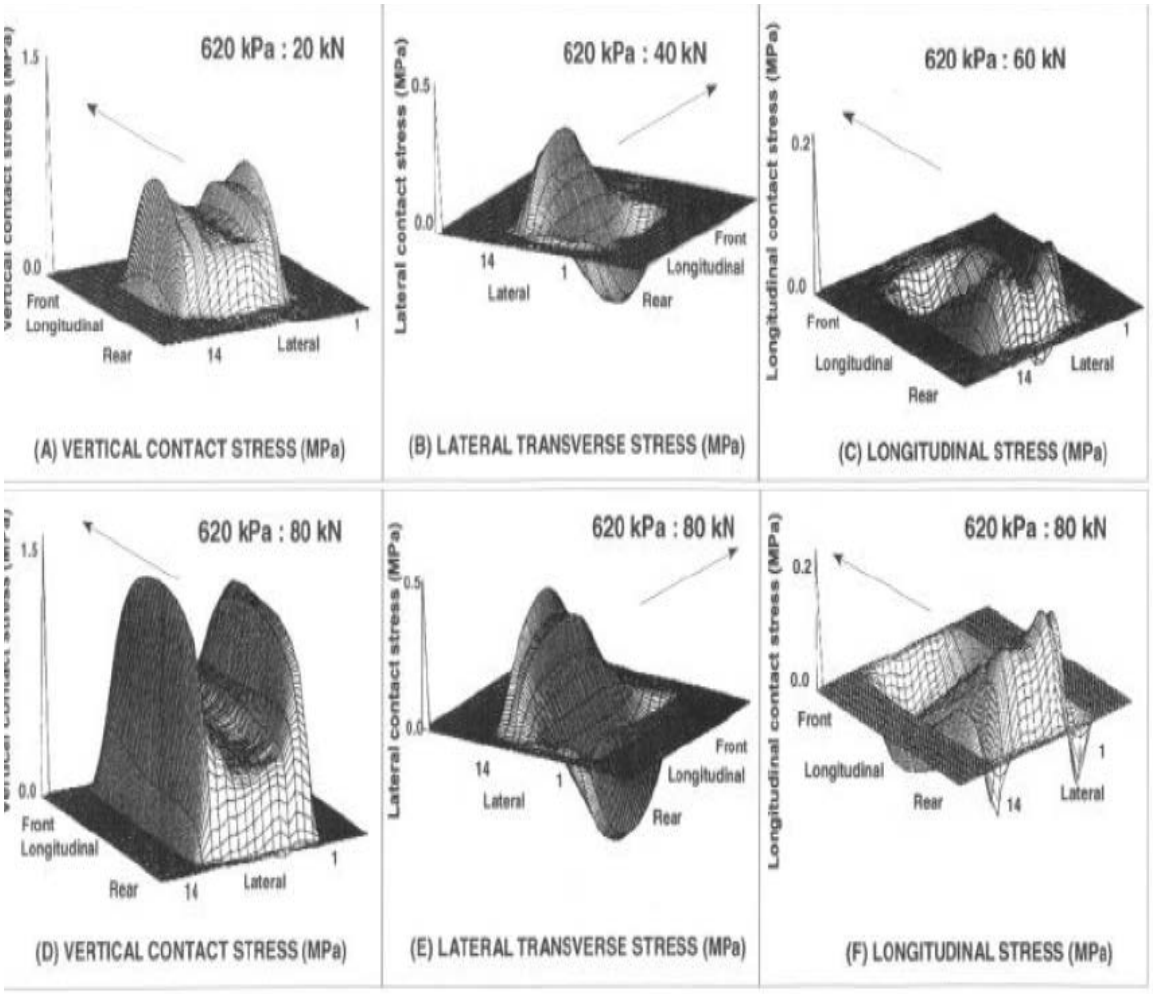

Figure 2.4: Typical Contact Stress Distributions (De Beer et at., 1997)

2.1.3. Pavement Responses

When a wheel moves on the pavement surface, the parts of pavement structure subjected to loading and unloading process. The stress types: axial and shear stresses are formed as shown in figure 2.5a; The axial stresses are compressive in unbound granular layers as a wheel load passes over pavement surface ; a reversal shear stress takes place and the rotation of principal axis induced. The deformation behaviour of pavement layers subjected to a moving wheel load composed of resilient (recoverable) and permanent (residual) deformation are formed as shown in figure 2.5b.

The elastic response of road pavement takes place when the repeated stress level is either lower or greater than the applied stress during the period preloading but below the maximum compressive strength of the pavement materials. The maximum stress level for elastic response of road pavement is known as shakedown limit. Below this limit, the pavement may behave plastically during initial loading but the elastic response takes place as further loading. The elastic behavior of the pavement has been validated through wheel tracking test in the laboratory There is further accumulation of plastic deformation after certain number of the repeated stress and when the pavement is subjected to an applied stress below the shakedown limit (Juspi, 2007).

The accumulation of permanent deformation is typical plastic response of the pavement. Rutting (permanent deformation in pavement) is caused by compaction (reduction in volume) and shear distortion at pavement surface. When the pavement experiences a repeated stress level above the shakedown limit, the permanent deformation constantly accumulates with the repetition of wheel loads (Monismith and Brown, 1999).

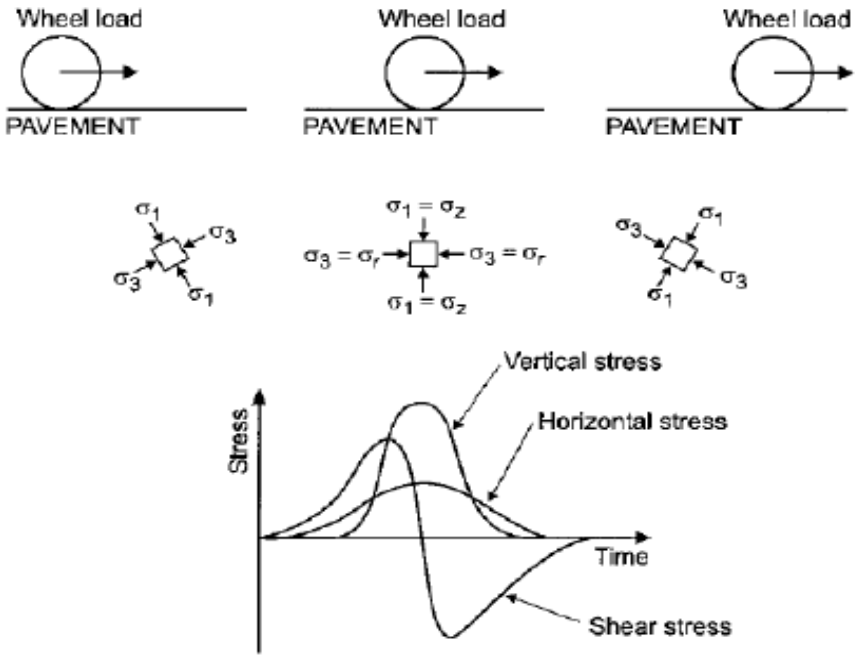

a) Stress Response

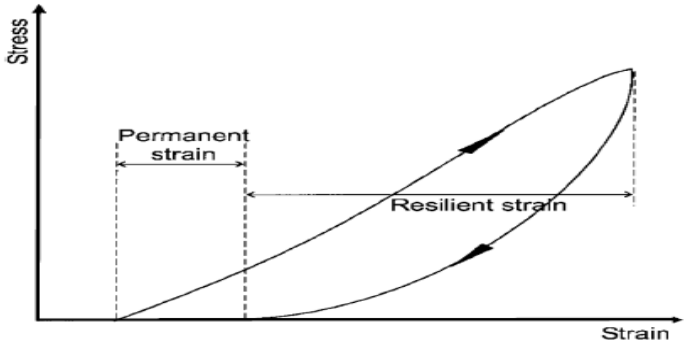

b) Strain Response

Figure 2.5: Stress and Strain responses of pavement (Lekarp et al., 2000)

2.1.4. Pavement Failure Modes

There are two types of pavement failure (Yoder and Witczak, 1975). The first is categorized as the structural failure. The pavement structure may collapse, one or more pavement components fail. As a result, the pavement is incapable of support the traffic load applied on its surface. The second is pavement functional failure: This pavement failure tends to take place due to discomfort to passengers induced by pavement roughness. According to Miller and Bellinger (2003), there are several types of pavement distress. The pavement distress modes generally observed in flexible pavement classified into five categories, namely fatigue cracking, permanent deformation or ratcheting; surface defects such as bleeding and raveling, patching and potholes and other miscellaneous distress like lane to shoulder drop off. The latter three problems could be solved by an appropriate resurfacing or removal of the excess bituminous binder. The fatigue cracking and permanent deformation induced by repeated traffic loads are the main characteristics of pavement distress.

The most common mode of distress in flexible pavements in the USA has been considered to be fatigue cracking (Monismith, 1973). As shown in Figure (2.6), fatigue cracking may be observed at the surface outside the loaded area or at the bottom of the bituminous layer directly under the load, where the tensile stress is largest (Wang, 2011). With reference to Hveem and Sherman (1962), for a thin asphalt layer, the fatigue cracking evidently occurs at the pavement surface, which is induced by horizontal tensile stresses or strains resulting from flexure of the pavement. As thicker bituminous layers were introduced, in situ measurements of tensile strains were carried out by Klomp and Niesman (1967) and the maximum value was apparently observed at the bottom of the layer rather than at the surface. In practical engineering, the cracks develop and connect to one another with the repetition of traffic loads, as shown in Figure 2.7.

Deterioration in flexible pavements is mainly indicated by permanent deformation, which is attributed to an accumulation of vertical plastic deformation in the pavement structure and the soil foundation subjected to repeated traffic loads (see Figure 2.8). The pavement structure includes the asphalt layer as well as the granular layer. These deformations may arise from shear deformation, viscous flow, compaction or consolidation. An initial sharp increase in the permanent deformation tends to occur for all flexible pavements, due to the densification of the pavement layers. For a well designed road pavement, only a small increase in the permanent

deformation appears with time. Figure 2.9 shows the permanent deformation of flexible pavements in practical engineering. Generally, when a value of 15mm for permanent deformation is measured from the original level, the pavement is considered to have reached a critical condition. Pavement maintenance is required to satisfy the future performance (Norman et al., 1973). Once the rut depth exceeds 20mm, the pavement condition is often classified as failed (Croney, 1977).

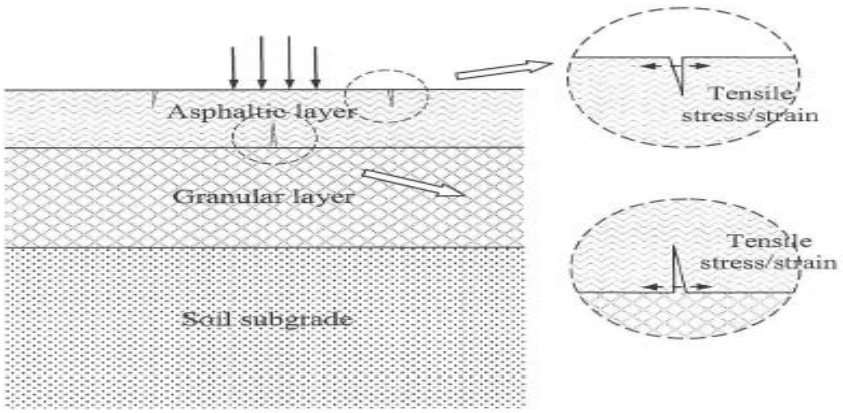

Figure 2.6: Fatigue cracking in road pavements outside and bottom of loaded area (Wang, 2011)

Figure 2.7: Fatigue Cracking in practical engineering (Wang, 2011)

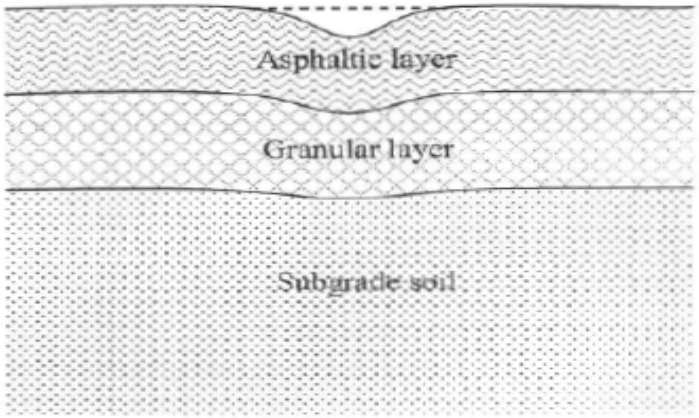

Figure 2.8: Rutting or Permanent Deformation in Road Pavements (Wang, 2011)

Figure 2.9: Rutting or permanent deformation in Practical Engineering (Quang, 2014)

2.1.5. Pavement Shakedown Analysis

Soil and Load Bearing Structures support the cyclic or repeated loading of earthquake, ocean wave and traffic loading. The shakedown theory used in Practical Engineering. Shakedown is a direct and effective way to explore bearing strength and stability capability of elastic plastic structure under cyclic load. Over the past three decades, the shakedown analysis played an important role in the safety of load assessment of the pavement. There exist a series of shakedown studies such as Johnson (1962); Sharp and Booker (1984); Collins and Cliffe (1987); Shiau and Yu (2000); Boulbibane and Collins (2000); Yu (2005); Wang (2011).

2.1.6. Shakedown Concept

When a cyclic load is applied to elastoplastic structure, four conditions are created due to various load level as shown in figure 2.10. First, if the load level is within the yield area of the structure, the behaviour of the materials is always purely elastic and no plastic strain occurs. When the load level exceeds the elastic limit but it is still lower than the critical limit, structure undergoes the plastic deformation at the beginning of loading cycles. Elastic shakedown happens and the critical limit is termed as the shakedown limit. Third ,if the load level is larger than the shakedown limit , where the closed plastic strain cycle substitute the purely elastic strain response is known as the plastic shake down limit. At this moment, irregular plasticity collapse may occur due to repeated closed loops developed between two plastic states. Finally, when the loading level is very large that is used to increase the plastic deformation with increasing the number load cycles, the structure will collapse, which termed as ratchetings.

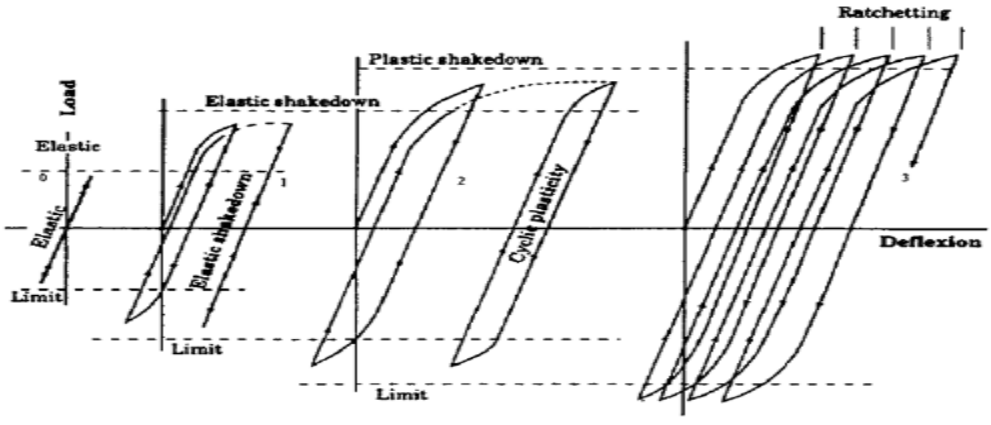

Figure 2.10: Elastoplastic Behaviour of Structure subjected to Cyclic Loads (Johnson, 1986)

2.1.7. Shakedown Analysis in Pavement Engineering

Ponter et al. (1985) used the kinematic shakedown theorem to study the deformation response of an elastic-perfectly plastic half-space under rolling and sliding point contacts. A Hertz pressure distribution and frictional traction acted on an elliptical area. Various traction coefficients and loaded ellipse shapes were used to obtain the optimal upper bound elastic and plastic shakedown limits. Radovsky and Murashina (1996) developed a model through a Mohr-Coulomb failure criterion to predict the shakedown occurrence of subgrade soils. The boundary shakedown loads and pressures increased with an augmentation of the shear strength of subgrade soils. The internal friction angle of the material had an effect on the ratio of the maximum to the smallest boundary shakedown load.

The mechanical behaviour of an unbound pavement under repeated traffic loads was studied by Collins and Boulbibane (2000). A procedure was proposed on the basis of the Mohr-Coulomb criterion and kinematic shakedown theorem. A shakedown limit was obtained above which pavements will eventually fail due to continuous accumulation of permanent deformation and below which pavements initially exhibit some plastic deformation but will eventually shakedown to a steady state. Some factors such as self weight, moisture content, dual loads, relative strengths of the different pavement layers and non-associated plastic flow were considered. Non-linear programming techniques and the displacement-based finite element method were used to perform shakedown analysis of structures by Li and Yu (2006). A general yield criterion and an associated flow rule were applied to the upper bound shakedown theorem. The efficiency and effectiveness of this numerical method were validated by shakedown analysis of pavements and tunnels

2.1.8. Residual Stress

Elastic and plastic deformations of the pavements are caused through the moving traffic load on the pavement surface. After the removal of the load, the elastic strain will recover and the elastic stress disappears. However, the plastic deformation remains in pavement and some stresses have occurred, called residual stress. Pavement shakedown was simulated using the finite element

method in 2D by Wang (2011). The size of the simulated pavement model was 84a long by 30a high (a is semi contact width). A Hertzian contact was used to model the wheel pressure. Tresca and Mohr Coulomb materials were used for the half-space simulation. Pure rolling contact was considered. The various residual stress distributions with pavement depth for a Tresca half-space are presented in Figure 2.11, where the wheel pass number was three. It was noted that the vertical and shear residual stresses could be disregarded, consistent with the equilibrium condition. For the horizontal and transverse residual stresses, the maximum value was close to the pavement surface. In the case of Mohr Coulomb material, the fully-developed horizontal residual stress fields for various internal friction angles and wheel pressures are demonstrated in Figure 2.12. Their peak points were all located beneath the pavement surface, approximately at z/a = 0.5. With the increase in friction angle, the residual stress distributed more and more widely with the increased magnitudes of compressive residual stresses.

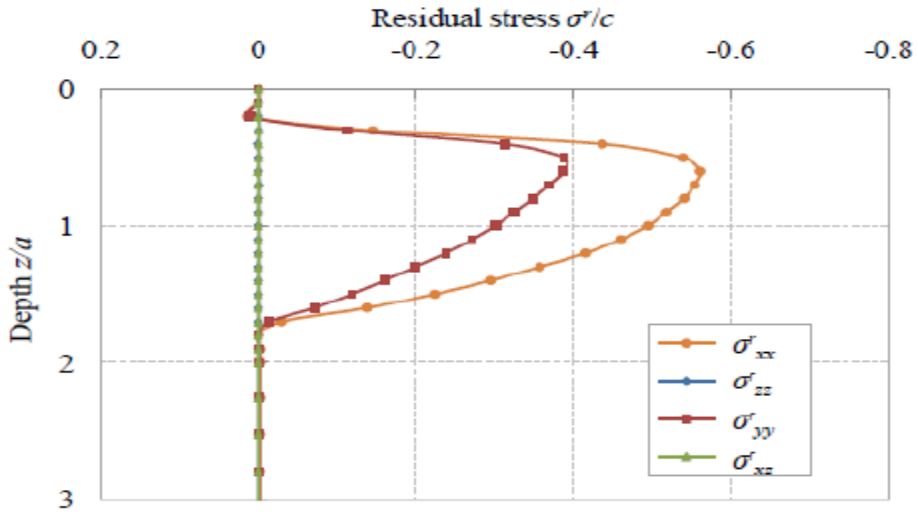

Figure 2.11: Distribution of normalized Residual Stress (Wang, 2011)

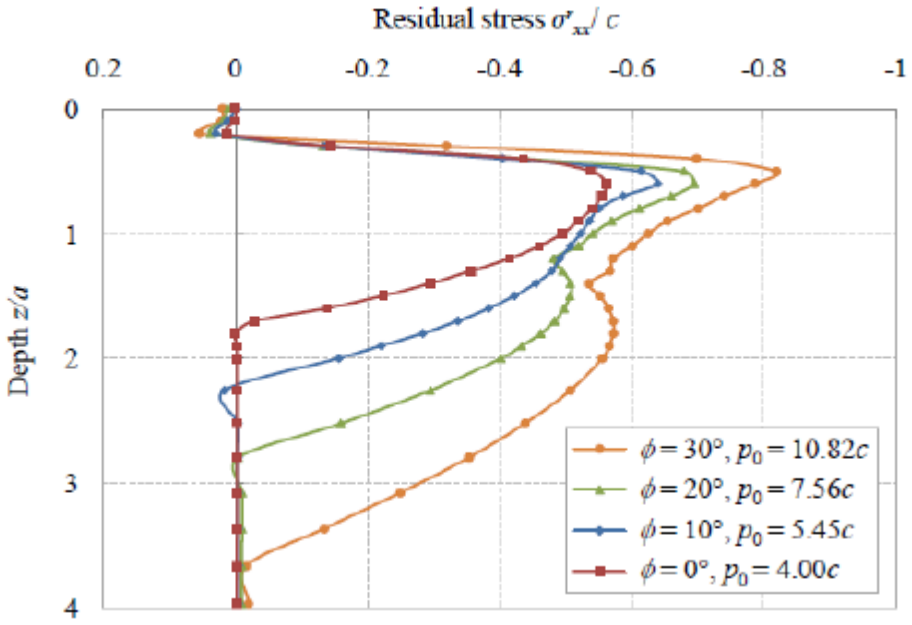

Figure 2.12: Distributions of normalized fully-developed horizontal residual stress (Wang, 2011)

2.2. Pavement Design Method

The growing of transportation needs and increments of traffic load had made rapid deterioration of existing road networks. This situation influences the road sectors to use alternatives materials to the natural aggregates in pavement structure. But, the applicability of alternative materials was a gap by the empirical nature of traditional design method. The need to overcome this gap has led worldwide research effort to develop the more adaptable and comprehensive pavement design method, namely mechanistic pavement design. This method is used to analyze the response of the pavement structure under specified traffic loads and environmental conditions. Understanding the behaviour of the pavement materials is a prerequisite for mechanistic approach. The behaviour of the granular material is a complex Elasto plastic. This has two type of deformational response under repeated traffic loading as a resilient response, which is important for the load carrying capacity of the pavement and a permanent strain response, which characterizes the long-term performance of the pavement and the rutting phenomenon (Werkmeister, 2003).

The mechanical properties of unbound granular layers in flexible pavements are important to the overall structural integrity of the pavement structure. The resilient (elastic) properties of unbound granular materials are non-linear and stress dependent (Hicks and Monismith, 1971; Uzan, 1985).

Prior to 1920s pavement was designed against subgrade shear failure by providing a subgrade support from the experience of previously completed projects. Afterward, the traffic volume increased and evaluation of pavement performance became the main focus points. These parameters have led the development of test track experiments. This experiment was AASHTO Road test track at 1960. From this, AASHTO Road test track seminar experiment, the AASHTO design guide was developed. This design guide was named as Empirical Methods (NCHRP, 2004).

Empiricism is behind the design of pavements still the current time. The thickness of a pavement is determined entirely through experience. A part of road pavements has the same thickness and different subgrade soil occurs in geotechnical engineering. A series of methods has been proposed by various agencies, based on experience, to determine the ideal thickness of road pavements. Flexible pavements usually consist of asphaltic and granular materials. Rutting and Cracking of pavement surfaces are the main causes of flexible pavement failures. The design methods of flexible pavements can be divided into five groups, namely the empirical method, the mechanistic-empirical method, the limiting deflection method, the limiting shear failure method, and the regression method (Huang, 1993).

Empirical methods are most wide used to design flexible pavements, like AASHTO Pavement design guide. The recent empirical approach is totally based on experimental data from in service pavement performance and full scale road tests. Some empirical equations such power equation, used to determine the permanent deformation of road pavements under repeated wheel loads (Monismith et al., 1975; Li and Selig, 1996). Though, the relationship between the elastic strain and the permanent deformation behaviour of road pavement tends not to be directly established (Shiau, 2001). In general, plastic strain is assumed not to be induced and the importance of plastic behaviour to the pavement life cycle is disregarded. Another weakness of the empirical method is related to the limitation of the environmental, material and loading conditions (Huang, 1993).

The mechanistic-empirical method of pavement design depends on the mechanical behaviour of materials, e.g. the stress or strain response of road pavements to a wheel pressure. According to laboratory tests and field performance data, prediction of pavement distress is performed using the response values. As first recommended by Kerkhoven and Dormon (1953), the vertical compressive strain on the surface of the subgrade can be applied as a failure criterion for pavement design. In addition, the horizontal tensile strain at the bottom of the asphalt layer is employed to reduce fatigue cracking (Saal and Pell, 1960). Moreover, a mechanistic-empirical design approach, i.e. the South African Mechanistic Design Method, has been used in South Africa (Theyse et al., 1996). Transfer functions are proposed to predict the permanent pavement deformation in terms of the unbound pavement layer, the individual pavement layers and the roadbed. In the mechanistic-empirical framework, there exist the linear elastic model, the linear elastic model with the viscoelastic response and *the* nonlinear finite element model (e.g. Monismith et al., 1977; Kenis, 1977; Lytton et al., 1993). The strengths of the mechanistic-empirical method are improvement in the reliability of pavement design, and the ability to predict types of pavement distress (Huang, 1993).

The thickness of pavements can be obtained using the limiting shear failure method so that shear failures will not take place (e.g. Barber, 1946; Yoder, 1959). The cohesion and internal friction angle are the main parameters to be determined in terms of pavement materials and subgrade soils. The limiting deflection method is applied to the design of road pavements so that the maximum limit of the vertical deflection is not exceeded (Huang, 1993). The evident strength of this method is that it can be easily measured in the field. However, pavement failures will be induced by excessive stresses and strains rather than deflections. For the regression method, the regression equations are proposed on the basis of the performance of existing pavements (e.g. Darter et al., 1985; Hall et al., 1989). The advantage of these equations is that the effect of various factors on pavement performance is considered, whereas there is a significant limitation on pavement design due to the many uncertainties concerned (Huang, 1993).

Destruction of road pavements subjected to repeated vehicle loads is generally brought about by progressive deterioration, instead of sudden failure. Therefore, the long-term plastic behaviour needs to be taken into consideration. Over the last three decades, a growing attention has been paid to the application of shakedown theorems so as to study the mechanical behaviour of road pavement structures under repeated traffic loads (e.g. Sharp and Booker, 1984; Collins et al.,

1993; Yu and Hossain, 1998; Yu, 2005). Theoretically, there exists a critical load limit below which the accumulation of plastic strain ceases because of the protective residual stress and above which the road pavements will be destroyed as a result of the continuous accumulation of plastic strain. This load limit is called the shakedown limit. Melan (1938) developed a fundamental theorem for static shakedown, which provides a lower bound to the shakedown limit. Later, Koiter (1960) proposed a kinematic shakedown theorem to give an upper bound to the shakedown limit. The shakedown limit load seems first to have been proposed as providing proper parameters for road pavement design by Sharp and Booker (1984). Determination of the shakedown limit for pavement design has been performed (e.g. Yu and Hossain, 1998; Shiau, 2001; Yu, 2005; Wang, 2011). The pavement shakedown phenomenon has also been validated by laboratory wheel tracking tests (e.g. Juspi, 2007) and by the AASHO road test records (see Sharp and Booker, 1984).

A few Discrete Element Modeling (DEM) simulations for road pavements have been proposed. A 2D flexible pavement structure was constructed by Vallejo et al. (2006), composed of a modelled asphalt concrete layer and a granular base. The particle degradation in the granular base was studied and particle crushing was not allowed in the modelled asphalt layer. It was found that particle breakage started at the top of the granular base course and went on to spread towards the bottom of the base layer during repeated wheel loads. In addition, a flexible pavement in three dimensions was established by Dondi et al. (2007), containing an asphalt layer, as well as granular subbase and subgrade courses. The asphalt layer was simulated using Burger's model. The visco-elastic behaviour of the simulated pavement subjected to two circular contact patches was studied. The contact stress distributions within the simulated pavement section were measured in terms of vertical, horizontal and shear stresses. Moreover, some DEM simulations have been performed on the mechanical behaviour of the elementary specimens, comprised of unbound granular materials subjected to quasi-static cyclic loading (e.g. Garca-Rojo and Herrmann, 2005; Luding et al., 2007). The development of permanent deformation with the repetition number of the external loads was recorded. For different load levels, shakedown (i.e. no further accumulation of permanent deformation) and ratchetting (i.e. the continuous accumulation of plastic strain in individual loading cycles) were observed. Therefore, as discussed above, DEM simulation of permanent deformation of road pavements under repeated traffic loads can be carried out. It is potentially useful in pavement structure design.

2.3. Pavement Mechanistic Modeling

The development of CIRCLY was based on layered elastic system (Gerrard, 1969). The work to develop analytical elastic solutions (Gerrard and Wardle, 1973) in software in FORTRAN language to explore different circular loadings on pavement surface combined CRANLAY and UCRANLAY (Harrison et al., 1972) programs into CIRCLY. The acronym of CIRCLY came from circular loads (circular contact area) and layered systems. CIRC was the short form of Circular loads and LY was an abbreviation for layered Systems, because at the time the CSIRO FORTRAN compiler had a limit of 6 characters for the program name (and any variable).

CIRCLY works based on integral transform techniques and offers significant advantages more than other linear elastic analysis techniques such as the finite element method. Input data for the program is much easier than the essential finite element programs. The analytical solutions for the stresses, strains and displacements are given by integral transform methods (Wardle, 1977a).The solutions involve integrals of this form:

$$I = \int_0^{\infty} A(k)\ J_{\eta}(k)\ J_{\tau}(kr)\ \exp(\pm \delta kz)\ k^{\mu}\ dk \qquad (1)$$

Where J denotes the Bessel function of the first kind, and r and z are expressed as multiples of the loaded radius. The coefficients A(k) are found by solving a set of simultaneous equations which represent the loading conditions at the surface, the interface conditions between the layers, and the conditions at the base of the lowest layer. The integrals are evaluated numerically.

CIRCLY was used to calculate the load-induced stresses, strains and displacements at any selected points in the layered system as represented in figure 4.2 and 4.3. Subgrade material and subgrade soil have anisotropic material properties, asphalt and cemented materials comprise isotropic properties. The interfaces between the layers can be either fully continuous (rough) or fully frictionless (smooth), or a combination of both types. From a practical standpoint the response of actual pavement interfaces will be somewhere between these theoretical limits. The fully continuous case is always assumed for pavement design.

The evolution of CIRCLY has been intimately linked to the development of Austroads flexible pavement design method. CIRCLY was officially adopted for flexible pavement design in Australia with the publication in 1987 of Pavement Design. This manual had moved forward empirical pavement design to comprehensive mechanistic design method. This design method acquired a mathematical model with inputs of engineering properties and outputs depended on material performance data. The advantages of the mechanistic approach in pavement design are the ability to take into consideration different variables and test these for quality, and the ability to assess the performance of new materials and loading conditions. Momentarily, the Austroads flexible pavement design method (Austroads, 2004) uses CIRCLY to calculate load-induced stresses, strains and deflections in model pavements as represented in Figure 2.13. The surface loading is the "standard axle" as represented in appendix figure C-4. Two critical strain components are used to design pavements. These are maximum vertical compressive strain at the top of the subgrade and subgrade layers is related to the repetitions to cause surface rutting failure and the maximum horizontal tensile strain at the bottom of the asphalt or cemented layers is related to repetitions to cause fatigue cracking of those layers as shown in figure 4.1 and C-4.

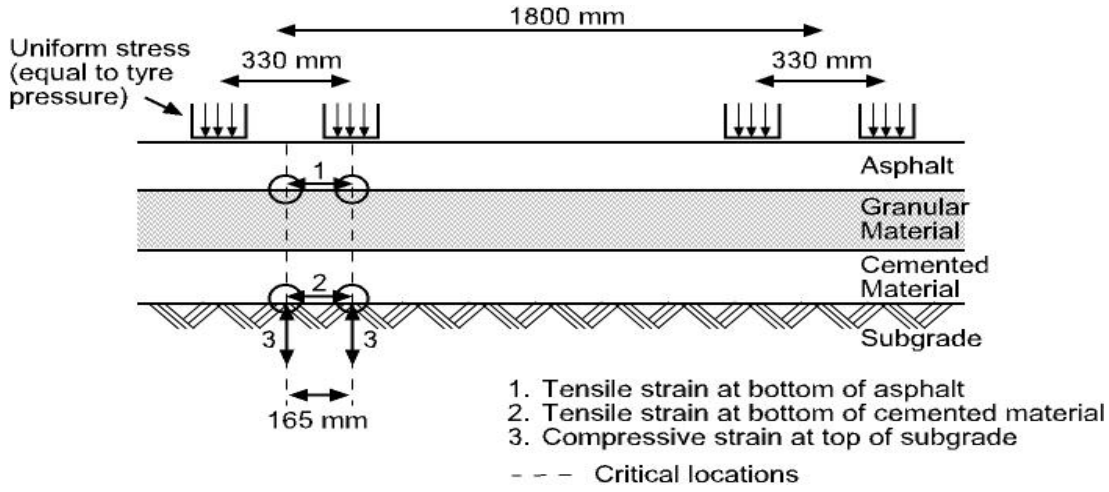

Figure 2.13: Pavement Model for Mechanistic Procedure (Austroads, 2004)

The 'mechanistic' design method involves calculating pavement damage from these critical strains using empirical equations called 'failure criteria' or 'performance relationships' of the form as indicated in appendix table B-3b of CIRCLY:

$$N = \left[\frac{k}{\varepsilon}\right]^{b} \quad (2)$$

where N is the predicted life (repetitions)

k is a material constant

b is the damage exponent of the material

ε is the induced strain (dimensionless strain)

The empirical parameters *k* and *b* are determined by calibrating the design method against observed performance of test pavements or of pavements in service.

2.3.1. Pavement Damage Model

Empirical pavement design method does not consider the Cumulative Damage Factor (CDF) theory; it has been considered through mechanistic design method determined in CIRCLY software by presenting results numerically and graphically. The CDF theory is used to predict the total damage as represented in figure 4.2. This presents the level of pavement strain response to vehicle loading as a direct indicator of pavement damage over the complete life of the pavement. The cumulative damage from all of the vehicles contributes to the failure of the pavement according to the strain imposed by the individual vehicles. The Damage Factor for the i-th loading is defined as the number of repetitions (ni) of a given strain divided by the 'allowable' repetitions (Ni) of the strain that would cause failure. The Cumulative Damage Factor is obtained by summing the damage factors over all the loadings in the traffic spectrum using Miner's hypothesis. The Total Damage Factor is defined by:

$$CDF_{Total} = \sum_{i=1}^{LoadCases} CDF_i \quad (3)$$

i is summed over the mix of loads, for example, different container vehicles. The pavement is presumed to have reached its design life when the cumulative damage reaches 1.0. If the CDF is less than 1.0, the pavement has excess capacity and the CDF represents the proportion of pavement life consumed by the design traffic. Conversely, if the CDF exceeds 1.0 then the pavement is deemed to be unacceptable and must be modified in the next trial so that the deficiency is overcome by increase in pavement thickness or a modification to stiffness. The process is repeated until a satisfactory result in achieved as prescribed in Austroads 2004.

2.3.2. Material Characterization

Isotropic materials have the same properties in all directions whereas anisotropic materials have not the same properties in all directions. The cross-anisotropic case has an axis of symmetry of rotation. The properties are equal in all directions perpendicular to this axis, but different to those parallel to the axis. Assuming the axis of symmetry to be vertical, the five parameters required are Vertical Moduli (Eν), Horizontal Moduli (Eh), Shear Force (Fν), Horizontal Poisson's Ratio (νh) and Vertical Poisson's Ratio (Vν) (Austroads, 2004).

The NAASRA working group had noted that measured deflection bowls were narrower than those estimated from elastic layer analysis using isotropic models. The view was taken by the working group that anisotropic models were appropriate for modeling granular and subgrade materials. To obtain a closer fit between observed and CIRCLY-estimated deflection bowls, a value of 2 for the modular ratio (Eν/Eh) was adopted for both granular and subgrade materials as a 'best estimate'. The values of Vh and Vν were taken to be the value of the isotropic V. The remaining cross-anisotropic parameter – Fν – was set equal to Eν / (1+ν). With these additional assumptions, the cross-anisotropic characterization of granular and subgrade materials was specified by values for Eν and V. Isotropic properties were considered to be appropriate for asphalt and cemented materials (Austroads, 2004). Unbound granular pavement materials such as graded crushed rock base course and natural gravels require special attention because their elastic stiffness depends on stress state at each point in the material. The layered elastic model cannot fully deal with stress dependence. This is the important limitation of the method that elastic moduli must be constant within each horizontal layer. Stress diminishes with distance from the wheels so the modulus will also change with distance from the wheels, both in the

horizontal and vertical directions. However, the layered elastic model can take stress-dependence into account to some degree by dividing granular layers into sublayers and assigning moduli to each sub layer. This allows the modulus to change with depth. CIRCLY automatically subdivides granular layers and assigns moduli in accordance with the method specified in the Austroads pavement design Guide.

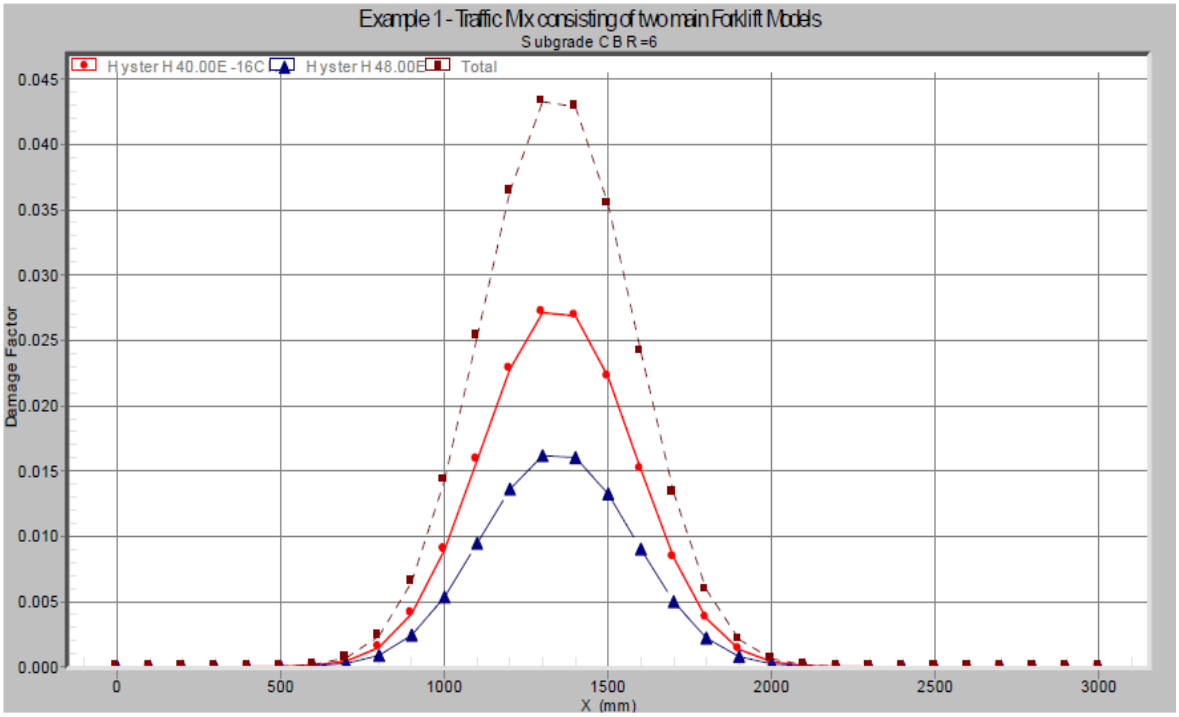

Figure 2.14: Cumulative Damage Factor Graph (Austroads, 2004)

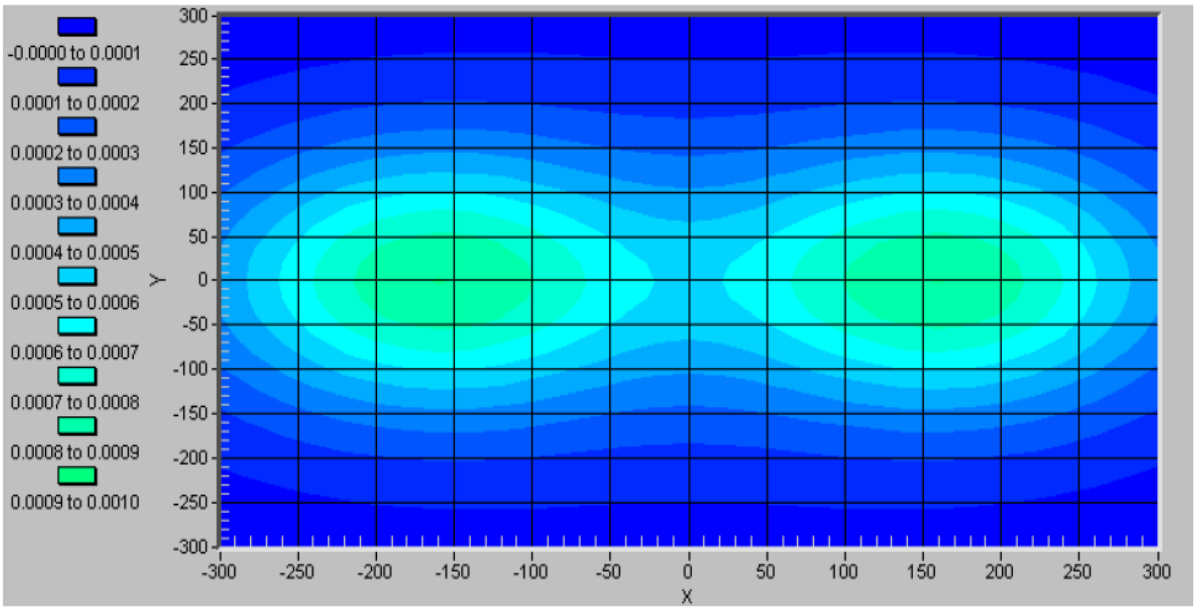

Figure 2.15: 2- Dimensional Contour Plot of Strain (Austroads, 2004)

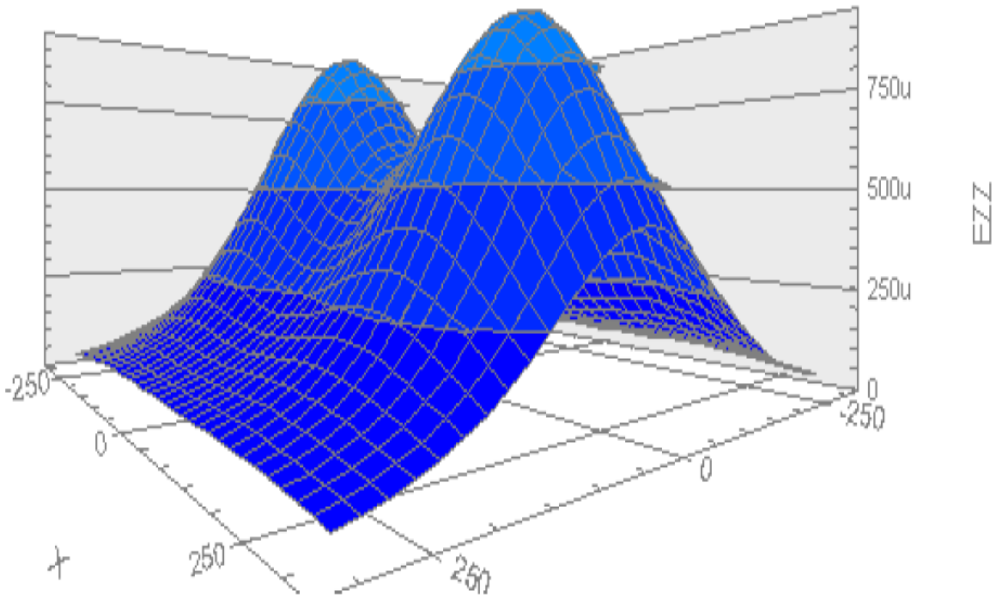

Figure 2.16: 3- Dimensional plot of Strain (Austroads, 2004)

3. Methodology

3.1. Material used for the Research

A triaxial compression test is more sophisticated test equipment for determining stiffness, deformation and shear strength of unbound subgrade material. In general, these test results used as input to explore response of subgrade pavement material to stress. The main use of this repeated load triaxial test equipment was to determine mechanical properties of unbound pavement materials and to access suitability of physical test results for mechanistic Models. The capping layer material or unbound subgrade material was used for this research. The standards classified subgrade materials mostly into two; G7 and G20 depending on their strength or California Bearing Ratio (CBR value). Basically, this material had a CBR value of 16% as determined in laboratory. Hence, unbound subgrade material sampled for this research from existing borrow pit of Shano Danaba gravel Road Construction project located in Oromia Regional State, North Shawa. And this project is located at 80km from Finfinne (Addis Ababa) City toward North Direction as indicated in Figure 3.1.

3.2. Material Location

Unbound pavement material used for this research was sampled from Shano Danaba unpaved road construction project located in Oromia Regional State, North Shawa. The location of this sample was at station 0+000 offset 500m to left hand side of road under construction as indicated in detail Engineering Design Report of project soil investigation, borrow materials for embankment construction. Strength evaluation of suitable borrow materials had been tied with test pits dug during subgrade soil investigation and obtained from laboratory tests as indicated in table A-10 . The material sampled for this research was disturbed and taken from existing borrow pit used previously by contractor.

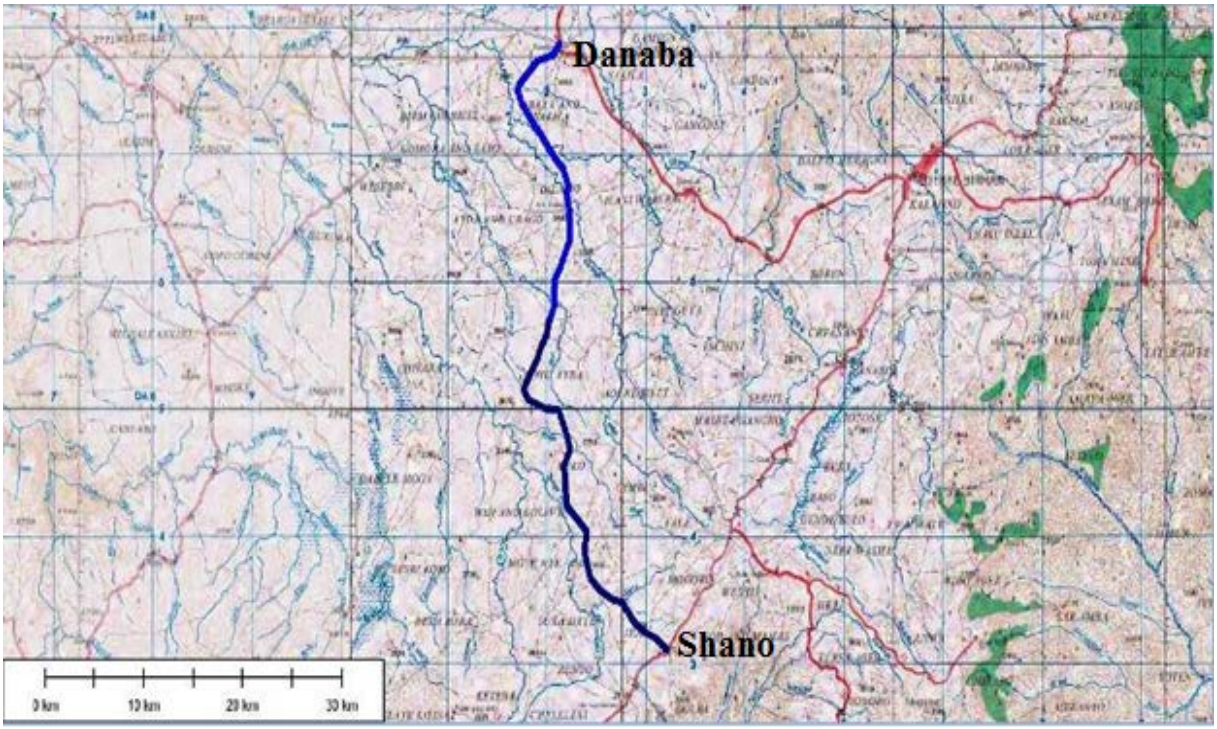

Figure 3.1: Project Location Map (www.globalmapper.com)

3.3. In-Situ Sampling Method

The borrow materials used for Shano Danaba Road Construction Project having different CBR values had shown in table A-10. The borrow pit located at 0+000 offset 500m left hand side of this project was selected for this research work, based on minimum CBR value from the four utilized borrow pits. Depending on purposive sampling method this borrow pit was selected. Selecting a borrow pit with a minimum CBR value from the utilized borrow pits required a special judgment of sampling method.

In-situ sample was required in this research, for taking disturbed sample from a borrow pit, at station 0+000 offset 500m to left hand side of road under construction, with vertical sides two meter square and which has been excavated in a natural deposit of soil by means of digging axle. Depth and area measuring tape , spade and materi material was utilized as subgrade material for a road under construction. A 40kg of subgrade material was sampled for laboratory test. A visual inspection of test pit was taken place and sampling of material had al sampling bag used to sample subgrade pavement material as shown in figure F-4. This sampled been done according to AASHTO material sampling techniques or disturibed sampling method . The material sampled from existing borrow pit was tested at the laboratory of Ethiopian Construction Design and

Supervision Work Corporation, Water and Energy sector located at Bole Subcity or near to Emperial Hotel in Addis Ababa City. The location of material and detail of test equipments had represented in table A-10 and figure F-3 respectively.

3.4. Triaxial Sample Preparation

The characterizations of material in physical tests in the laboratory were the main input parameters of this research. Variety of tests was carried out in laboratory to ensure that the material performs as intended for this research work. One of these tests was the gradation test that used to determine the distribution of UGM particles by size within a given sample. In this research, UGM size analysis was conducted according to AASHTO sieve size distribution that common used for test of unbound subgrade pavement material . The series of sieve sizes used for this research work were; 37.5mm, 25mm, 19mm, 16mm, 12.5mm 9.5mm 4.75mm and 2.36mm, 1.18mm , 0.300mm ,0.150mm and 0.075mm with atterberg limit for material classifcation as indicated in table A-3,A-4 and A-5.

Mostly the materials retained on these sieves 2.36mm, 1.18mm , 0.300mm ,0.150mm and 0.075mm had utilized for triaxial sample prepartion of this research. Two kilogram of material sampled on these size required for triaxial sample preparation. The apparatus used for this sample preparation and test procedure of particle size analysis had done according to AASHTO materials test specification in the laboratory as represented table A-1. The laboratory test performed to determine the relationship between moisture content and dry density of subgrade materials sampled from the site as indicated A-2. The laboratory employed compaction test using Proctor method. AASHTO T99 method used to determine the maximum dry density and optimum moisture content of subgrade materials as in shown in figure F-1. The density ratio of specimen should be related to density normally achieved in field. Normally three specimens prepared and tested at Optimum Moisture Content and Maximum Dry Density (MDD) obtained in laboratory. The size of specimen used for this research was 38 mm in diameter with a height of 76 mm prepared in the laboratory for conducting Repeated Load Triaxial Test as shown in figure F-4 in appendix. The material was compacted according to standard Proctor compaction method, in a split cylinder lined with a rubber membrane usually up to a level corresponding to standard compaction energy.

3.5. Testing Equipment

The sample prepared was tested in triaxial testing apparatus suitable for specimen 38 mm diameter and 76mm high with a working pressure of 3000KPa. Dynamic loading equipment capable of applying a vertical dynamic force and a static confining pressure via the air in the triaxial cell and Load and pressure measurement devices to measure vertical dynamic force and static confining pressure and devices to measure vertical displacement of sample. Apparatuses used for this research ; hammer, split mould, and sealing membrane, triaxial cell, and vertical load actuator and stand, and small air pressure cell as shown in figures 3.2.

Specimen in triaxial cell

Triaxial Test Equipment

Figure 3.2: Triaxial Test Equipment at laboratory of ECDSWC

These procedures were used to test the specimen prepared for this research in triaxial test

1. Place triaxial cell with the specimen inside it on the platform of the compression machine.
2. Make proper adjustments so that the piston of the triaxial cell just rests on the top platen of the specimen.
3. Fill the chamber of the triaxial cell with water. Apply a hydrostatic pressure, σ_3 to the specimen through the chamber fluid. All drainage to and from the specimen should be closed *now* so that drainage from the specimen does not occur.

4. Check for proper contact between the piston and the top platen on the specimen. Zero the dial gauge of the proving ring and the gauge used for measurement of the vertical compression of the specimen. Set the compression machine for a strain rate of about 1.5mm per minute, and turn the switch on.
5. Take initial proving ring dial readings for vertical compression intervals of 0.01 mm. This interval can be increase or more later when the rate of increase of load on the specimen decreases. The proving ring readings will increase to a peak value and then may decrease or remain approximately constant. Take about four to five readings after the peak point.
6. After completion of the test, reverse the compression machine; lower the triaxial cell, and then turn off the machine. Release the chamber pressure and drain the water in the triaxial cell. Then remove the specimen and determine its moisture content.

3.6. Modeling Method

The responses to stress of pavement layers strongly influenced in moving loads on the pavement surface and play a very important role in determination of damage factor of pavement layers during design process. The layered elastic model or CIRCLY was used to determine pavement layer responses to stress. The development of CIRCLY was based on layered elastic system (Gerrard, 1969). CIRCLY is used to explore different circular loadings on pavement surface. The acronym of CIRCLY came from circular loads (circular contact area) and layered systems. CIRC was the short form of Circular loads and LY was an abbreviation for layered Systems.

These models can easily be run on personal computers and required data that easily obtainable. A layered elastic model used to analysis engineering problems, namely stresses, strains and deflections at any point in a pavement structure resulting from application of a circular load. This model was basically developed for pavement structural modeling. The analytical solutions for the stresses, strains and displacements are given by integral transform methods (Wardle, 1977a).

This mechanistic model required mathematical models to analysis pavement responses to surface loadings. Although, there are different functional models utilized for pavement structural modeling. These function models are layered elastic model (Gerrard, 1969) and finite elements model (FEM) typically used in pavement structural analysis and design. These models can easily be run on personal computers and required data that easily obtainable. A layered elastic

model used to analysis engineering problems, namely stresses, strains and deflections at any point in a pavement structure resulting from application of a circular load.

CIRCLY was used to calculate the load-induced stresses, strains and displacements at any selected points in the layered system. Subgrade material and subgrade soil have anisotropic material properties, asphalt and cemented materials comprise isotropic properties. The interfaces between the layers can be either fully continuous (rough) or fully frictionless (smooth), or a combination of both types. From a practical standpoint the response of actual pavement interfaces will be somewhere between these theoretical limits. The fully continuous case is always assumed for pavement design. Thus, it was essential to use layered elastic system to determine critical stress, strain and deformations in pavement layers. Hence, this modeling method was used for this research to explore responses of unbound subgrade pavement material to stress.

3.7. Data Analysis and Presentation

To make complete the primary data, the review of secondary material was used to make more rational thesis work. Materials from scholarly output literatures such as theses, edited books, Engineering Journal Articles, dissertations and pavement design guides were reviewed during thesis work to generate data analysis models. Data analysis and presentation was done in quantitative methods. This quantitative method was used for data analysis and presented in tables and figures of this research. Data analyzing models used for this research illustrated as pursue.

Data obtained from the laboratory experiments and in-situ were used for this research work. These data were represented in tables A-1 to A-9 and A-10 to A-12 in appendices section of this research. These primary data had analyzed in models or equations shown in table 3.1. The layered elastic model required input data that significant to model pavement responses. These input data analyzed in correlation and anisotropic models represented in table 3.2. The output of layered elastic model represented in graphicals and numericals.This output represented in graphical was used to analysis the results obtained in discussion section of this research. These results were appropriately utilized during design of the pavement structures. These results were pavement layers; deflections, strains and stresses occurred from the traffic loadings. The damage of the pavement was estimated in damaging models represented in a table 3.2 or equations 18 and 20.

Models used to analysis data obtained from laboratory

Models Description	Models	Equation No.
Initial area of specimen	$A_0 = \frac{\pi d_0^{\,2}}{4}$	(4)
Corrected Area	$A_c = \frac{A_0}{1-\varepsilon}$	(5)
Moisture Content	$w = \left(\frac{W_1 - W_2}{W_2}\right)100$	(6)
Vertical strain	$\varepsilon_v = \frac{\Delta h}{H_0}$	(7)
Horizontal strain	$\varepsilon_h = \frac{\Delta d}{D_0}$	(8)
Poisson's Ratio	$V = \frac{\varepsilon_h}{\varepsilon_v}$	(9)
Deviator Stress	$\sigma_d = \frac{F}{A_C}$	(10)
Major Principal Stress	$\sigma_1 = \sigma_3 + \sigma_d$	(11)
Modulus of Elasticity	$E = \frac{\sigma_1}{\varepsilon}$	(12)
Maximum Shear Stress	$\tau_f = c + \sigma\tan\emptyset$	(13)
Cohesion and Angle of Internal Friction(c, φ)	$\frac{(\sigma_1 - \sigma_3)}{2} - \frac{(\sigma_1 + \sigma_3)}{2}\sin\emptyset - c\cos\emptyset = 0$	(14)

Table 3.1: Models used to analysis data obtained from laboratory (Braja M. Das, 2002)

Table 3.2: Models used to analysis data (Austroads 2004 and NCHRP 1-37A, 2004)

Models Description	Models	Equation No.
Californian Bearing Ratio to stiffness	$E = 17.6[CBR(\%)]^{0.64}$	(15)
Moduli (E)	$E_h = \frac{Ev}{2}$	(16)
Poisson's Ratio (V)	$V_h = V_v$	(17)
Shear Force(F_S)	$F_s = \frac{E_V}{1+V}$	(18)
Number of repetitions to failure (N)	$N = \left[\frac{K}{\varepsilon}\right]^b$	(19)
Cumulative Damage Factor (CDF)	$CDF = \frac{N_i}{N_A}$	(20)

4. Results and Discussion

This chapter presented the experimental test result obtained from laboratory and layered elastic system simulation to characterize properties and responses of unbound subgrade material to stress.

4.1. Physical Test Results

The classification of subgrade material was carried out in laboratory. This process was used to analysis grain size and determination of Atterberg limits. Six hundred thirty nine gram of material utilized to characterize grain size as represented in figure 4.1 and table A-3, however 28.57% of this material passed 0.075mm sieve size. This material also had liquid limit and plastic index of 42% and 18% as indicated in table A-4 and A-5 respectively. According to AASHTO general classification, the material that passed 0.075mm sieve size with less than or equal to 35% of total weight, then, with minimum of liquid limit 41% and minimum plasticity index 11% is considered as a granular materials. This shown us; the material under study was granular material. Subsequently, this material was classified as A-2-7 or silty or clay gravel as represented in table C-1 of AASHTO material classification.

Material under study that passed 4.75mm sieve size and retained on 2.36mm, 1.18mm, 0.300mm, 0.150mm and 0.075mm was used for specimen preparation at laboratory of this research. More than 50% of sampled material was passed 4.75mm sieve size. This shown that the specimen prepared for triaxial test was appropriately represent the sampled material as indicated in table A-3.

The natural moisture content of subgrade material sampled for preparation of triaxial sample was determined in laboratory. This determined moisture content (w) of sampled soil was 11.47% as indicated in table A-1. Two kilogram of subgrade material used to prepare three specimens for triaxial test. The difference between optimum moisture content and sample moisture content used to prepare these triaxial specimens.

The preparation of triaxial sample was done at the laboratory. The sample prepared at optimum moisture content and maximum dry density at standard compaction method. The sample prepared for triaxial test represented subgrade material sampled at road construction project. The OMC and MDD of sample 28.1% and 1496KN/m^3 as shown in figure 4.2 and table A- 2

respectively. Although, this research test results had certain differences to in-situ test result. This was shown that, there was difference in material size used at in-suit and laboratory. As material size decreased OMC increased and MDD decreased. This shown as that changing size of material was affecting its property.

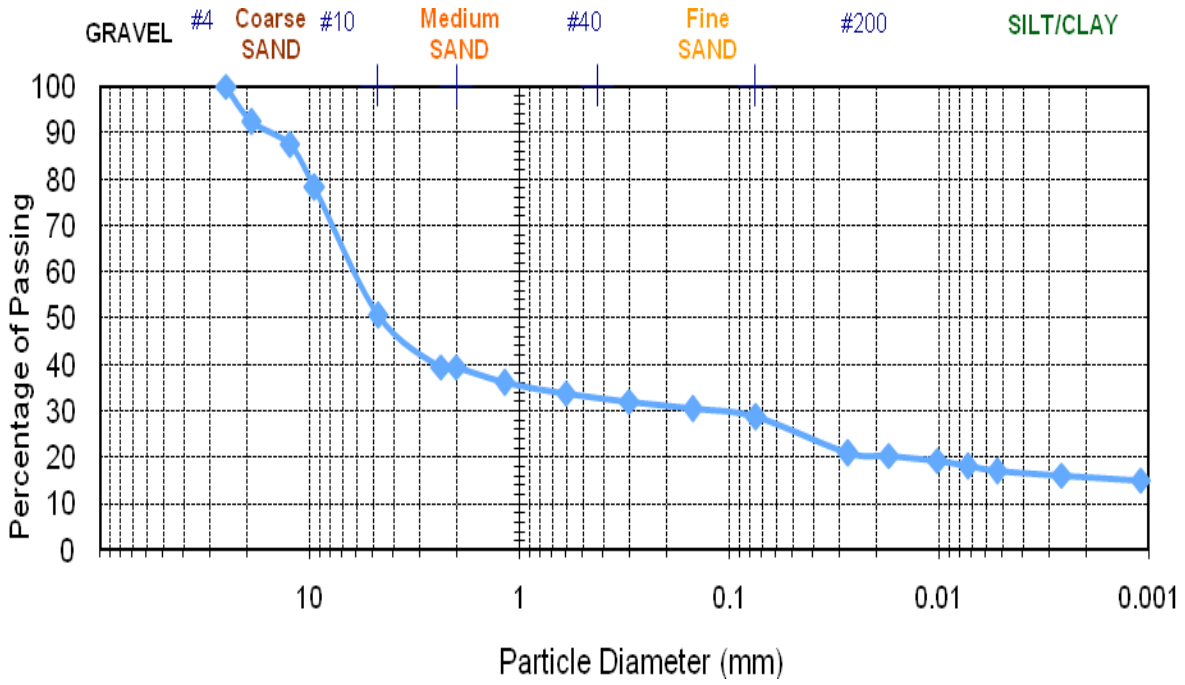

Figure 4.1: Particle Size Distribution Curve of Subgrade Material

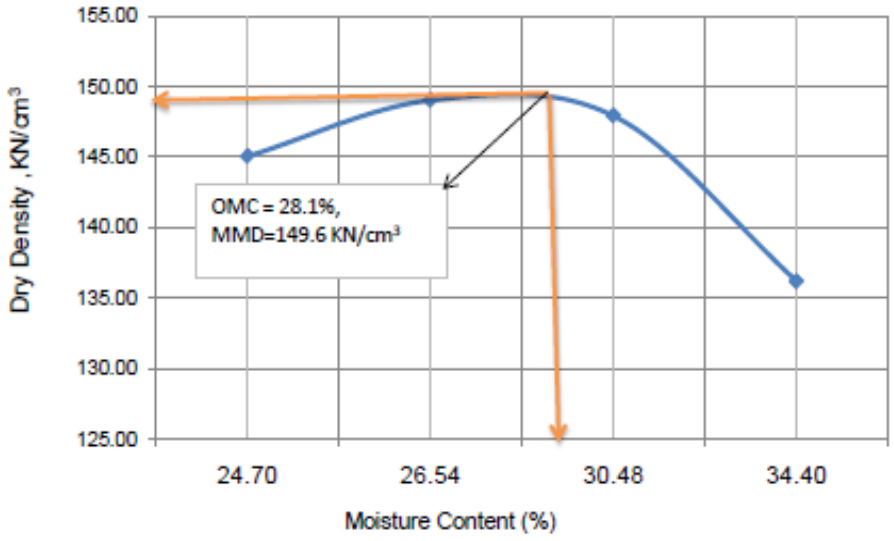

Figure 4.2: Optimum Moisture Content and Maximum Dry Density

4.2. Mechanical Test Results

4.2.1. Stiffness of the Material

Repeated load triaxial test was conducted for subgrade material in laboratory; mainly for subgrade material having minimum CBR value seven percent (15%) sampled from borrow pit. The triaxial tests were conducted at 100KPa, 200KPa and 300KPa cell confining stresses for three specimens prepared. These cell confining stresses were used to pressurize water in triaxial cell. This water was used as cell stress when pressurized by air. These stresses and strains were calculated from test results obtained in laboratory as presented in table A-6, A-7 and A-8. These measured stresses and strains from test results were represented in figure 4.3 for samples conducted at different cell confining pressures. These specimens were failed at their maximum deviator stress. These shown that deviator stress on specimen increased as cell confining pressure of increased. Basically, as cell confining pressure increased the modulus of elasticity of materials also increased, meaning cell confining pressure directly proportional to stiffness of materials as shown in table 4.3. As the magnitude of load level increased the modulus elasticity also increased upto ultimate stage and reverse to decrease its stiffness until it get to fail. This shown that material had supported the stresses lower than the maximum stress. Additionally, three specimens were tested at same optimum moisture content and MDD to support stresses imposed on it. But, these specimens were failed at different stress level in laboratory. This was to show that total stress and stiffness of the materials were directly proportion to each other. The diagram 4.4 has used to represent the stiffness and strain of material. The modulus of elasticity of given material had a linear slope at the first straining stage of specimen or stresses and strains were proportional to each other. And this stiffness used as inputs of layered elastic model.

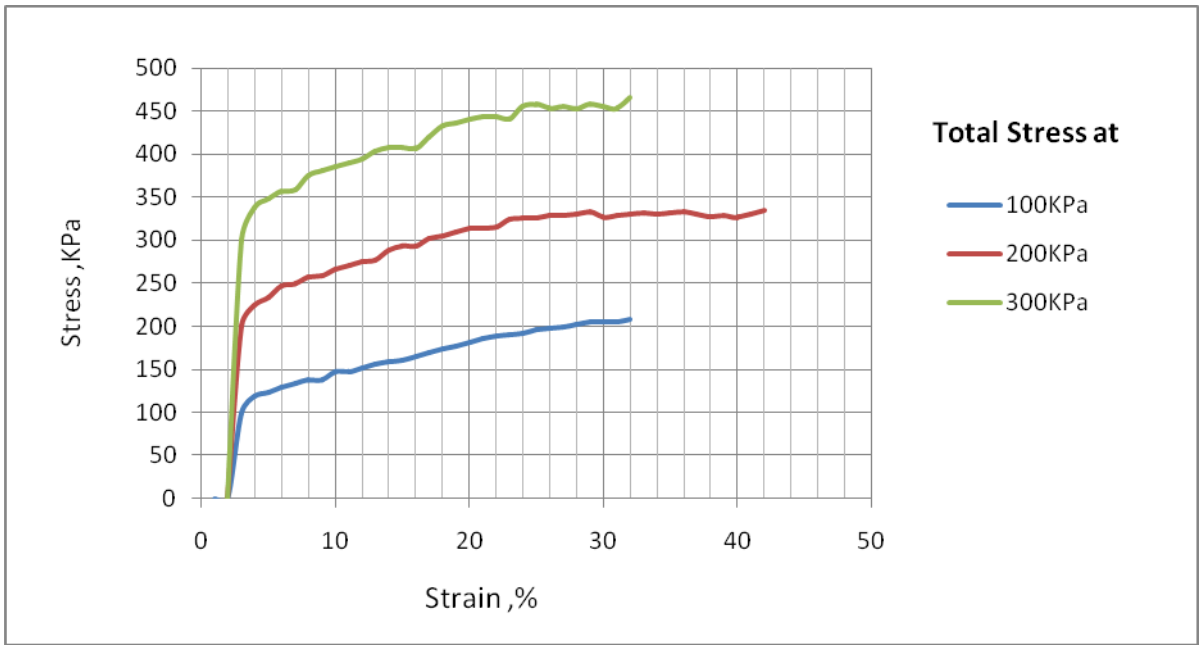

Figure 4.3: Stress-Strain Curve of specimens in different cell stresses

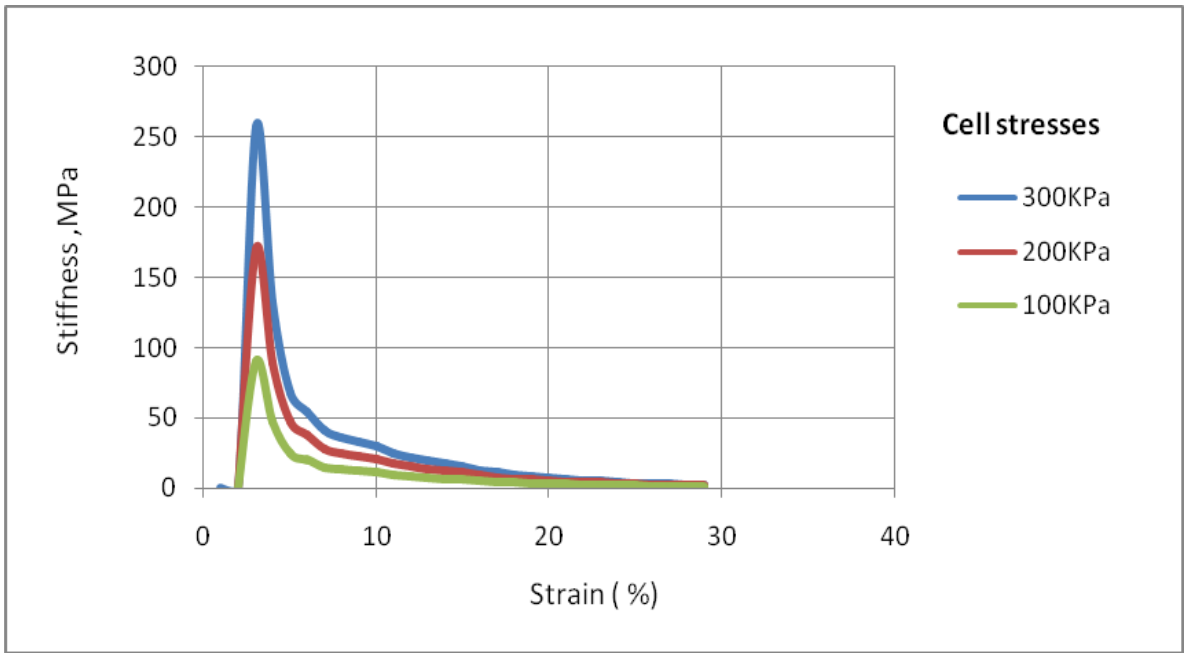

Figure 4.4: Stiffness of the Material

Summarized Test Results of Subgrade Material

No.	Specimen Deformation = ΔL(mm) (3)	Vertical strain ε = ΔL/Lo	Axial load (p),N	Cell Confining Pressure (σ_3),Kpa	Deviator Stress (σ_d),Kpa	Total Stress (σ_1) ,Kpa	P ($\sigma_1+\sigma_3$)/2	q ($\sigma_1 - \sigma_3$)/2	Stiffness (Kpa)
Test 1	15.00	0.1974	15	100	107	207	154	54	544
Test 2	25.00	0.3289	23	200	135	335	267	67	409
Test 3	16.00	0.2105	24	300	166	466	383	83	788

Table 4.1: Summarized Test Results of Subgrade Material.

4.2.2. Shear Strength

Shear strength calculated from test results of subgrade pavement material at laboratory as shown in appendices section table A-6, A-7 and A-8. Summarized test results of subgrade material represented in table 4.1. These summarized results represent maximum strains and stresses at samples failed. These measured shear strength represented by stress path in figure 4.5 and A-1 for three specimen of different cell confining pressure at 100KPa, 200KPa and 300KPa conducted in triaxial test. And these diagrams and tables also used to represent shear angle and cohesive property of material and state of stresses. The cohesive and internal friction angle of this material calculated using stress path equation represented appendix E. In applying this equation in table A-9 shear angle and cohesive property of this material determined as represented in table A-9. Angle of internal friction and cohesive determined used to increase shear strength of subgrade material as indicated figure 4.5 and A-1. Shear strength of this material determine in equation indicated in table A-9. This material shear strength increased as normal stress increases as indicate in figure 4.5. In this research, the Mohr coulomb failure criterion used to determine maximum shear strength and stress that this material can withstand without failure under normal stress. This to show that increasing the normal stress of material can increase shear strength of required subgrade material. Material under this research failed at its maximum shear strength equal to its shear stress.

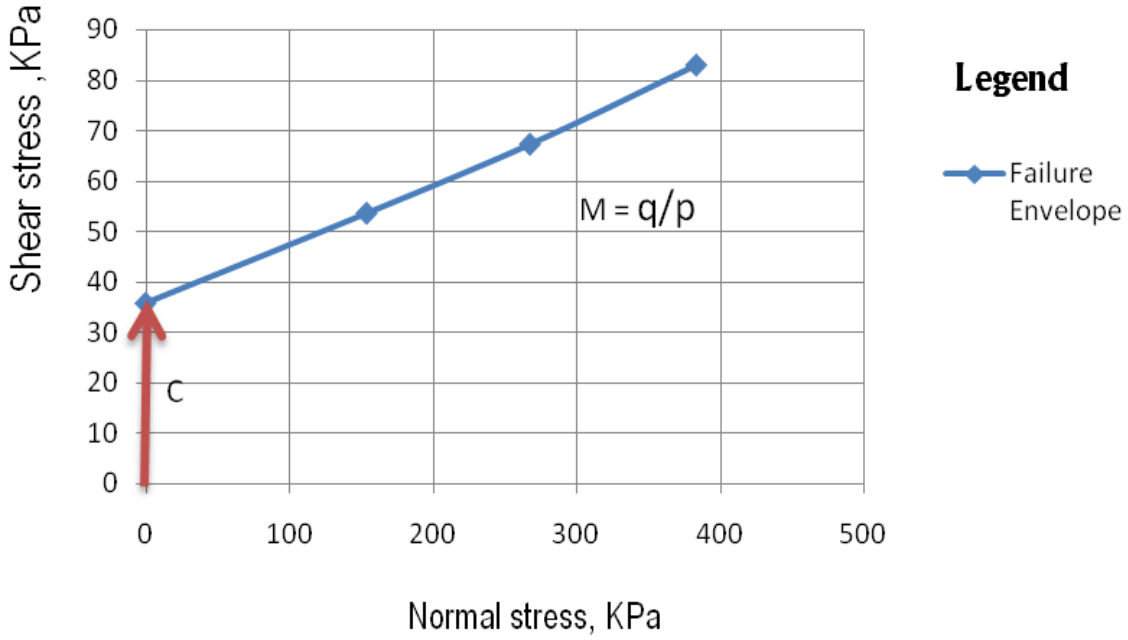

Figure 4.5: Triaxial test results represented on Stress Path Curve.

5.3.3 Specimen Strain Character

The strains were calculated from the test results of subgrade pavement materials in laboratory as indicated in table A-8. These measured strains from the test results were represented graphically in figure 4.6 for a sample of maximum cell confining pressure or 300KPa conducted by triaxial test; this diagram was used to represent the response of a specimen during loading. When the specimen loaded the change in length was taken place. As the magnitude of deviator stress increases the change in length of the material was increased. This was shown that as the magnitude of load increased the straining character of the materials also increased. The Poisson's ratio of the subgrade material obtained from the laboratory test at the three cell stresses of 100KPa, 200KPa and 300KPa were 0.35 and 0.44 as determined in table 4.3.

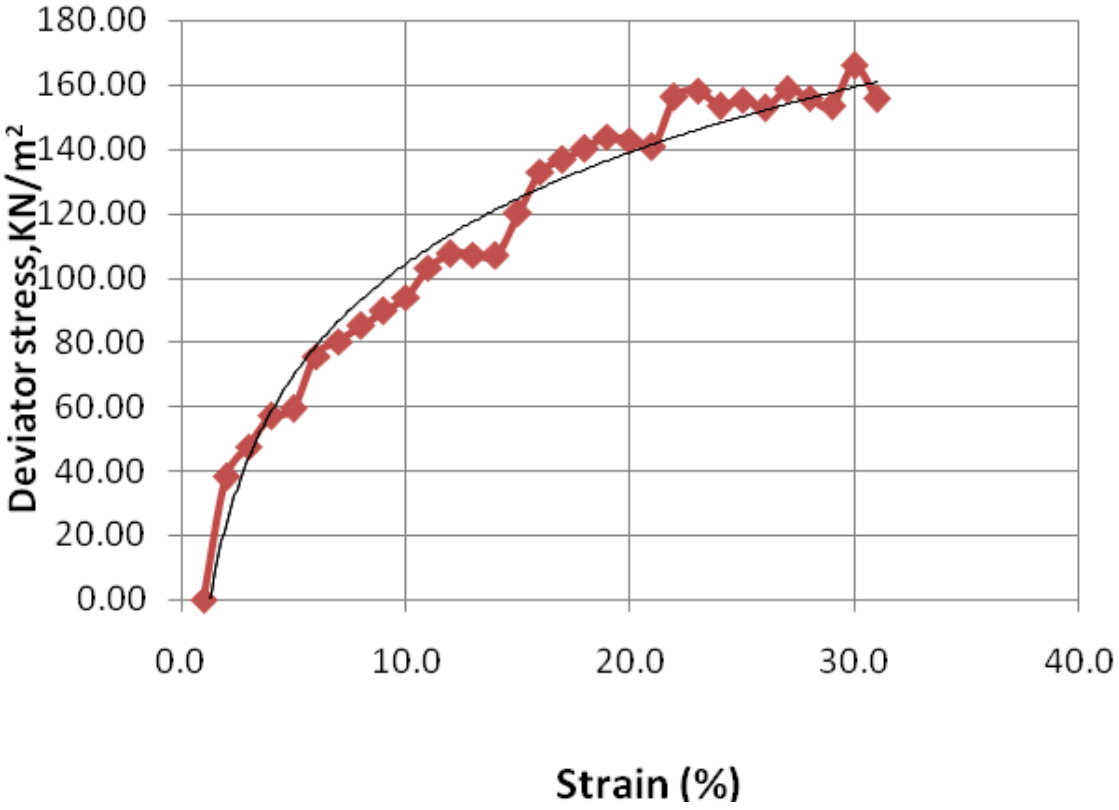

Figure 4.6: Stress - Strain Curve shown straining character of the Material

4.3. Pavement Responses Modeling

4.3.1. Pavement Model Inputs

The following input parameters required to explore responses of unbound pavement material to stress;

1. Unbound subgrade materials considered as anisotropic in Layer Elastic Model that have different properties when measured in different direction. Consequently, anisotropic property required for this research. Subgrade materials cross-anisotropic parameters namely vertical modulus, horizontal modulus and Poisson's ratio, and shear force determined in equations (14), (15) and (16) as indicated in table 3.2. Young modulus of subgrade material obtained from the laboratory was determined using in equation (12) represented in table 3.1 and calculated in table A-6. Subsequently, CBR value correlation required for determination of stiffness of wearing course and subgrade soil using equation (15) in table 3.2. Accordingly, three CBR values used for determination of input parameters to explore responses of unbound pavement material in layered elastic system described as pursued.

    a) Subgrade soils having an average CBR value 4% was required along route of project as shown in table A-9.
    b) Minimum an average CBR value 15% of subgrade material used along route of project as shown in table A-10.
    c) Minimum an average CBR value 30% of pavement material used along route of project as shown in table C-2.

    Based on the above three parameters, the vertical stiffness of pavement materials correlated using equation (15) as shown in table 3.2.

$$E = 17.6[CBR(\%)]^{0.64} \quad (15)$$

CBR = 4%, E= $17.6(4)^{0.64}$ = 40MPa

CBR=15%, E= $17.6(15)^{0.64}$ = 100MPa

CBR =30%, E= $17.6(30)^{0.64}$ = 150M Pa

Input parameters, namely vertical moduli, horizontal moduli and ,poisson's ratio and shear force required for modeling of unbound pavement material. The models used to determine these input parameters of unbound pavement materials had shown in table 3.2 of this research. Subsequently,these input parameters calculated as pursued and summarized in table 4.3.

a) Input parameters of wearing course calculated using equations (16),(17) and (18)

$$E_h = \frac{Ev}{2} \quad (16)$$

Ev = 2Eh, Ev =150MPa,

Eh = 150/2= 75MPa

Vh=Vv= 0.35,taken from Austroads 2004 (17)

F= Ev/(1+v) = 150/(1.35)= 111MPa (18)

b) Input parameters for subgrade material determined at laboratory

Ev = 2Eh, Ev =100MPa,

Eh = 100/2= 50MPa

Vh=Vv= 0.45 , determined at laboratory as shown table in 4.3

F= Ev/(1+v) = 100/(1.45)= 69MPa (18)

c) Input parameters for subgrade soil

Ev = 2Eh, Ev = 40MPa,

Eh = 40/2= 20MPa

Vh=Vv= 0.45,taken from Austroads 2004

F= Ev/(1+v) = 40/(1.45)= 28MPa

2. Responses of the pavement are analyzed in layered elastic model, namely the computer program CIRCLY 5.1 edition.
3. Standard axle loading consists of a dual-wheeled single axle, applying a load of 80KN considered on this gravel pavement as indicated figure C-4.
4. Standard Axle loading is represented by four uniformly-loaded circular areas of equal area separated by centre-to-centre distances of 330 mm, 1470 mm, and 330 mm respectively used as illustrated in figure 4.9 and C-4.
5. The contact stress is assumed to be uniform over the wheel contact area and, for this study 750 KPa required for inputs of CIRLY. The contact stress is related to the tyre pressure which is assumed to be in the range 500KPa – 1000KPa for highway traffic (Austroads, 2004).

The Poisson's ratio of unbound pavement material used for this research had determined at the laboratory. The following procedures utilized to characterize vertical and horizontal dimensional change of the samples. Initially, measuring and recording the vertical and horizontal sizes of samples before triaxial test had conducted in different cell confining stresses. After triaxial test had conducted, vertical and horizontal sizes of the samples measured in measuring devices at laboratory. From these characterizations, the change in vertical and horizontal dimensions of the sample determined. This characterization of sample was significant to attain lateral and vertical strains. The Poisson's ratio of the sample estimated from lateral strain to vertical strain of the samples using equation (7), (8) and (9) as indicated in table 3.1. Different Poisson's ratio; 0.35, 0.44 and 0.50 obtained at 100KPa, 200KPa and 300KPa of cell confining stresses respectively, though, average of three was 0.45 as represented in table 4.2 and it required for input parameter of CIRCLY.

Poisson's Ratio determination at the laboratory			
Cell stress at 100KPa	Vertical strain	Original height(H_o),mm	76
		Chang height, mm	20
		Vertical strain (ε_V)	0.26
	Horizontal strain	Original Diameter(D_o),mm	38
		Total length, mm	41.5
		Chang length, mm	3.5
		Lateral strain(ε_L)	0.09
	Poisson's Ratio=$\varepsilon_L/\varepsilon_V$		0.35
Cell stress at 200KPa	Vertical strain	Original height(Ho),mm	76
		Chang height, mm	26
		Vertical strain (ε_V)	0.34
	Horizontal strain	Original Diameter(D_o),mm	38
		Total length, mm	43.7
		Chang length, mm	5.7
		Lateral strain(ε_L)	0.15
	Poisson's Ratio=$\varepsilon_L/\varepsilon_V$		0.44

Table 4-2: Subgrade Material Poisson's Ratio determination at laboratory

Figure 4.7: Pavement Model for Mechanistic Design Method of Gravel Road

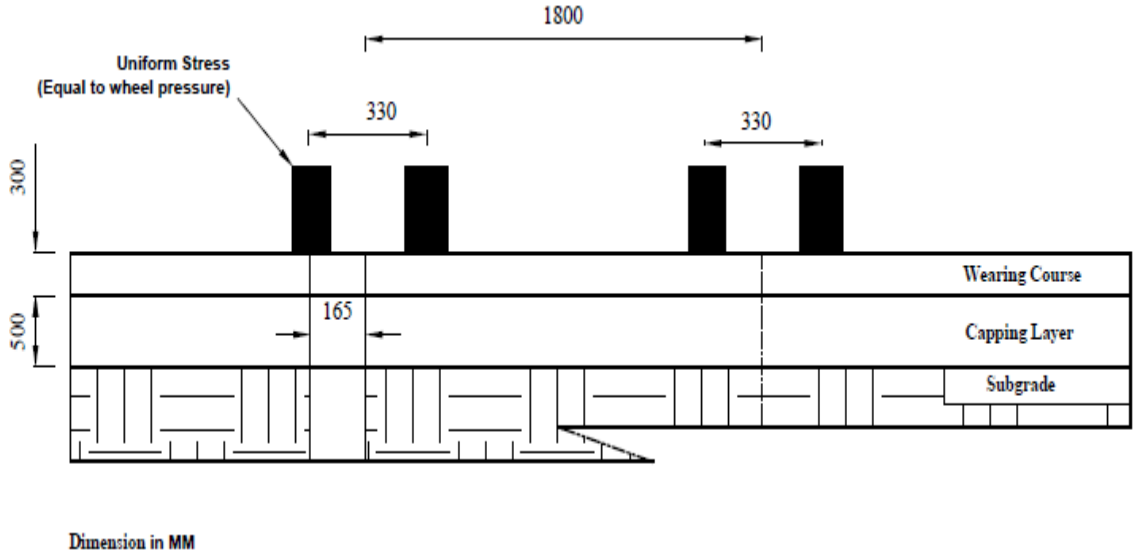

Table 4.3: Summarized Input Parameters for Layered Elastic Model

Layers	Input Parameters	Value
Wearing Course	Vertical stiffness (MPa)	150
	Horizontal stiffness (MPa)	75
	Poisson's Ratio	0.35
	Shear stress (MPa)	111
Subgrade Layers	Vertical stiffness (MPa)	100
	Horizontal stiffness (MPa)	50
	Poisson's Ratio	0.45
	Shear stress (MPa)	69
Subgrade Soil	Vertical stiffness (Map)	40
	Horizontal stiffness (MPa)	20
	Poisson's Ratio	0.45
	Shear stress (MPa)	28

4.3.2. Pavement Responses

CIRCLY was used for this research to model the response of unbound pavement material to stress. CIRCLY uses inputs features to model these responses. These input parameters were described in detail in pavement model inputs section. Then, these parameters used for layered elastic model to analysis the critical responses of this pavement. The deflections, strains and stresses of pavement layers as well as damage of pavement structures were critical responses explored under this research.

In this research, the main purpose of pavement responses analysis is to determine stress, strain and deformation of pavement structures due to applied loads. These applied repeated loads were taken as a cause of compression and tension in layers of pavement. This compression at upper and tension at lower of pavement layers brought up change in depth in pavement structure. This change in depth is considered as deflection of layers as analyzed from the model output. The Maximum vertical deflection of this pavement layer during loading time was found at center of wheel contact area as shown in figures 4.8. The deflection of pavement layers was increased from outer to center of wheel contact area as indicate in figure 4.8b. Deflection of pavement surface reduced away from wheel contact area in both vertical and horizontal directions as represented in this figures.

In analysis of pavement responses to stress, the vehicular movements on pavement surface would be always expected in order to form various values of compression and tension strain in pavement layers depending on locations of load intensities. In short, the compressive strain was found at the top of unbound pavement and subgrade layers with different value of load intensity based on distance from wheel contact area on pavement surface. The load intensity at wheel contact area is not the same as to some distance from the wheel contact area. High load intensity was found at center of wheel contact area. This to show that critical strain obtained in subgrade pavement layers are diminished in distance away from vehicular wheel contact area in pavement layers in both horizontal and vertical directions as represented in figure 4.9b . As indicated in figure 4.9, the critical vertical strain during loading of the pavement was found at wheel contact area. Strains in pavement layers increased from outer to center of wheel contact area and the maximum value of critical strain obtained from this analysis was indicated in figure 4.9.

In addtion to normal strain, the shear strain of unbound pavement layers was analyzed under this study. The shear strain intensity location on the pavement surface was identified at two sides of wheel contact area,but not at center of wheel contact area as analyzed in layered elastic model and indicated in figure 4.10. As represented in figures 4.10 , the maximum shear strain of the pavement layer was found at the two sides of wheel contact area. The shear strain in pavement layers was increased from the outer and inner to two sides of the wheel contact area as indicate in figure 4.10 and the maximum value of shear strain represented in this figures. This maximum value of shear strain obtained from this analysis was 0.0022. This to show that critical shear strain responses obtained in subgrade pavement layers are diminished in distance away from center of two sides vehicular wheel contact area on pavement surface in both horizontal and vertical directions.

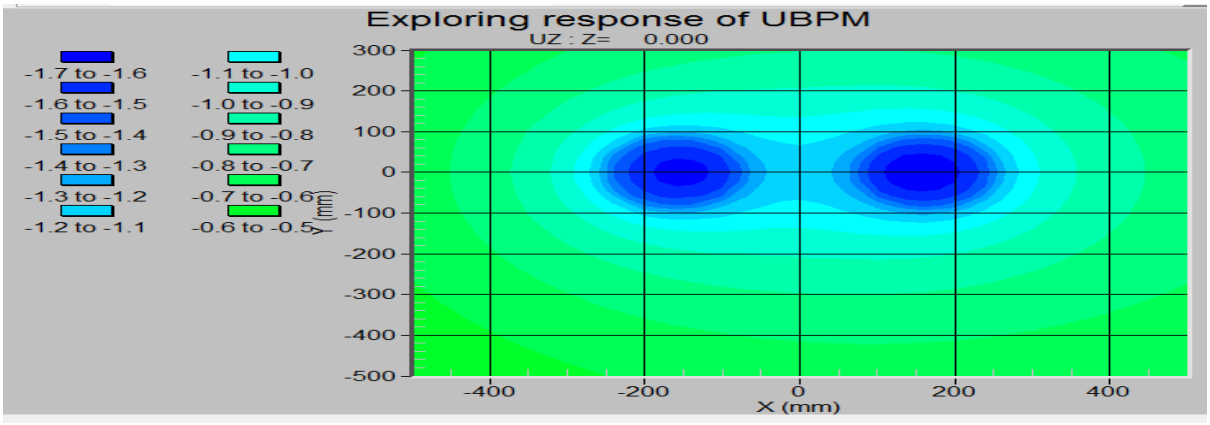

Figure 4.8(a): Deflection of pavement Layers in 2D

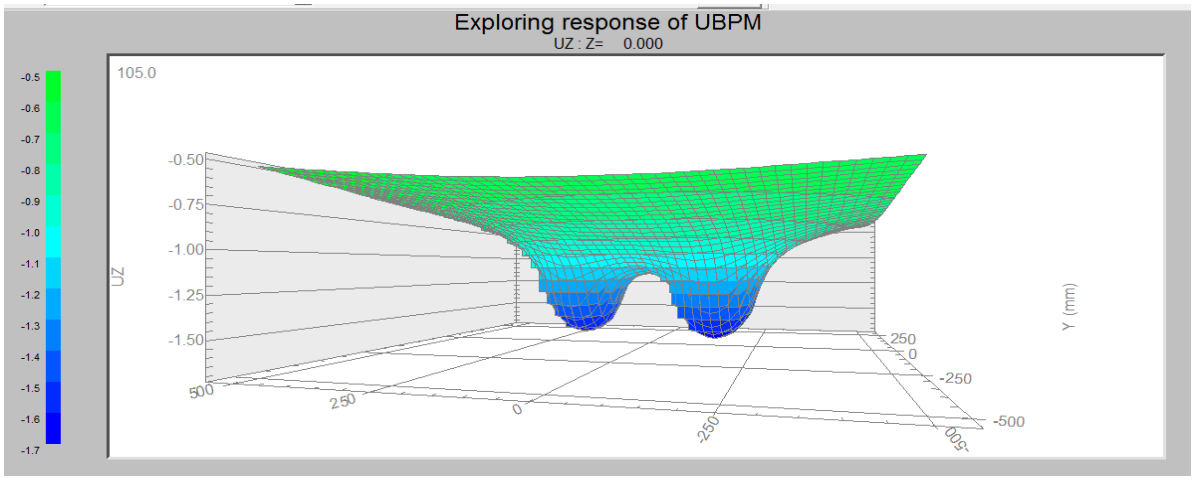

Figure 4.8(b): Deflection of pavement Layers in 2D.

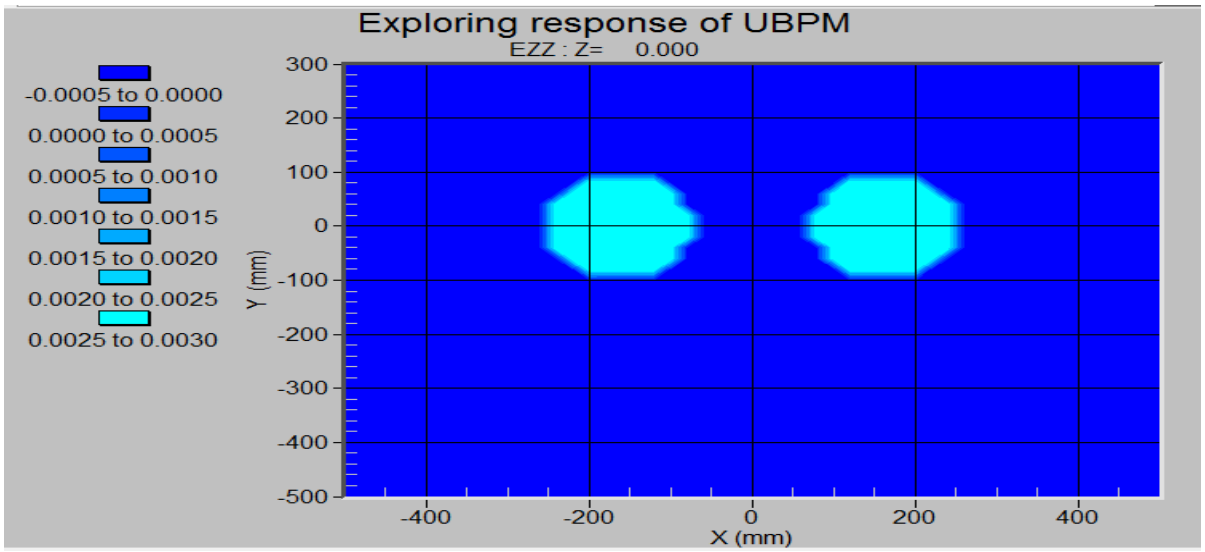

Figure 4.9(a): Strain in Pavement Layer in 2D.

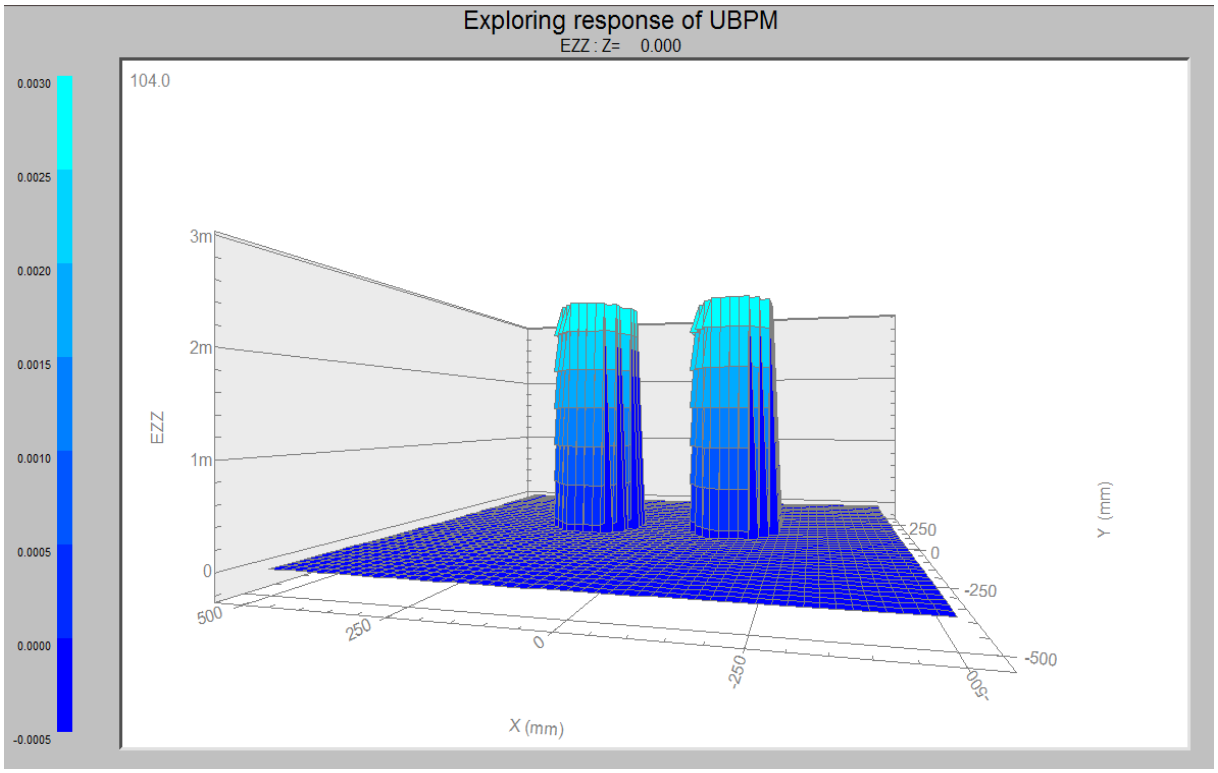

Figure 4.9(b): Strain in Pavement Layer in 3D

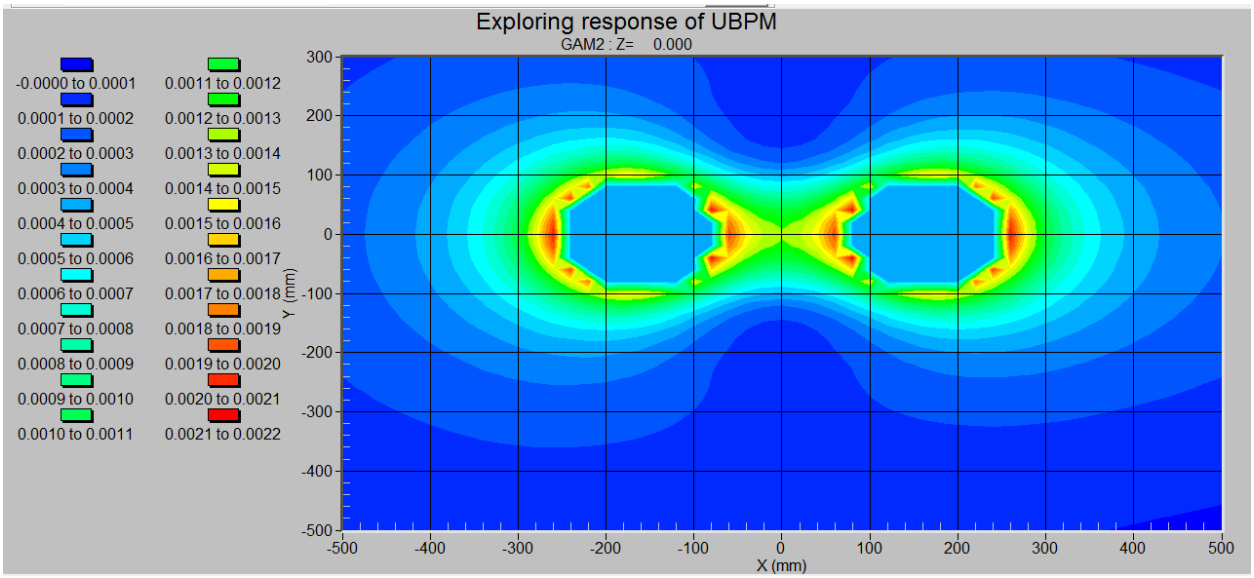

Figure 4.10(a): Shear Strain in Pavement Layer 2D

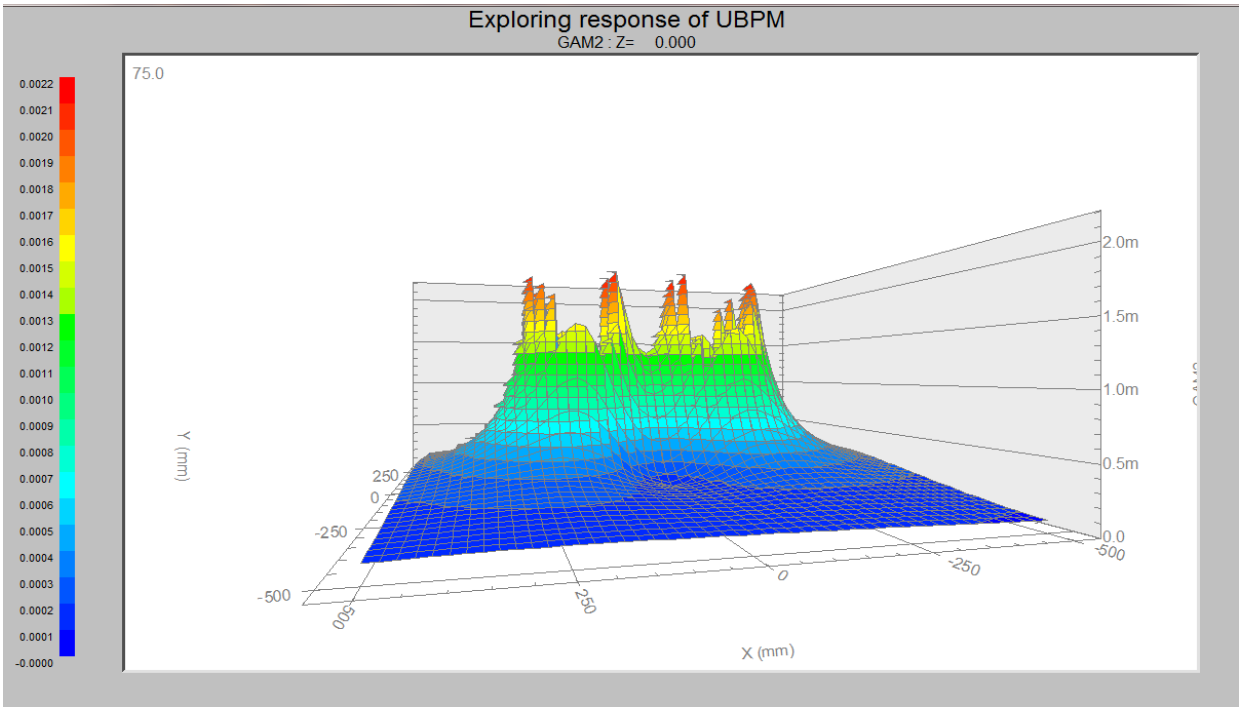

Figure 4.10(b): Shear Strain in Pavement Layer 3D

4.3.3. Stresses in Pavement Layers

There are two stresses acting in pavement layers; the compressive stress or contact stress or wheel stress which acts perpendicular to pavement surface and shearing stress which acts parallel to pavement layers. Standard axle loading used for layered elastic model to be represented in four uniformly loaded circluar area was acting perpendicular to pavement surface as described in model input parameters section. The stresses in pavement layers are formed from the vehicular axle load. This vehicular load on single axle distributed to dual wheeled and transferred to pavement surface at circular area. The load of vehicle per conatct area considered as stress transferred to pavement surface in different values based on the distance or radius from the center of wheel contact area. This stress intensity diminished or increased depend on the radius from the center of wheel load as represented in figures and tables generated from this model output. Bassicaly as represented in figure 4.11, the maximum contact stress was found at wheel contact area . The contact stress in the pavement layers was increased from outer to center of wheel contact area. And this contact stress are diminished in distance or radius away from vehicular wheel in pavement layers in both horizontal and vertical directions. The maximum value of vertical compressive stress at center of wheel contact area was 750KPa, but as it away some distance from this contact area the value of stress reduced. This is because of stress intensity depend on the distance or radus in both verical and horizotal direction as represented in figure 4.11 . This stress was equal to the wheel contact stress used as an input feature of CIRCLY.

In addtion to the vertical stress analyzed in this section, there was a hozizontal stress created along horizotal direction of pavement surface. This stress considered as shear stress moves along the direction of motion of vehicle in forward and backward based on vehicle wheel. This stress or shear stress intensity also depended on the distance or radius from wheel contact area. This stress reduced in distance away from the center of wheel contact area. Generally, as represented in figure 4.12, the maximum shear stress in pavement layer was located at vehicle wheel contact area. This shear stress in pavement layers was increased from outer to center of wheel contact area. The maximum value of shear stress obtained from this analysis was 160KPa, but as it away some distance from this center the value of stress reduced, this is because of stress intensity

depend on the distance or radus as indicated in figure 4.12. And this shear stress diminished in distance away from vehicular wheel contact area in both directions.

Third response of pavement analyzed under this research and model output was strain energy in pavement structure. The axle load of vehicle transferred to the pavement through wheel contact area. This load of vehicle per contact area considered as stress transferred to pavement surface in different values based on the distance or radius from the center of wheel contact area. This stress in pavement layer created deformation of pavement structure. The product of axle load and deformation of pavement layer formed strain energy in the pavement layers. In a short descrption, Strain Energy in the pavement was induced due to the axle load and deformation formed. The product of axle load or exteral applied load (stress multiplied by area) and deformation is the internal work done in pavement layers. This work was stored as deformation of internal elastic energy or strain energy. Entirely, as shown in figure 4.13, the maximum strain energy of vehicle wheel was found at wheel contact area. This strain energy in the pavement layers was increased from outer to center of wheel contact area and the maximum value of vertical strain energy is described in graph 4.13. And this strain energy diminished as stress diminished in distance away from vehicular wheel contact area in both horizontal and vertical directions. This strain energy in pavement layers was increased from outer to center of wheel contact area. The maximum value of strain energy obtained from this analysis was 0.0220, but as it away some distance from this center the value of strain energy reduced, this because of stress intensity depend on the distance or radius from wheel contact area.

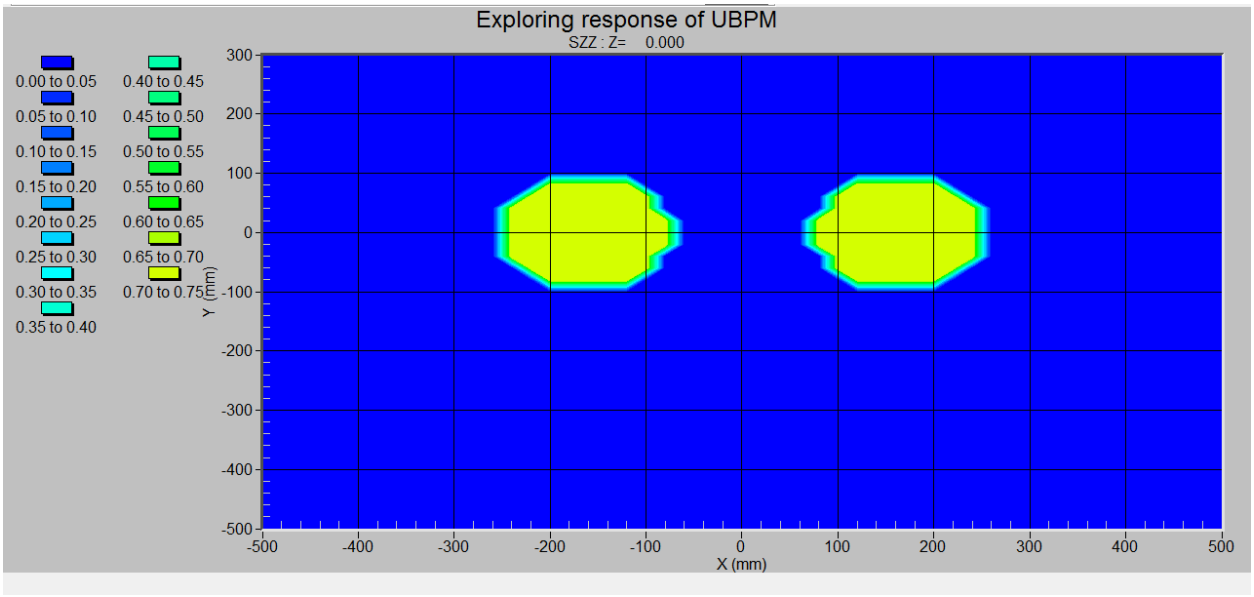

Figure 4.11(a): Stress in Pavement Layer 2D

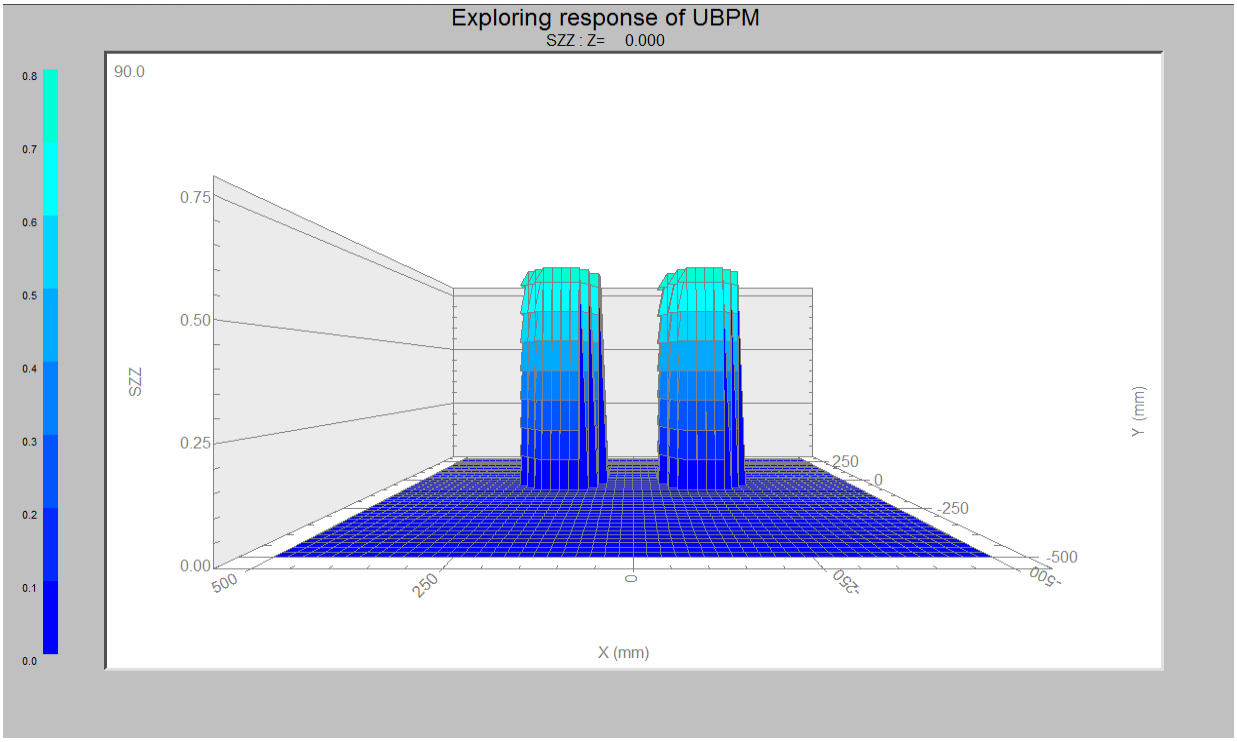

Figure 4.11(b): Stress in Pavement Layer 3D

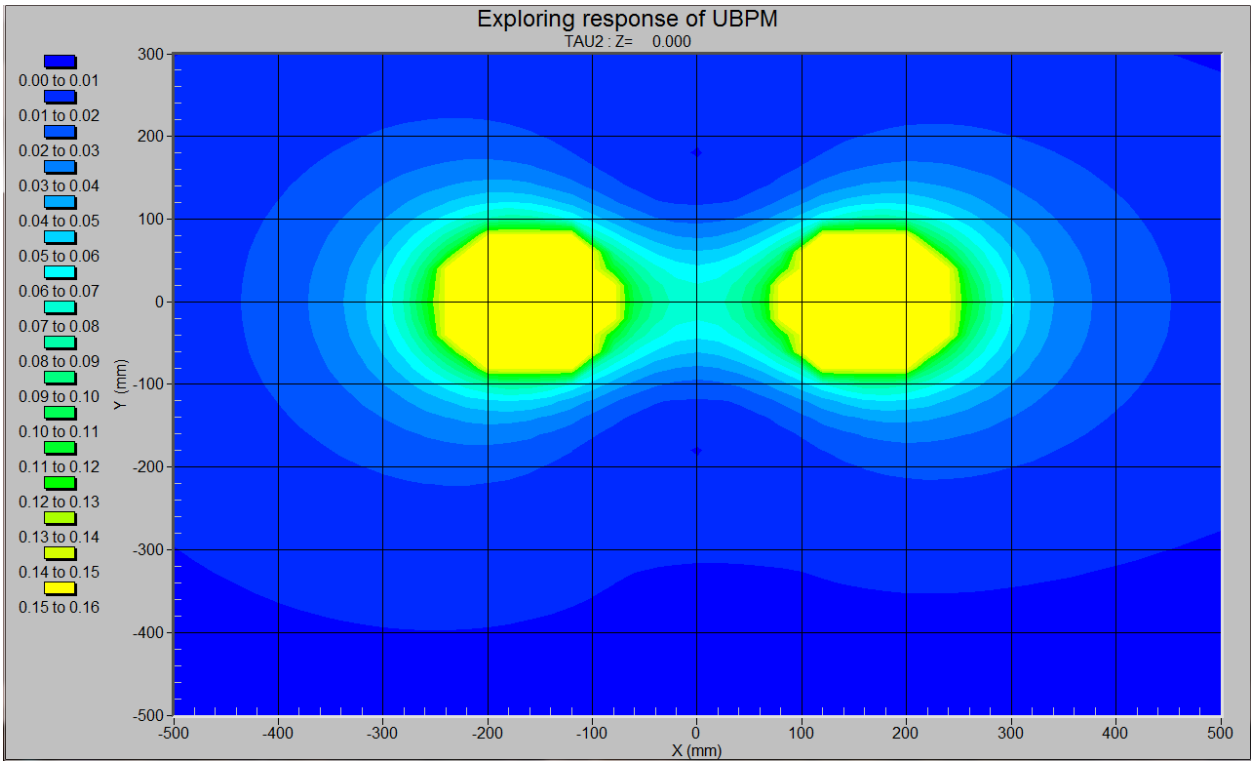

Figure 4.12(a): Shear Stress in Pavement Layer 3D

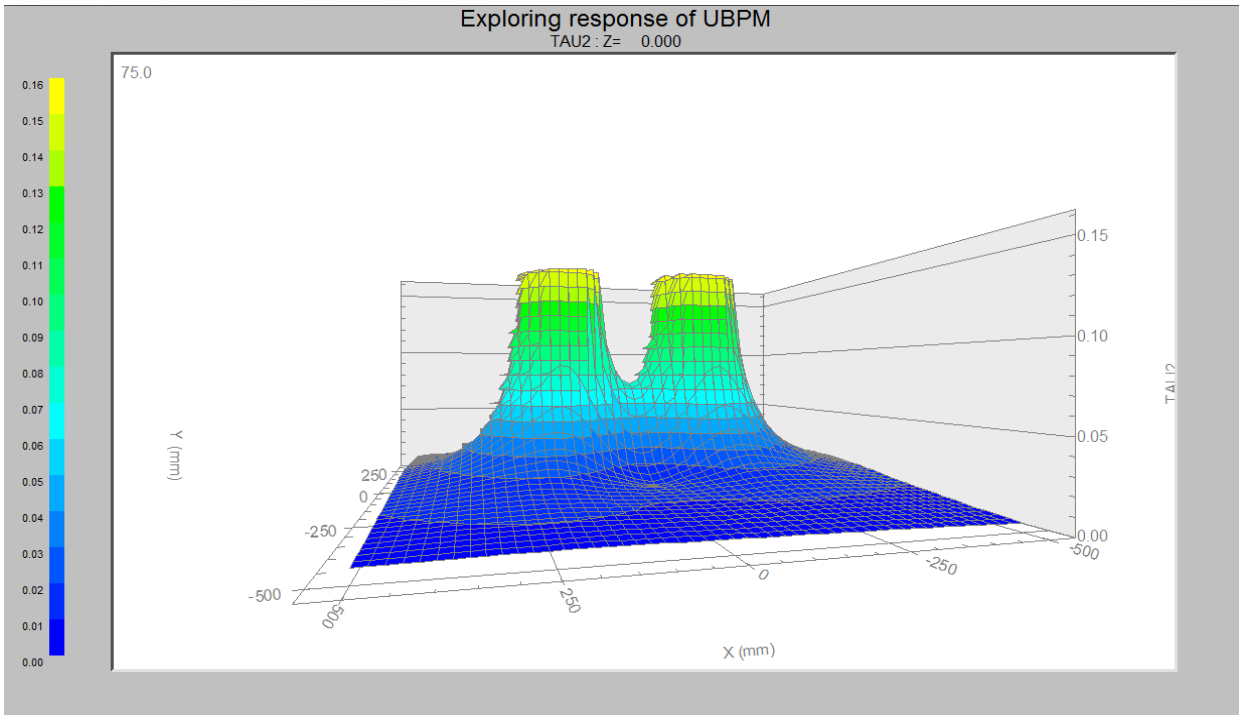

Figure 4.12(b): Shear Stress in Pavement Layer 3D

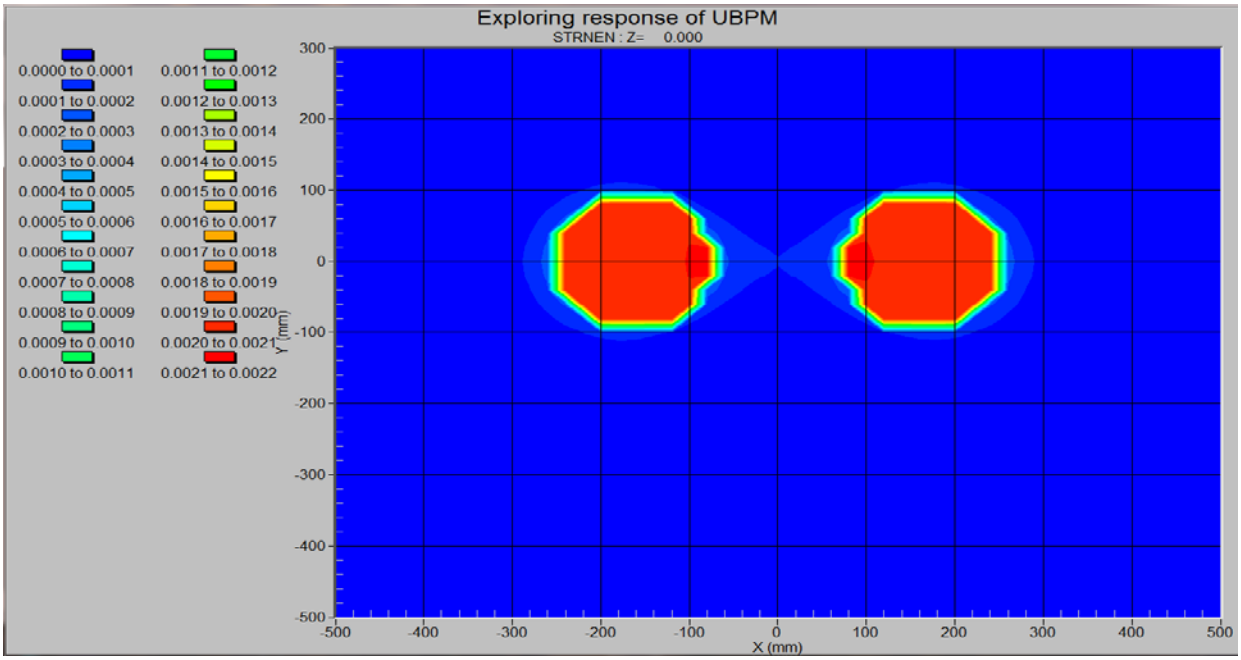

Figure 4.13(a): Strain Energy in Pavement Layer 2D

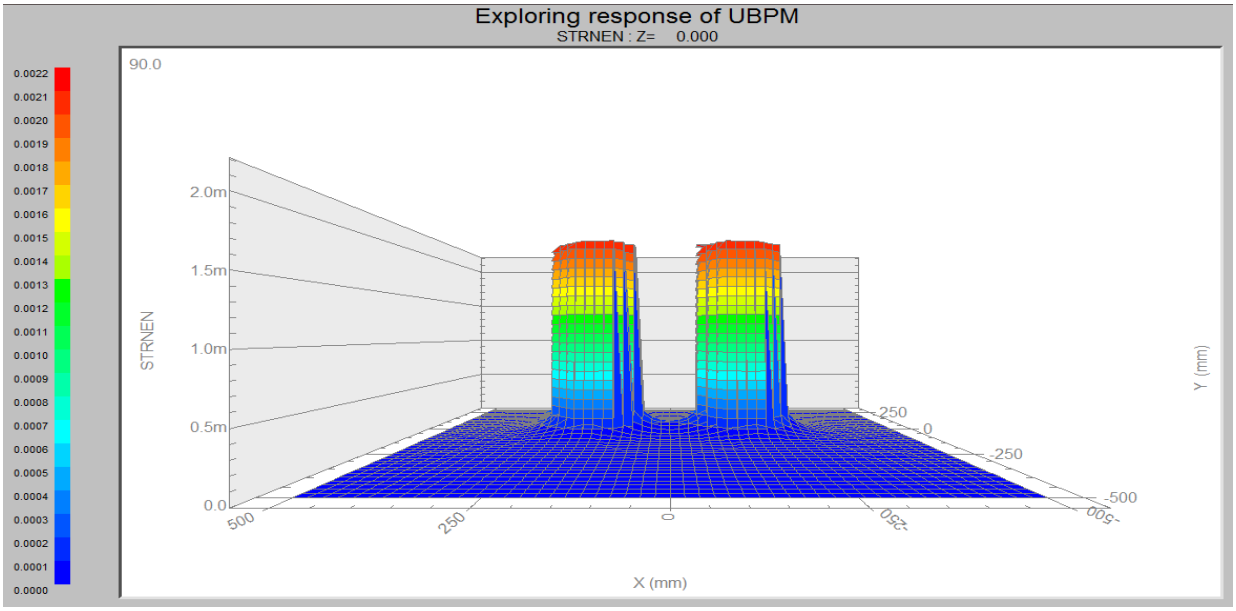

Figure 4.13(b): Strain Energy in Pavement Layer 3D

4.3.4. Pavement Deformations

In pavement design moving vehicular load on surface of pavement usually transferred through dual wheeled to subgrade soil at much wider area. This system usually needs a thick pavement layer in order to reduce intensity and distribute uniformly vehicular load at wider area on lower pavement layer to resist excessive deformation of subgrade soil. This deformation in mechanistic pavement design can be classified in two based on the condition of loading time. These deformations are recoverable and permanent. The recoverable deformation was directly related to the presence of moving load on pavement surface meaning as moving load present on pavement surface the deformation pavement taken place as moving load removed from the pavement the deformed layer certainly recovered, but the unrecovered part of the pavement due to this moving load is considered as permanent deformation. This is shown that some stress remained in material inform of residual stress. These two strains induced from traffic loading as represented in diagram 4.14(a), these strains are recoverable and permanent; the most strain induced is recoverable strain, but all vertical strain induced by contact stress is not recoverable after many load repetitions, the permanent strain accumulated at subgrade level and these permanent strain accumulation produce rutting in the pavement. This vertical compressive strain at the top of subgrade is taken as determinant for surface rutting in unbound portions of the pavement structure. The maximum recoverable strain from this diagram was 1.68 while the maximum non recoverable strain was 0.58 as indicated in figures generated from the model output. Entirely, as represented in graph 4.14(a), the maximum resilient strain during loading time wheel was found at center wheel contact area. This resilient strain on the pavement layers was increased from outer to center of wheel contact area and the maximum value of resilient strain was shown in this figure. And this resilient strain diminished in distance away from vehicular wheel contact area in loading time in both horizontal and vertical directions.

4.3.5. Pavement Damage

In mechanistic pavement design method the damaging factor of the pavement layers estimated based on repetition of standard axle load and vertical strain or permanent deformation. In empirical pavement design damaging factor of pavement layers was not predictable, but all damages of pavement layers under this study estimated in mechanistic pavement design method.

In this research damaging factor of this gravel pavement estimated in using the layered elastic model which used to represent damage in numerical and graphical. This model also required formulas to calculate damaging factor in equation represented in appendix E. Generally, layered elastic model used under this study estimated the cumulative damage factor of subgrade soil and subgrade layers of pavement. The output of this model represented in graphical in figure 4.14(b) and 4.14(c). The cumulative damage factor of subgrade soil layer under study was 0.0096 and the cumulative damage of subgrade material layer was 0.79. This value was obtained from the CIRCLY model output or from the equation (19) as indicated in table 3.2. The maximum of the two was taken as cumulative damage factor. Thus a cumulative damage factor of this pavement was 0.79 as shown in table 4.4.

Based on output layered elastic model, Austroads 2004 is presumed that the pavement have reached its design life when the cumulative damage reaches 1.0. If the cumulative damage is less than 1.0 the system has excess capacity and the cumulative damage represents the proportion of life consumed. If the cumulative damage is greater than 1.0 the system is predicted to 'fail' before all of the design traffic has been applied.

Therefore, the critical cumulative damage factor of this pavement under study was less than 1.0. This is shown that this pavement has excess capacity and the cumulative damage represents the proportion of this pavement life used by design traffic.

As represented in graph 4.14(b) and 4.14(c), the maximum critical cumulative damage factor of this pavement was found at center of wheel contact area. This critical cumulative damage factor on the pavement layers was increased from outer to center of wheel contact area and the maximum value of resilient strain was shown in this figure. And this critical cumulative damage factor diminished in distance away from vehicular wheel contact area in both horizontal and vertical directions.

Material	Vehicle Type	Damage Factor	Critical Strain	Maximum of total damage
Subgrade Pavement Materials =15	ESA750-Full	.79218E+00	0.10586E 02	0.79
Subgrade, CBR4, Anis	ESA750-Full	.96136E-02	0.56366E-03	9.61E-03

Table 4.4: Maximum damage values for each vehicle type of CIRCLY output

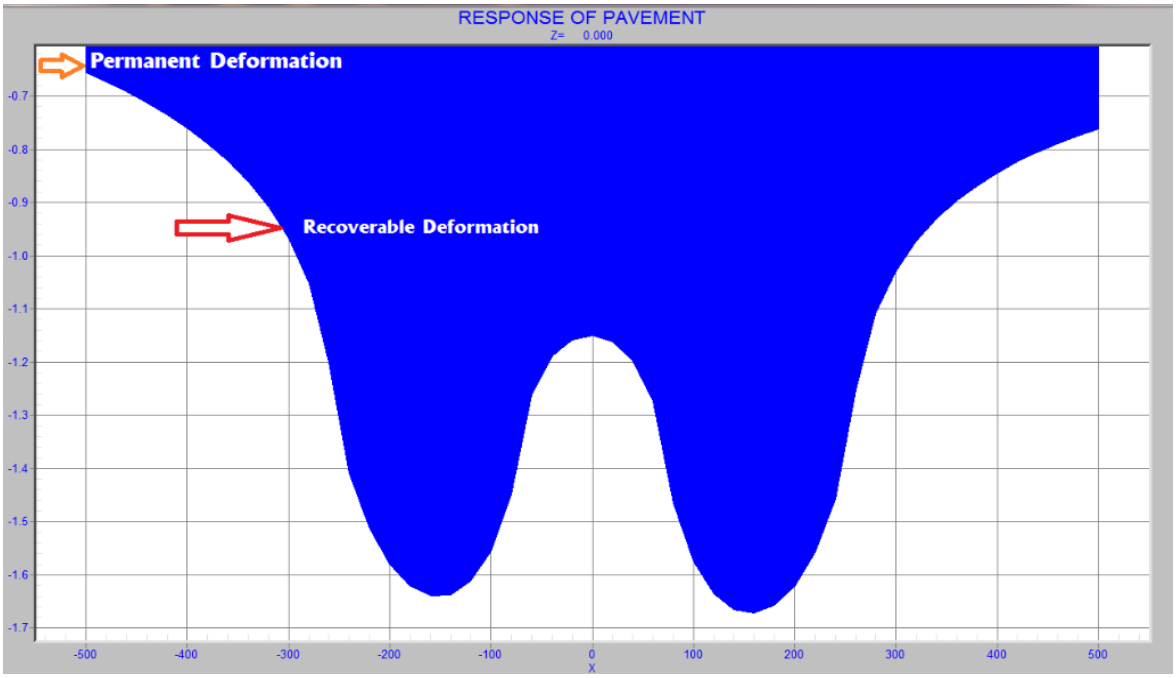

Figure 4.14(a): Recoverable and Permanent Strain of pavement

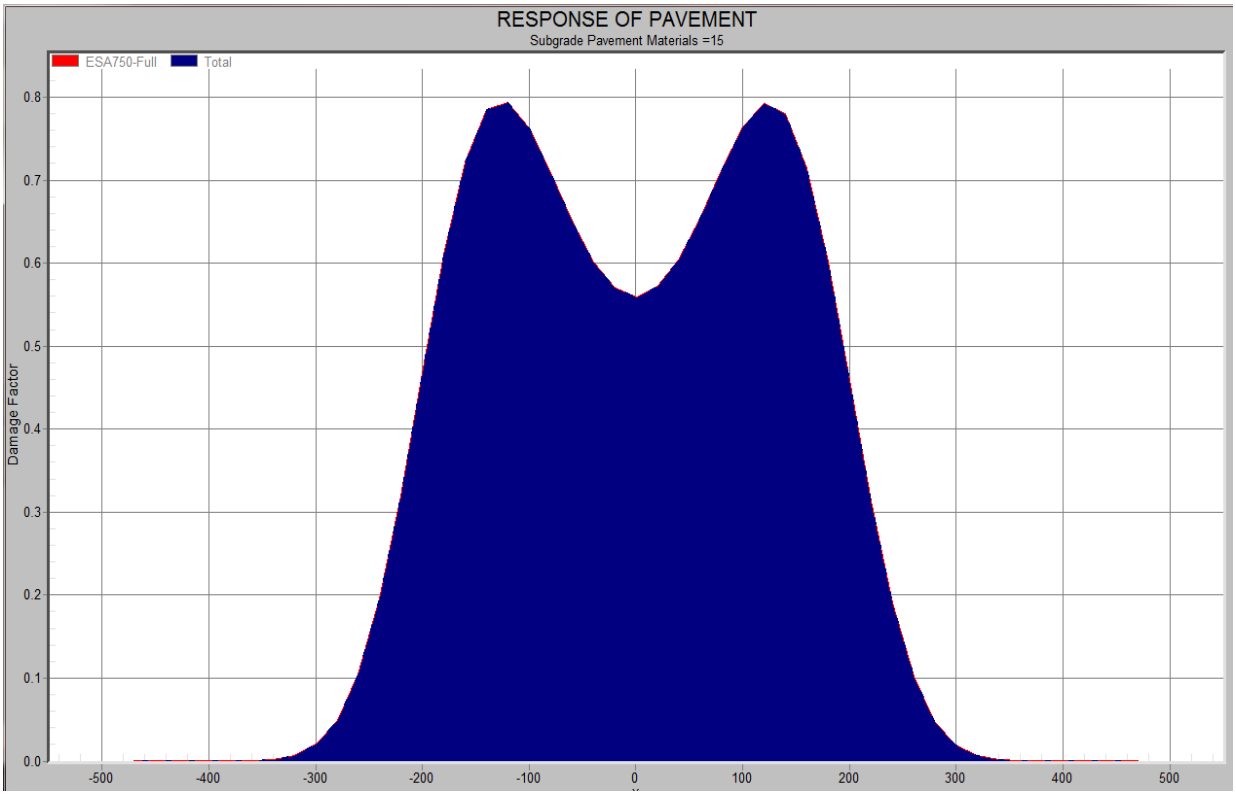

Figure 4.14(b): Cumulative Damage Factor of subgrade material

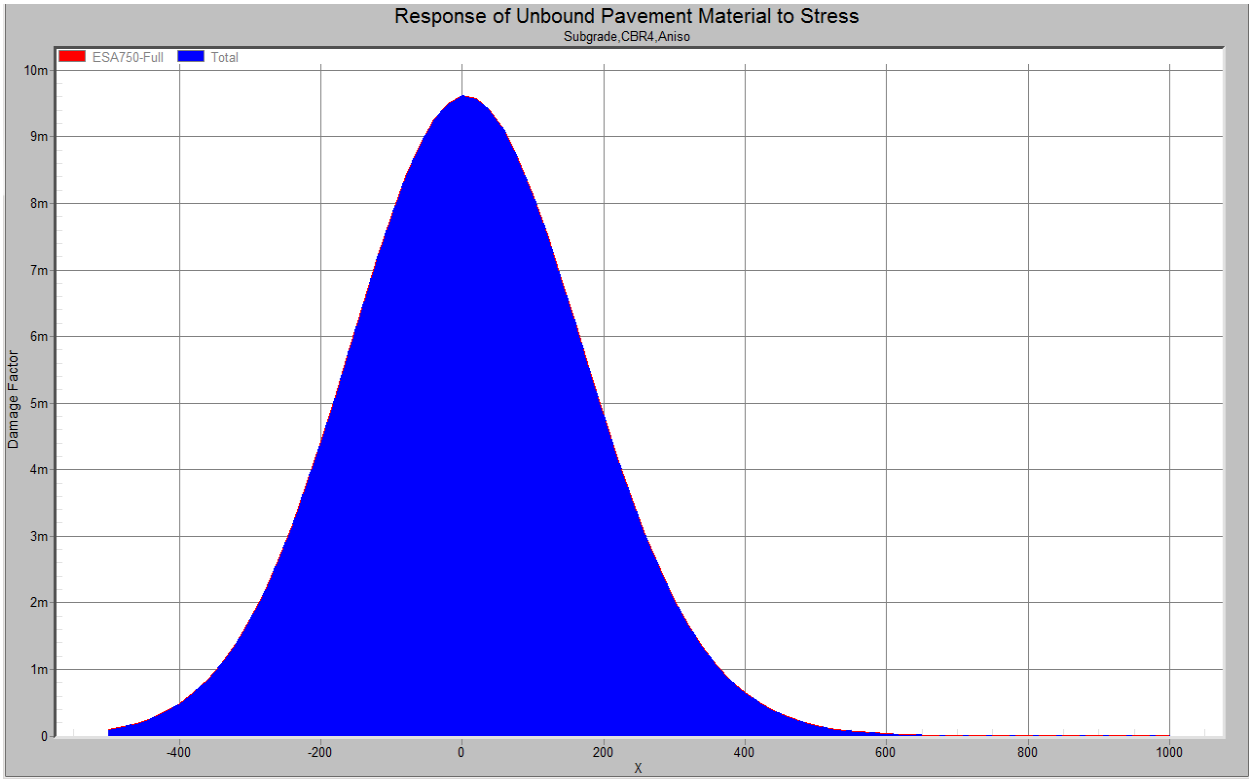

Figure 4.14(c): Cumulative Damage Factor of subgrade soil

In addition to determining the cumulative damage factor, the significance of determining different stresses and strains are used to;

1. Determine the critical stress and strain with their locations from these different stresses and strains during pavement design process.
2. Require different stiffness (deformation characteristics) of pavement materials for stability of various pavement structural systems for different stresses and strains condition in various directions.
3. Consider internal resistance for pavement structures to resist pavement failure and sliding along any section inside it.
4. Help to consider different stresses and strains as there are different pavement design factors for most reliable pavement design.

5. Conclusions and Recommendations

5.1. Conclusions

Unbound subgrade pavement materials with minimum CBR value greater than fifteen percent used to conduct this research. This material sampled in purposive sampling techniques from existing borrows pit located along the project rout. The size of sampled material determined in laboratory using AASHTO series of sieve size and materials passed 4.75mm and retained above 0.075mm sieve sizes used for triaxial sample preparation. Maximum dry density and optimum moisture content of this sample determined in proctor compaction method at laboratory. This triaxial sample has a size of 38 mm in diameter with a height of 76 mm prepared in laboratory to conduct Repeated Load Triaxial Test.

The sample prepared in laboratory was tested in triaxial equipment in applying vertical dynamic load and static confining stress through air in triaxial cell with load, pressure and vertical displacement measurement devices; namely ring and dial gauges. This material test result was used as input for layered elastic model. Layered elastic model used to explore unbound subgrade material responses to axle loadings. This layered elastic model works by integral transform method and calculate stress, strain and deflection in pavement layers.

Test results obtained at laboratory represented in tables and figures of this research. These laboratory results analyzed and discussed using stress stain relationships and stress path method. Stress strain relationship used to represent stiffness of material sampled at in-situ. Stress path method represented triaxial test result obtained at laboratory in graph. This stress path method used to connect points on Mohr circles to form failure envelope line. These points on Mohr circles illustrated maximum shear stresses and maximum shear strength of triaxial samples. Using these methods of analysis stiffness, shear and Poisson's ratio of the subgrade material determined for model inputs parameters.

CIRCLY, layered elastic model required to explore responses of unbound pavement material. This model utilized different inputs for simulation of pavement layer responses to axle load. The following input parameters used for CIRCLY; material properties, pavement layers, minimum CBR value of material in stiffness form and standard axle load, load distribution and contact stress. Material stiffness obtained at laboratory was used as input of this model. Consequently,

this research used minimum stiffness value of gravel wearing from standard for input of CIRCLY. Whereas, others input parameters of this software were used from Austroads mechanistic design standard. Furthermore, using this layered elastic model for simulation of pavement layers the following results obtained.

1. Maximum vertical deflection of pavement layer at loading time was found at wheel contact area and deflection of pavement layers increased from outer to center of wheel contact area, but it reduced away from wheel in both vertical and horizontal directions.
2. The critical strain responses obtained in subgrade pavement layers diminished in distance away from vehicular wheel in both horizontal and vertical directions. Critical vertical strain at loading time on pavement surface was found at wheel contact area. And strains in pavement layers increased from outer to center of wheel contact area.
3. Maximum shear strain of pavement layer was found at the two sides of wheel contact area. And shear strain in pavement layers was increased from outer and inner to two sides of wheel contact area.
4. Maximum contact stress was found at wheel contact area. And contact stress on pavement layers was increased from outer to center of wheel contact area, but this contact stress are diminished in distance away from vehicular wheel in pavement layers in both horizontal and vertical directions.
5. The maximum damages value of pavement layers was taken as critical cumulative damage. The maximum of the two was taken as critical cumulative damage. Thus critical cumulative damage of the pavement was 0.79. Hence, the cumulative damage factor of pavement was less than 1.0 .This shown that this pavement has excess capacity to sustain design traffic.

In this conclusion, layered elastic model explored responses of unbound pavement material to stress in form of pavement layers deflection, strain and shear and, predict pavement layers cumulative damages.

5.2. Recommendations

Based on conclusion of this research two attributes will be recommended for utilization and further research. ERA pavement design guide used throughout the country as pavement design stanadrd. This stanadrd needs response based pavement design method namely mechanistic pavement design guide that significant to analysis responses of pavement layers to stress. This response based pavement design method used softwares particularly layered elastic model and Discrete Element Modeling. As a result, this standard needs to embrace this numerical simulation models. Pavement layers damage estimation models will need to be recommended for this standard pavement design guide. Additionaly, the models input data for unbound pavement materials specially stiffness and shear test specification will need to be included in this pavement design guide.

For researchers, now a day mostly pavements designed in empirical way that could not determine pavement layers response to stress in numerical analysis. Mechanistic pavement design method used as an option to solve gaps of empirical pavement design. Responses of unbound pavement material to stress determined in three ways; namely, theoretical analysis, physical test and numerical simulation (Cundall and Strack, 1979a). These three parameters used to investigate response of granular materials with their own limitations; the theoretical analysis is used for analytical model based on uniform size granular materials but, it has gaps on loading path and particle shape. A physical test is time – consuming to determine contact forces, displacements and rotations. The numerical simulation method is the most powerful way of modeling behaviour of granular assemblies due to its flexibility in application of loading paths, granular shape, particle parameters and boundary condition as well as data acquisition at any stage of test.

In study of behavioral condition of granular material, discreteness of particles and force of transmission between particles at contact points make complex constitutive relationship of granular material. Additionally, the stress existing inside sample was difficult to measure in a traditional laboratory test. These behavioral constraints of granular material were determined through an alternative boundary condition. From these point of view, numerical simulation selectable to characterize response of unbound pavement material for this recommendation of future research , due to its flexibility in application of loading paths, granular shape, particle parameters and boundary condition as well as data acquisition at any stage of test in Discrete

Element Modeling detail description found at appendix section of this research. Consequently, Response of unbound subbase and base pavement material to stress in Discrete Element Modeling recommeded for future research .

6. References

1. Aaron Austin (2009), Fundamental Characterization of Unbound Base Course Materials under Cyclic Loading (Thesis), B.S., Louisiana Tech University
2. Alemgena Alene Araya (2010), Characterization of Unbound Granular Materials for Pavements, thesis, Transport and Road Engineering, IHE/TUDelft, the Netherlands
3. Anthony Sebastian Cabrera (2012), Evaluation of the Laboratory Resilient Modulus Test Using a Fine-Grained New Mexico Subgrade Soil (Thesis), Civil Engineering Department, the University of New Mexico Albuquerque, New Mexico
4. Anuroopa Kancherla (2007) ,Resilient Modulus and Permanent Deformation Testing of Unbound Granular Materials (thesis), Civil Engineering Department, Texas A&M University ,USA.
5. Arnold, G. K.(2004), Rutting of granular pavements, Ph.D. dissertation, School of Civil Engineering, the University of Nottingham, the United Kingdom.
6. Austroads (2004), Pavement design – a guide to the structural design of road pavements, APG17/ 04, Austroads, Sydney, NSW
7. Austroads (2008a), Guide to Pavement Technology - Part 2: Pavement Structural Design AGPT02/08, Austroads, Sydney, NSW
8. Austroads (2008b), Technical Basis of Austroads Guide to Pavement Technology - Part 2: Pavement Structural Design. Austroads Publication No. AP-T98/08
9. Barksdale, R.D. and, J.L. Alba (1993), Laboratory. Determination of Resilient Modulus for Flexible Pavement Design," Interim Report No. 2 for NCHRP, Transportation Research Board (TRB), NRC, Washington, D.C.
10. Barry R. Christopher and Charles Schwartz (2006), Geotechnical Aspects of Pavements, U.S. Department of Transportation, Federal Highway Administration, Publication No. FHWA NHI-05-037,
11. Belt J, Ryynänen T, Ehrola E (1997), Mechanical properties of unbound base course. Proceedings of the 8th International Conference on Asphalt Pavements, Seattle, Vol.
12. Bereket Yohannes, Kimberly Hill, and Lev Khazanovich (2009), Mechanistic Modeling of Unbound Granular Materials, Department of Civil Engineering University of Minnesota and Minnesota Department of Transportation, Minneapolis, USA .

13. Braja M. Das (2002), Soil Mechanics Laboratory Manual, Sixth Edition, College of Engineering and Computer Science California State University, Sacramento, USA.
14. BRAJA M. DAS (2006), Principle of Geotechnical Engineering, Fifth Edition, Californian State University, Sacramento, USA.
15. Brown, S. F. and Chan, F.W. K. (1996). Reduced rutting in unbound granular pavement layers through improved grading design. Proceedings of the ICE-Transport, 117(1):40–49.
16. CEM KARAGÖZ(2004), Analysis of Flexible Pavements Incorporating Nonlinear Resilient Behavior of Unbound Granular Layers, Middle East Technical University,
17. Charles W. Schwar Regis L. Carvalho tz (2007) , Evaluation of Mechanistic-Empirical Design, Department of Civil and Environmental Engineering ,The University of Maryland, College Park, MD 20742,USA
18. Charles W. Schwartz, A. P. (2007), "Evaluation of Mechanistic-Empirical Design Procedure, Civil and Environmental Engineering the University of Maryland, USA."
19. Chen, L. H., Tang, S. T., and Zhang, H. T. (2010), Excel method in triaxial test data processing. Journal of Beijing Jiaotong University, 34(1):54–57.
20. Collins I F, Boulbibane M (1988), the application of shakedown theory to pavement design. Metals and Materials, Vol.4.
21. Croney, D. (1977), the Design and Performance of Road Pavements. Transport and Road Research Laboratory, London.
22. CSIR – Central Road Research Institute (2011), Pavement Engineering and Materials Flexible and Rigid Pavement Evaluation, annual report.
23. De Beer, M., Fisher, C., and Jooste, F. J. (1997). Determination of pneumatic tyre/pavement interface contact stresses under moving loads and some effects on pavements with thin asphalt surfacing layers. In Proceedings of the 8th International Conference on Asphalt Pavements, volume.
24. ERDEM ÇÖLERİ (2007), Relationship between Resilient Modulus and Soil Index Properties Of Unbound Materials (thesis), Civil Engineering, Middle East Technical University
25. Fredrick Lekarp (2000), Permanent Strain Response of Unbound Aggregates, Dept. of Civ. Engrg., Univ. of Nottingham, University Park, Nottingham NG7 2RD, U.K.

26. Gregory S. Williamson (2005), Investigation of Testing Methods to Determine Long-Term Durability of Wisconsin Aggregate Resources Including Natural Materials, Industrial By-Products, and Recycled/Reclaimed Materials, thesis, Faculty of the Virginia Polytechnic Institute and State University, Blacksburg, Virginia.
27. Hicks G R, Monismith CL (1971), Factors influencing the resilient response of granular materials. Highway Research Record, No.345, pp 15-31.
28. John Peter Lambert (2007), Novel Assessment Test for Granular Road Foundation (Dissertation Thesis), Materials Department of Civil & Building Engineering, Loughborough University, Loughborough, Leics, LE11 3TU,England
29. Jorge Alberto Prozzi (2001), Modeling Pavement Performance by Combining Field and Experimental Data (Dissertation),Civil and Environmental Engineering ,university of California Berkeley ,USA
30. Juspi, S. (2007). Experimental validation of the shakedown concept for pavement analysis and design. PhD thesis, University of Nottingham, the United Kingdom.
31. Kolisoja P, Resilient Deformation Characteristics of Granular Materials. PhD Thesis, Tampere University of Technology, 1997.
32. Komsun Siripun,2010, Mechanical Behavior of Unbound Granular Road Base Materials under Repeated Cyclic Loads, Curtin University of Technology, Perth, Australia,
33. Lekarp F (1997), Permanent deformation behaviour of unbound granular materials; Licentiate Thesis, Kungl Tekniska Högskolan.
34. Lekarp, F. (2004),"Permanent Strain Response of Unbound Aggregates" Journal of transportation Engineering
35. Lekarp, F., Isacsson, U., and Dawson, A. (2000), State of the art. I: Resilient response of unbound aggregates. Journal of Transportation Engineering,
36. Lillian Uthus (2007), Deformation Properties of Unbound Granular aggregates (PhD Thesis),Norwegian University of Science and Technology ,Faculty of Engineering Science and Technology ,Department of Civil and Transport Engineering
37. Luo, R. and Prozzi, J.A. (2007), Calibration of Pavement Response Models for the Mechanistic- Empirical Pavement Design Method. University of Texas at Austin, September 2007 (167264-1).

38. Shabbir Hossain, Ph.D. Research Scientist (2010), Characterization of Unbound Pavement Materials from Virginia Sources for Use in the New Mechanistic-Empirical Pavement Design Procedure, Research Report, Virginia Transportation Research Council, 530 Edgemont Road, Charlottesville, VA 22903 -2454, www.vtrc.net,
39. Thompson and Q.L Robnett (1979), "Resilient Properties of Subgrade Soils," J. of Transportation Engineering, vol. 105.
40. Makhaly Ba, Meissa Fall, Oustasse Abdoulaye Sall, Fatou Samb (2011), Effect of Compaction Moisture Content on the Resilient Modulus of Unbound Aggregates from Senegal, Journal of Scientific Research
41. Maria Arm(2013), Mechanical Properties of Residues as Unbound Road Materials, PhD Thesis, Stockholm, Sweden
42. Matti Huhtala (1995), The Effect of Wheel Loads On Pavements, University of Michigan Transportation Research Institute, Ann Arbor
43. Nahla Yassub Ahmad, Elaf Jasim Mahan (2014), Evaluation the Factors Affecting Permanent Deformation Using Cyclic Loading Test for Stabilized Subgrade Soil, Babylon University - Civil Engineering
44. Selezneva and M. Hallenbeck (2013), Long-Term Pavement Performance Pavement Loading User Guide, PUBLICATION NO. FHWA-HRT-13-089, U.S. Department Of Transportation, The Federal Highway Administration, Research, Development, And Technology, Turner-Fairbank Highway Research Center,6300 Georgetown Pike Mclean, VA 22101-2296Research, Development, And Technology, Turner-Fairbank Highway Research Center.
45. OGUZ ACIKGÖZ & REZHIN RAUF(2010), Analysis of Parameters Affecting Permanent Deformation in Road Pavement, Department of Civil and Environmental Engineering, Chalmers University Of Technology, Goteborg, Sweden
46. Radovsky, B. S. and Murashina, N. V. (1996), Shakedown of subgrade soil under repeated loading. Transportation Research Record: Journal of the Transportation Research Board, 1547(1):82–88.
47. Regis L. Carvalho (2006), Mechanistic-Empirical Design of Flexible Pavements: A Sensitivity Study, Thesis, Faculty of the Graduate School of the University of Maryland, College Park,

48. Sabine Werkmeister (2003), Permanent Deformation Behavior of Unbound Granular Materials in Pavement Constructions, dissertation, Dresden University of Technology, Dresden, Germany.
49. Sharp R W (1985), Pavement Design Based on Shakedown Analysis. Transportation Research Record 1022, Transportation Research Board, Washington, D.C., pp. 99-107.
50. Sharp R W (1983), Shakedown-Analyses and the design of pavement under moving surface load. PhD Thesis, University of Sydney, 1983.
51. Shaw P S (1980), Stress-Strain Relationships for Granular Materials under Repeated Loading. PhD Thesis, Department of Civil Engineering, University of Nottingham.
52. Shiau, S.-H. (2001). Numerical methods for shakedown analysis of pavements under moving surface loads. PhD thesis, University of Newcastle.
53. Simon Y. Oloo, D.G. Fredlund, and Julian K-M. Gan (1997), Bearing capacity of unpaved roads, Department of Civil Engineering, University of Saskatchewan, Saskatoon's S7N 5A9, Canada
54. Siripun.K, (2011), "Mechanical Behavior of Unbound Granular Road Base Materials under Repeated Cyclic Loads," International Journal of Pavement Research and Technology Vol.4.
55. South African Pavement Engineering Manual (2013), South African National Roads Agency Ltd, South Africa.
56. Sweere G T H (1990), unbound granular bases for roads. PhD Thesis, Delft University of Technology.
57. Theyse HL (2000), the Development of Mechanistic-Empirical Permanent Deformation Design Models for Unbound Pavement Materials from Laboratory and Accelerated Pavement Test Data.
58. Thomas Mase and George E. Mase (1999), Continuum Mechanics for engineers, Second Edition, Flint, Michigan, USA.
59. Transportation Research Board (2008). Mechanistic Empirical Design Guide accessed, Van Niekerk A
60. (2002), Mechanical behavior and performance of granular bases and sub-bases in pavements; PhD Thesis, Delft University of Technology, Delft.

61. W.F. CHEN and J.Y. Richard Liew (2003), the Civil Engineering Handbook, Second Edition.
62. Wang, J. (2011). Shakedown analysis and design of flexible road pavements under moving surface loads. PhD thesis, University of Nottingham, the United Kingdom.
63. WASANTHA KUMARA(2005), Analysis and Verification of Stresses and Strains and Their Relationship to Failure in Concrete Pavements under Heavy Vehicle Simulator Loading (PhD thesis), University of Florida
64. Yang H. Huang, (2004), "Pavement Analysis and Design, Second Edition" University of Kentucky, USA.

7. Appendices

Appendix A: Laboratory Test Results

Determination of sample Moisture Content and Mass

Trial No.	1.00
Wet weight of Sample, gram	130.90
Dry weight of Sample, gram	117.43
Weight of Water, gram	13.47
Moisture Content %	11.47
OMC Table A-2 and Figure 5.2 of sample, %	28.10
Total mass used to prepare triaxial sample(M) ,gram	2000.00
Water used to prepare the triaxial sample(g) =((OMC-W)/100)*M in gram	332.59
Determination of mass of specimen from MDD and OMC ρ = M/V; M = MDD (1+OMC)*V, volume of Mold used to prepare the specimen; M= 1.496(1+.281)*86.19 = 165.17g	
The mass of one Specimen =165.17g	

Table A-1: Determination of water content and mass of specimen

Trial No.	1.00	2.00	3.00	4.00
Water in CC	180.00	240.00	300.00	360.00
Mould Weight + sample(g)	3340.20	3412.90	3454.70	3360.50
mold weight (gm)	1632.90	1632.90	1632.90	1632.90
sample weight(gm)	1707.30	1780.00	1821.80	1727.60
Mold volume cm3	944.00	944.00	944.00	944.00
Bulk density(g/cm3)	1.81	1.89	1.93	1.83
Moisture Content				
Tin No.	67.00	10.00	A12	65.00
Wet weight + Tin(g)	129.10	168.60	170.60	155.40
Dry weight +Tin(g)	106.80	136.60	134.70	119.80
weight of tin(g)	16.50	16.40	16.90	16.30
weight of dry soil	90.30	120.20	117.80	103.50
weight of water	22.30	32.00	35.90	35.60
Moisture Content %	24.70	26.62	30.48	34.40
Dry Density(kg/m3)	1450.40	1489.15	1479.11	1361.71

Table A-2: Determination Maximum Dry Density and Optimum Moisture Content

Determination of Material Gradation

Sieve size(mm)	Weight Ret. Soil	Percentage Retained	Cumulative percentage Retained	Percentage Passed
75.00	0.00	0.00	0.00	100.00
50.00	0.00	0.00	0.00	100.00
37.50	0.00	0.00	0.00	100.00
25.00	0.00	0.00	0.00	100.00
19.00	49.00	7.66	7.66	92.34
12.50	30.80	4.82	12.48	87.52
9.50	59.20	9.26	21.74	78.26
4.75	177.10	27.70	49.44	50.56
2.36	71.20	11.14	60.57	39.43
2.00	0.00	0.00	60.57	39.43
1.18	21.70	3.39	63.97	36.03
0.60	14.30	2.24	66.20	33.80
0.30	10.90	1.70	67.91	32.09
0.15	11.00	1.72	69.63	30.37
0.075	11.50	1.80	71.43	28.57
Pan	182.70	28.57	100.00	0.00
	639.40			

Table A-3: Material Size Determination Using Series of Sieve

Determination Liquid Limit, plastic limit and Plasticity Index

Sample No.	**1**	**2**	**3**	**4**
Wet Weight + Tin(g)	134.1	182.6	188.6	170.4
Dry Weight +Tin(g)	106.8	136.6	134.7	119.8
Weight of Tin(g)	16.5	16.4	16.9	16.3
Weight of Dry Soil	90.3	120.2	117.8	103.5
Weight of Water	27.3	46	53.9	50.6
Moisture Content %	30.23	38.27	45.76	48.89
No. of drops (N)	45	30	20	15

Table A-4: Determination of Liquid Limit Determination

Sample No.	1	2	3
Wet Weight + Tin(g)	110.10	150.60	155.60
Dry Weight +Tin(g)	100.80	122.60	120.70
Weight of Tin(g)	16.50	16.40	16.90
Weight of Dry Soil	84.30	106.20	103.80
Weight of Water	9.30	28.00	34.90
Moisture Content %	11.03	26.37	33.62
PL(%) = (W1+W2+W3)/3	24		
LL (%)	42		
PI(%) = LL -PL	18		

Table A-5: Determination of Plasticity and Plastic Index

A triaxial test axial stress-strain calculation at cell stresses 100KPa, 200KPa and 300Kpa

Dial Division	Ring cal kgf/Div	Specimen Deformation = ΔL(mm)	Vertical strain ε = ΔL/Lo	Axial load (p)	Corrected Area (A)	Deviator stress (Δσ)= p/A	Total stress (KN/m^2)	Stiffness E= Δσ/ε (MPa)
0.0	0.0	0.00	0.000	0.00	0.001130	-	100.00	
10.0	3	0.10	0.001	3.24	0.001131	26.63	128.63	98
20.0	3.5	0.20	0.003	3.78	0.001133	33.36	133.36	55
40.0	3.5	0.40	0.005	3.78	0.001136	33.36	128.52	25
50.0	4	0.50	0.007	3.78	0.001137	33.23	133.23	20
70.0	4.0	0.70	0.009	4.32	0.001141	37.88	137.88	15
80.0	4.0	0.80	0.011	4.32	0.001142	37.83	137.83	13
90.0	5.0	0.90	0.012	5.40	0.001144	47.22	147.22	12
100.0	5.0	01.00	0.013	5.40	0.001145	47.16	147.16	11
20.0	5.5	1.20	0.016	5.94	0.001148	51.74	151.74	10
140.0	6.0	1.40	0.018	6.48	0.001151	56.29	156.29	8
160.0	6.3	1.60	0.021	6.75	0.001154	58.48	158.48	8
180.0	6.5	1.80	0.024	7.02	0.001157	60.65	160.65	7
200.0	7.0	2.00	0.026	7.56	0.001161	65.14	165.14	6
250.0	7.5	2.50	0.033	8.10	0.001168	69.32	169.32	5
300.0	8.0	3.00	0.039	8.64	0.001176	73.44	173.44	4
350.0	8.5	3.50	0.046	9.18	0.001185	77.50	177.50	4
400.0	9.0	4.00	0.053	9.72	0.001193	81.49	181.49	3
450.0	9.5	4.50	0.059	10.26	0.001201	85.42	185.42	3
500.0	10.0	5.00	0.066	10.80	0.001210	89.29	189.29	3
550.0	10.3	5.50	0.072	11.07	0.001218	90.88	190.88	3
600.0	10.5	6.00	0.079	11.34	0.001227	92.43	192.43	2
700.0	11.0	7.00	0.092	11.88	0.001245	95.45	195.45	2
800.0	11.5	8.00	0.105	12.42	0.001263	98.34	198.34	2
1000.0	12.0	10.00	0.132	12.96	0.001301	99.60	199.60	2
1100.0	12.5	11.00	0.145	13.50	0.001321	102.18	202.18	1
1200.0	13.0	12.00	0.158	14.04	0.001342	104.63	204.63	1
1300.0	13.3	13.00	0.171	14.31	0.001363	104.98	204.98	1
1400.0	13.5	14.00	0.184	14.58	0.001385	105.26	205.26	1
1500.0	14.0	15.00	0.19737	15.12	0.001408	107	207.40	1
1600.0	14.0	16.00	0.211	15.12	0.001431	106	205.64	1
1700.0	14.0	17.00	0.224	15.12	0.001456	104	203.88	1
1800.0	14.0	18.00	0.237	15.12	0.001481	102.11	202.11	1
1900.0	13.5	19.00	0.250	14.58	0.001507	96.77	196.77	1
2000.0	13.0	20.00	0.263	14.04	0.001534	91.55	191.55	1

Table A-6: Triaxial test axial stress-strain calculation for cell stress 100Kpa

No.	Dial Division	Ring Cal kgf/Div	Specimen Deformation = ΔL(mm)	Vertical strain ε = ΔL/Lo	Axial load (p)	Corrected Area	Deviator Stress (Δσ)= P/A	Total stress (KN/m^2)	Stiffness E= Δσ/ε (MPa)
1	0.0	0.0	0.00	0.000	0.00	0.001130	-	200	
2	10.0	2.5	0.10	0.001	2.70	0.001131	23.86	224	170
3	20.0	3.5	0.20	0.003	3.78	0.001133	33.36	233	89
4	40.0	5.0	0.40	0.005	5.40	0.001136	47.54	248	47
5	50.0	5.3	0.50	0.007	5.67	0.001137	49.85	250	38
6	70.0	6.0	0.70	0.009	6.48	0.001141	56.82	257	28
7	80.0	6.25	0.80	0.011	6.75	0.001142	59.11	259	25
8	90.0	7.0	0.90	0.012	7.56	0.001144	66.11	266	22
9	100.0	7.5	1.00	0.013	8.10	0.001145	70.74	271	21
10	120.0	8.0	1.20	0.016	8.64	0.001148	75.25	275	17
11	140.0	8.25	1.40	0.018	8.91	0.001151	77.40	277	15
12	160.0	9.5	1.60	0.021	10.26	0.001154	88.88	289	14
13	180.0	10.0	1.80	0.024	10.80	0.001157	93.31	293	12
14	200.0	10.0	2.00	0.026	10.80	0.001161	93.06	293	11
15	250.0	11.0	2.50	0.033	11.88	0.001168	101.67	302	9
16	300.0	11.5	3.00	0.039	12.42	0.001176	105.57	306	8
17	350.0	12.0	3.50	0.046	12.96	0.001185	109.41	309	7
18	400.0	12.5	4.00	0.053	13.50	0.001193	113.18	313	6
19	450.0	12.8	4.50	0.059	13.77	0.001201	114.64	315	5
20	500.0	13.0	5.00	0.066	14.04	0.001210	116.07	316	5
21	550.0	14.0	5.50	0.072	15.12	0.001218	124.12	324	4
22	600.0	14.3	6.00	0.079	15.39	0.001227	125.44	325	4
23	700.0	14.5	7.00	0.092	15.66	0.001245	125.82	326	4
24	800.0	15.0	8.00	0.105	16.20	0.001263	128.27	328	3
25	1000.0	15.5	10.00	0.132	16.74	0.001301	128.65	329	2
26	1100.0	16.0	11.00	0.145	17.28	0.001321	130.79	331	2
27	1200.0	16.5	12.00	0.158	17.82	0.001342	132.80	333	2
28	1300.0	16.0	13.00	0.171	17.28	0.001363	126.76	327	2
29	1400.0	16.5	14.00	0.184	17.82	0.001385	128.65	329	2
30	1500.0	17.0	15.00	0.197	18.36	0.001408	130.41	330	2
31	1600.0	17.5	16.00	0.211	18.90	0.001431	132.04	332	2
34	1900.0	18.5	19.00	0.250	19.98	0.001507	132.61	333	1
35	2000.0	18.5	20.00	0.263	19.98	0.001534	130.28	330	1
36	2100.0	18.5	21.00	0.276	19.98	0.001561	127.96	328	1
37	2200.0	19.0	22.00	0.289	20.52	0.001590	129.03	329	1
38	2300.0	19.0	23.00	0.303	20.52	0.001620	126.64	327	1
39	2400.0	20.0	24.00	0.316	21.60	0.001652	130.79	331	1
40	2500.0	21.0	25.00	0.329	22.68	0.001684	135	335	1
41	2600.0	19.0	26.00	0.342	20.52	0.001718	119	319	1

Table A-7: Triaxial test axial stress-strain calculation for cell stress 200Kpa

No.	Dial Division	Ring Cal kgf/Div	Specimen Deformation = ΔL(mm)	Vertical Strain ε = ΔL/Lo	Axial load (p)	Corrected Area (A)	Deviator Stress (Δσ) =P/A	Total stress (KN/m²)	Stiffness E= Δσ/ε (MPa)
1	0.0	0.0	0.00	0.000	0.00	0.001130	-	300	
2	10.0	4.0	0.10	0.001	4.32	0.001131	38.18	338	257
3	20.0	5.0	0.20	0.003	5.40	0.001133	47.66	348	132
4	40.0	6.0	0.40	0.005	6.48	0.001136	57.04	357	68
5	50.0	6.3	0.50	0.007	6.75	0.001137	59.34	359	55
6	70.0	8.0	0.70	0.009	8.64	0.001141	75.76	376	41
7	80.0	8.50	0.80	0.011	9.18	0.001142	80.38	380	36
8	90.0	9.0	0.90	0.012	9.72	0.001144	85.00	385	33
9	100.0	9.5	1.00	0.013	10.26	0.001145	89.60	390	30
10	120.0	10.0	1.20	0.016	10.80	0.001148	94.07	394	25
11	140.0	11.00	1.40	0.018	11.88	0.001151	103.20	403	22
12	160.0	11.5	1.60	0.021	12.42	0.001154	107.60	408	19
13	180.0	11.5	1.80	0.024	12.42	0.001157	107.31	407	17
14	200.0	11.5	2.00	0.026	12.42	0.001161	107.02	407	15
15	250.0	13.0	2.50	0.033	14.04	0.001168	120.16	420	13
16	300.0	14.5	3.00	0.039	15.66	0.001176	133.11	433	11
17	350.0	15.0	3.50	0.046	16.20	0.001185	136.76	437	9
18	400.0	15.5	4.00	0.053	16.74	0.001193	140.34	440	8
19	450.0	16.0	4.50	0.059	17.28	0.001201	143.87	444	7
20	500.0	16.0	5.00	0.066	17.28	0.001210	142.86	443	7
21	600.0	16.0	6.00	0.079	17.28	0.001227	140.85	441	6
22	700.0	18.0	7.00	0.092	19.44	0.001245	156.19	456	5
23	800.0	18.5	8.00	0.105	19.98	0.001263	158.20	458	4
24	1000.0	18.5	10.00	0.132	19.98	0.001301	153.55	454	3
25	1100.0	19.0	11.00	0.145	20.52	0.001321	155.31	455	3
26	1200.0	19.0	12.00	0.158	20.52	0.001342	152.92	453	3
27	1300.0	20.0	13.00	0.171	21.60	0.001363	158.45	458	3
28	1400.0	20.0	14.00	0.184	21.60	0.001385	155.94	456	2
29	1500.00	20.00	15.00	0.20	21.60	0.00	153.42	453	2
30	1600.0	22.0	16.00	0.211	23.76	0.001431	166.00	466	2
31	1700.0	21.0	17.00	0.224	22.68	0.001456	155.81	456	2
32	1800.0	19.0	18.00	0.237	20.52	0.001481	138.58	439	2

Table A-8: Triaxial test axial stress-strain calculation for cell stress 300Kpa

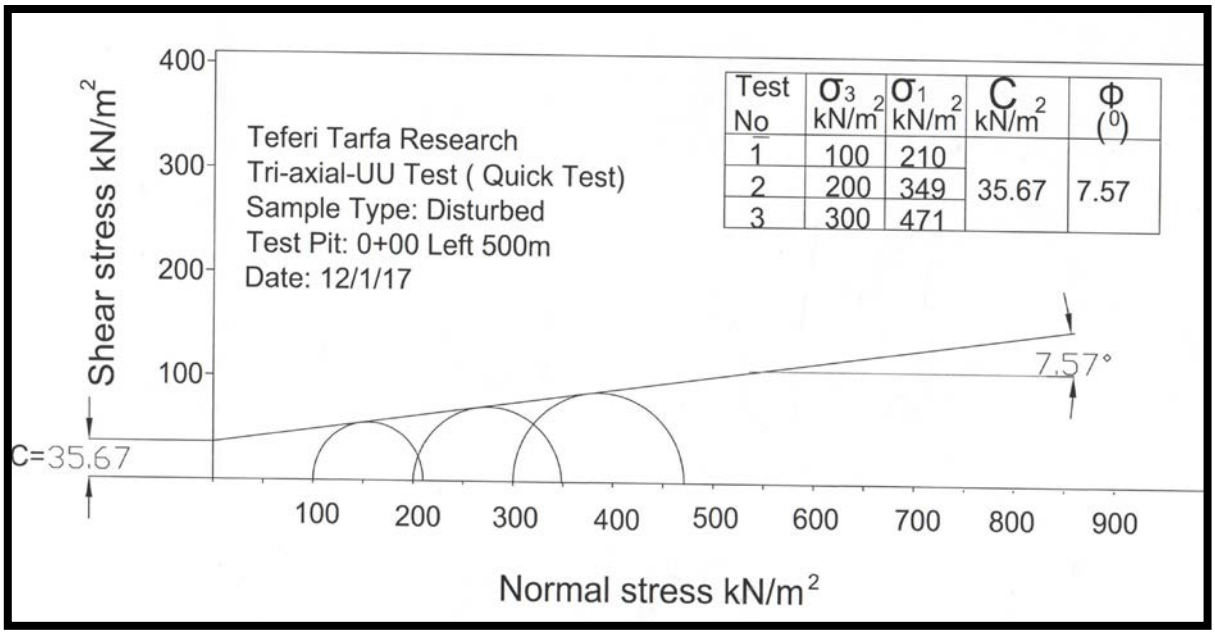

Figure A-1: Shear strength determination of specimen in triaxial test

Shear strengh of subgrade material
Using equation of stress path $\frac{\sigma_1-\sigma_3}{2} = (\frac{\sigma_1+\sigma_3}{2}) * \sin\emptyset + c(\cos\emptyset)$ value of cohesion and internal angle of friction calculate as follow confining stress represented in table (210-100)/2 = (210+100)/2*sinØ+CcosØ 55 = 155sinØ+ccosØ ----------1 67 = 267 sinØ+ccosØ ----------2 By solving both equation 1 and 2 in simultaneously cohesion (c) and angle of internal friction (Ø) 35.7MPa and 8º respectively. Maximum Shear Strength of material , $\tau_f = c + \sigma tan\emptyset$ Sample 1= 35.7+(100+110)/2)tan(8) = 50.5KPa Sample 2 = 35.7+(200+119)tan(8) =60KPa Sample 3 = 35.7+ 300+171)tan(8) = 68.8KPa =70KPa

Table A-9: Shear Strength of subgrade material obtained at laboratory

THE REGIONAL STATE OF OROMIA
ROADS AUTHORITY

Detailed Engineering Design
and
Tender Document Preparation
of
Shanno - Dannaba Road Project

Soils/Materials Investigation & Pavement Design Report

(Final)

YIDIDIYA ENGINEERING CONSULTANTS PLC /YECON/

Tel 251 – 115 53 73 69/251 – 115 53 73 38

Fax 251 – 115 53 74 18

E-mail: yeconplc@yahoo.com
P.O.Box 102014
Addis Ababa, Ethiopia

June 2009

Subgrade Soil Investigation and Chacterization

Sr. No	Station (Pit No)	Lab. Material Description	Depth Sampled (cm)	% pass (mm)			LL %	PL %	PI %	AASHTO Soil Class	OMC %	MDD T-99 g/cm³	1 - Point CBR %	
				2.000	0.425	0.075							CBR	Swell %
1	0 + 500	Dark brown Silty CLAY	50 - 70	96	92	87	71	32	39	A-7-5 (20)	25.5	1.303	1	9.88
2	2 + 000	Dark Silty CLAY with few gravel	50 - 60	77	75	74	72	37	35	A-7-5 (20)	23.5	1.308	1	7.70
3	5 + 000	Dark Silty CLAY	50 - 70	100	99	98	67	31	36	A-7-5 (20)	29.0	1.363	1	8.33
4	7 + 000	Dark Silty CLAY	50 - 80	95	94	91	72	35	37	A-7-5 (20)	32.0	1.362	2	7.02
5	8 + 000	Dark Silty CLAY	50 - 75	100	97	95	80	35	45	A-7-5 (20)	26.3	1.294	1	9.84
6	10 + 000	Dark Silty CLAY	60 - 70	92	88	86	79	36	43	A-7-5 (20)	30.0	1.382	2	7.71
7	11 + 300	Dark brown Silty CLAY	60 - 80	100	100	100	84	43	41	A-7-5 (20)	36.0	1.290	3	5.57
8	12 + 400	Light dark Silty CLAY with very few gravel	80 - 95	88	85	84	78	35	43	A-7-5 (20)	24.0	1.322	1	10.29
9	15 + 000	Dark brown Silty CLAY	50 - 70	100	98	96	67	37	30	A-7-5 (20)	33.5	1.297	2	6.09
10	16 + 100	Dark brown Silty CLAY	50 - 70	99	96	94	84	36	48	A-7-5 (20)	33.0	1.330	2	6.37
11	17 + 050	Dark brown Silty CLAY	40 - 70	100	98	94	67	30	37	A-7-5 (20)	24.5	1.365	1	6.81
12	18 + 300	Dark Silty CLAY	50 - 60	100	96	94	78	36	42	A-7-5 (20)	26.5	1.218	1	8.56
13	19 + 500	Light brown Silty CLAY	50 - 70	89	85	81	50	30	20	A-7-5 (14)	27.5	1.449	8	0.51
14	21 + 600	Dark brown Silty CLAY with few gravel	50 - 70	99	94	90	56	35	21	A-7-5 (16)	34.5	1.319	3	2.99
15	24 + 200	Dark brown Silty CLAY	50 - 80	99	94	91	78	33	45	A-7-5 (20)	26.5	1.286	1	8.38
16	26 + 300	Dark brown Silty CLAY	50 - 70	97	93	89	67	35	32	A-7-5 (20)	29.5	1.359	3	3.26
17	29 + 000	Light brown sandy Silty CLAY	50 - 60	85	81	79	64	39	25	A-7-5 (18)	27.5	1.360	2	4.15
18	31 + 650	Dark brown Silty CLAY	50 - 60	99	95	93	77	45	32	A-7-5 (20)	31.5	1.315	2	7.14
19	33 + 600	Dark brown Silty clayey GRAVEL	45 - 60	41	40	39	71	37	34	A-7-5 (6)	34.0	1.310	4	3.64
20	35 + 900	Light brown Silty CLAY	50 - 70	100	96	93	77	45	32	A-7-5 (20)	35.0	1.272	2	7.69
21	39 + 000	Dark brown sandy Silty CLAY with very few gravel	50 - 80	90	87	79	65	32	33	A-7-5 (20)	23.5	1.413	2	7.56

Sr. No	Station (Pit No)	Lab. Material Description	Depth Sampled (cm)	% pass (mm) 2.000	0.425	0.075	LL %	PL %	PI %	AASHTO Soil Class	OMC %	MDD T-99 g/cm³	1 - Point CBR % CBR	Swell %
22	42 + 100	Brown Silty clayey GRAVEL	50 - 80	26	25	24	64	41	23	A-2-7 (1)	30.5	1.460	7	2.53
23	Aragesa + 2km	Light brown Gravelly silty CLAY	50 - 80	68	67	66	66	31	35	A-7-5 (17)	26.5	1.470	2	4.54
24	Aragesa + 4.5km	Dark Silty CLAY	50 - 70	100	99	98	79	39	40	A-7-5 (20)	30.0	1.268	1	10.39
25	Aragesa + 6.5km	Dark brown Silty CLAY	50 - 80	99	96	94	78	37	41	A-7-5 (20)	35.5	1.290	1	8.60
26	Deneba - 500m	Dark brown sandy silty CLAY with few gravel	50 - 70	83	81	78	65	31	34	A-7-5 (20)	26.0	1.412	1	6.33

Table A-9: Subgrade Soil Investigation and Characterization

Sr. No	Station (Pit No)	Lab. Material Description	Depth Sampled (cm)	% pass (mm) 2.000	0.425	0.075	LL %	PL %	PI %	AASHTO Soil Class	OMC %	MDD T-180 g/cm³	1 - Point CBR % CBR	Swell %
1	0 + 500 offset 500m left (Select 1)	Light brown Silty Clayey GRAVEL	-	30	26	24	41	24	17	A-2-7 (1)	12.5	2.050	16	0.26
2	7km offset 150m right (Select 3)	Light gray Silty Clayey GRAVEL	-	5	4	3	49	30	19	A-2-7 (0)	10.5	2.299	96	0.15
3	36 + 900 offset 250m right (Select 5)	Light gray Silty Clayey GRAVEL	-	10	6	5	48	35	13	A-2-7 (0)	14.5	2.289	170	0.17
4	End offset 4.9 km from Deneba on Deneba - Lemi Road	Light gray Silty Silty Clayey GRAVEL	-	5	4	4	51	24	27	A-2-7 (0)	12.3	2.125	64	1.00

Table A-10: Subgrade Material Location, Investigation and Characterization

Gondwana Engineering Plc.

WET SIEVE ANALYSIS (AASHTO T - 27)

Project:-	Sheno - Deneba Road Project
Client:-	Yididiya Consulting Engineers Plc.
Station:-	0 + 500 offset 500m left (Select 1)
Sample of:-	Select
Sampled by:-	The Client
Test specified by:-	The Client
Description of Sample:-	Light brown Silty Clayey GRAVEL
Depth Sampled:-	-
Lab. Number:-	SDRP-Grad.-Select-1/2009
Date Started:-	28/07/09
Date Issued:-	07/08/09

Weight Before Washing 1025 gm Weight After Washing 781.00 gm

ASTM SIEVE (MM)	CUMULATIVE WT. RETAINED (gm)	CUMULATIVE % RETAINED	% PASS
50	0.0	0.0	100.0
37.5	90.5	8.8	91.2
25	191.0	18.6	81.4
19	339.5	33.1	66.9
12.5	487.5	47.6	52.4
9.5	544.0	53.1	46.9
6.3	617.5	60.2	39.8
4.75	654.5	63.9	36.1
2.36	707.5	69.0	31.0
2	721.3	70.4	29.6
1.18	735.0	71.7	28.3
0.85	742.5	72.4	27.6
0.6	750.5	73.2	26.8
0.425	756.0	73.8	26.2
0.3	761.0	74.2	25.8
0.15	768.5	75.0	25.0
0.075	781.0	76.2	23.8

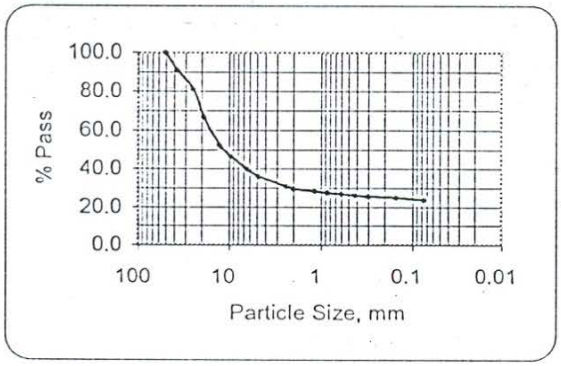

Table A-11: Gradation of Subgrade Material

Gravel Pavement Design

Input design parameters used in pavement design of Shano Danaba gravel road project; AADT, soil data and climate condition of area. The AADT of this project was less than 200 vehicles per day and CBR value of subgrade soil determined in laboratory as shown figure A-2. The average CBR value of subgrade soil for this project was 4%. This area climate condition is wet zone, having average rainfall 80mm per month with route alignment transverse through elevations more than 2000m above sea level. Based on these data Shano Danaba Road pavement had designed. This pavement design had two capping layers and gravel wearing course. The need of capping layers depended on subgrade soil strength, the CBR value of soil. Standards recommended 600mm cut for weak soil and replaced subgrade material CBR value more than 7% with thickness 300mm and second layers with CBR value more than 20% with 200mm thickness, along with gravel wearing course with 300mm thickness having CBR value more than 30% used as represented in table A-12. PI value and CBR value of this of project route shown in table A-9 and figure A-3. From this pavement design, the thickness of pavement had determined based on subgrade soil and subgrade material strength as represented in table A-12.

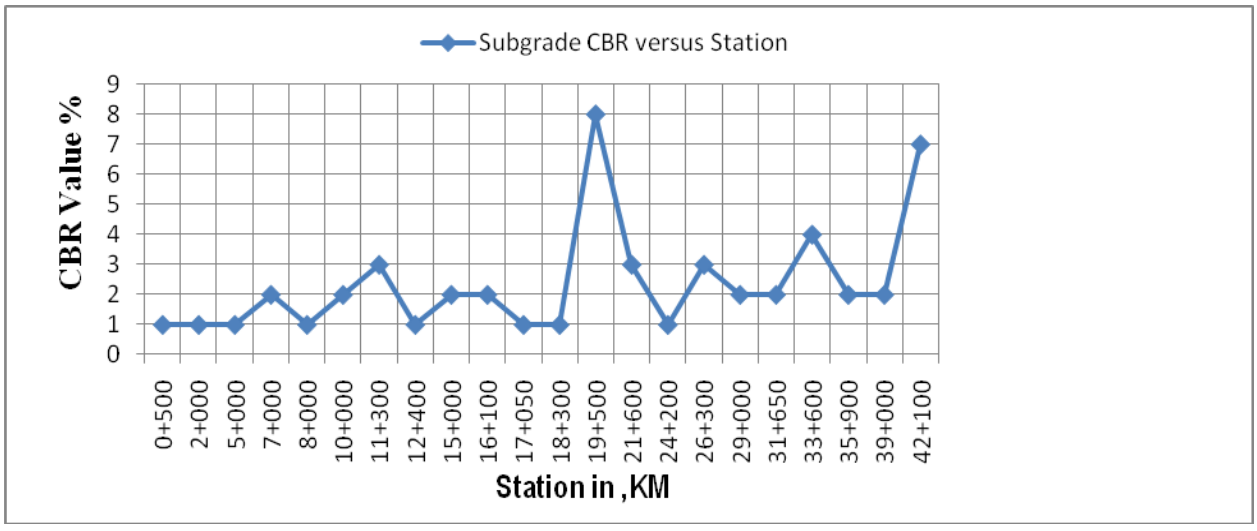

Figure A-2: CBR value versus project Chainage at laboratory

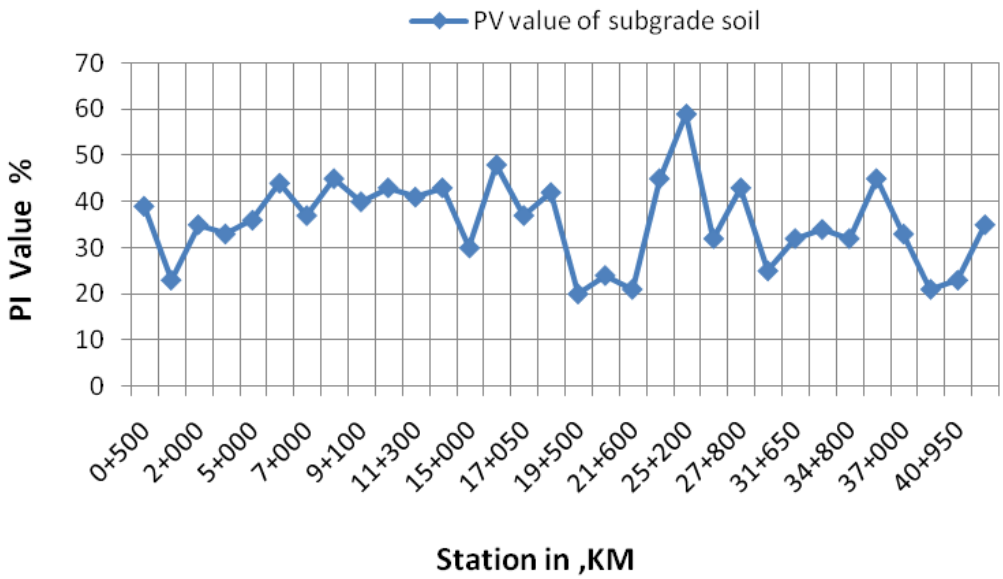

Figure A-3: PI value Shana Danaba project at laboratory

Stations		Homogeneous Section	Subgrade Materials		Gravel Wearing Course
			G7	G20	GW
0+000	27+900	HS1	300	200	300
28+900	34+200				
34+600	End				
27+900	28+800	HS2		200	
34+200	34+600				

Table A-12: Pavement Thickness Required for Shana Danaba project

Appendix B: Modeling Input and Output

```
*******************************************************************************

*                      Program- CIRCLY


*                Version- 5.1c

*          (C) Copyright MINCAD Systems Pty. Ltd., Australia 2015.


*           LAYERS BLOCK WORKSPACE                (MLYBLK)...  125000

*           COORDINATES BLOCK WORKSPACE       (MCOORD)...    5000


*           CONVERGENCE TOLERANCE                 (EPS)... 1.0E-02

*           MINIMUM INTEGRATION RANGE             (RKUPMN)... 2.0E+00

*           MAXIMUM INTEGRATION RANGE             (RKNMTR)... 1.0E+01

*           MAXIMUM EXPONENTIAL FN. ARG.          (EXPMAX)... 2.0E+01

*           MAXIMUM NODES IN QUADRATURE           (MXKNOD)...     127


*******************************************************************************
```

Job Summary File

CIRCLY Version 5.1c

Job Title: Response of Unbound Pavement Material to Stress

Damage Factor Calculation

Assumed number of damage pulses per movement:

One pulse per axle (i.e. use NROWS)

Traffic Spectrum Details:

ID: MSc Thesis Title: Response of Unbound Pavement Material to Stress

Table B-1: Layered Elastic Model Data Inputs

Details of layered system

Detail of Loads

Layer	Type	Elastic Constants			Thickness	Interface
1	CROSS-ANISOTROPIC	EH = 0.7500E+02 VH= 0.3500E+00	EV = 0.1500E+03 VH = 0.3500E+00	F=0.1111E+03	0.3000E+03	Rough
2	CROSS-ANISOTROPIC	EH =0.5000E+02 VH= 0.4500E+00	EV = 0.1000E+03 VH = 0.4500E+00	F= .6900E+02	0.5000E+03	Rough
3	CROSS-ANISOTROPIC	EH = 0.2000E+02 VH= 0.4500E+00	EV = 0.4000E+02 VH = 0.4500E+00	F= .2758E+02	INFINITE	Rough

Load Group No.	Load Type	Radius stress	Reference stress	Average per Location	Load /moment	Power
1	Vertical force	0.9210E+02	0.7500E+00	0.7500E+00	0.1999E+05	000

Traffic Spectrum

Load No	Load ID	Movements
1	ESA75-Ful	2.00E+06

Details of Load Groups

Load No	Load ID	Load Category	Load Type	Radius	Pressure/Ref stress	Exponent
1	ESA75-full	SA750-Full	Vertical force	92.1	0.75	0.00

Load Locations

Location No.	Load ID	Gear No.	X	Y	Scaling Factor	Theta
1	ESA75-Full	1	-165	0	1	0
2	ESA75-Full	1	165	0	1	0
3	ESA75-Full	1	1635	0	1	0
4	ESA75-Full	1	1965	0	1	0

Layout of result points on horizontal plane

Xmin	Xmax	Xdel	Y
-500	1000	20	0

Details of Layered System

ayer No.	urface type	Material ID	Isotropy	Modulus EV	Poisson's Ratio H	lodulus EH	Poisson's Ratio V	F(shear)
1	Rough	Gran_150	Anisotropic	150	.35	75	0.35	111
2	Rough	G15	Anisotropic	100	.45	50	.45	69
3	Rough		Anisotropic	40	.45	20	.45	45

Performance Relationships

Layer No.	Location	Performance ID	Component	Performance Constant	Performance Exponent	raffic Multipliers
2	top	selAust2004	EZZ	0.009300	7	1.600
3	top	Sub_2004	EZZ	0.009300	7	1.600

CIRCLY OUTPUT

No.	Coordinates				Displacements		
	X	Y	Z	L	UX	UY	UZ
1	-5.00E+02	0.00E+00	3.00E+02	2	2.65E-02	2.31E-09	-0.663
2	-4.80E+02	0.00E+00	3.00E+02	2	3.05E-02	2.67E-09	-0.679
3	-4.60E+02	0.00E+00	3.00E+02	2	3.47E-02	3.03E-09	-0.696
4	-4.40E+02	0.00E+00	3.00E+02	2	3.88E-02	3.39E-09	-0.714
5	-4.20E+02	0.00E+00	3.00E+02	2	4.28E-02	3.74E-09	-0.733
6	-4.00E+02	0.00E+00	3.00E+02	2	4.64E-02	4.06E-09	-0.752
7	-3.80E+02	0.00E+00	3.00E+02	2	4.95E-02	4.33E-09	-0.772
8	-3.60E+02	0.00E+00	3.00E+02	2	5.19E-02	4.54E-09	-0.792
9	-3.40E+02	0.00E+00	3.00E+02	2	5.34E-02	4.67E-09	-0.813
10	-3.20E+02	0.00E+00	3.00E+02	2	5.39E-02	4.71E-09	-0.834
11	-3.00E+02	0.00E+00	3.00E+02	2	5.32E-02	4.65E-09	-0.854
12	-2.80E+02	0.00E+00	3.00E+02	2	5.13E-02	4.48E-09	-0.874
13	-2.60E+02	0.00E+00	3.00E+02	2	4.82E-02	4.21E-09	-0.893
14	-2.40E+02	0.00E+00	3.00E+02	2	4.40E-02	3.85E-09	-0.911
15	-2.20E+02	0.00E+00	3.00E+02	2	3.89E-02	3.40E-09	-0.928
16	-2.00E+02	0.00E+00	3.00E+02	2	3.31E-02	2.90E-09	-0.944
17	-1.80E+02	0.00E+00	3.00E+02	2	2.69E-02	2.35E-09	-0.958
18	-1.60E+02	0.00E+00	3.00E+02	2	2.05E-02	2.00E-09	-0.97
19	-1.40E+02	0.00E+00	3.00E+02	2	1.43E-02	2.27E-09	-0.981
20	-1.20E+02	0.00E+00	3.00E+02	2	8.35E-03	2.52E-09	-0.99

21	-1.00E+02	0.00E+00	3.00E+02	2	2.93E-03	2.76E-09	-0.998
22	-8.00E+01	0.00E+00	3.00E+02	2	-1.91E-03	2.97E-09	-1.005
23	-6.00E+01	0.00E+00	3.00E+02	2	-6.14E-03	3.13E-09	-1.01
24	-4.00E+01	0.00E+00	3.00E+02	2	-9.84E-03	3.23E-09	-1.015
25	-2.00E+01	0.00E+00	3.00E+02	2	-1.31E-02	3.24E-09	-1.018
26	0.00E+00	0.00E+00	3.00E+02	2	-1.62E-02	3.16E-09	-1.02
27	2.00E+01	0.00E+00	3.00E+02	2	-1.93E-02	2.97E-09	-1.022
28	4.00E+01	0.00E+00	3.00E+02	2	-2.26E-02	2.67E-09	-1.023
29	6.00E+01	0.00E+00	3.00E+02	2	-2.63E-02	2.25E-09	-1.022
30	8.00E+01	0.00E+00	3.00E+02	2	-3.06E-02	1.72E-09	-1.021
31	1.00E+02	0.00E+00	3.00E+02	2	-3.54E-02	1.09E-09	-1.019
32	1.20E+02	0.00E+00	3.00E+02	2	-4.08E-02	3.71E-10	-1.015
33	1.40E+02	0.00E+00	3.00E+02	2	-4.67E-02	-4.06E-10	-1.01
34	1.60E+02	0.00E+00	3.00E+02	2	-5.29E-02	-1.22E-09	-1.003
35	1.80E+02	0.00E+00	3.00E+02	2	-5.92E-02	-1.42E-09	-0.995
36	2.00E+02	0.00E+00	3.00E+02	2	-6.53E-02	-1.41E-09	-0.985
37	2.20E+02	0.00E+00	3.00E+02	2	-7.10E-02	-1.41E-09	-0.973
38	2.40E+02	0.00E+00	3.00E+02	2	-7.60E-02	-1.40E-09	-0.961
39	2.60E+02	0.00E+00	3.00E+02	2	-8.00E-02	-1.40E-09	-0.947
40	2.80E+02	0.00E+00	3.00E+02	2	-8.30E-02	-1.39E-09	-0.932
41	3.00E+02	0.00E+00	3.00E+02	2	-8.48E-02	-1.38E-09	-0.916
42	3.20E+02	0.00E+00	3.00E+02	2	-8.54E-02	-1.38E-09	-0.9
43	3.40E+02	0.00E+00	3.00E+02	2	-8.49E-02	-1.37E-09	-0.884
44	3.60E+02	0.00E+00	3.00E+02	2	-8.33E-02	-1.36E-09	-0.868
45	3.80E+02	0.00E+00	3.00E+02	2	-8.08E-02	-1.36E-09	-0.852

46	4.00E+02	0.00E+00	3.00E+02	2	-7.75E-02	-1.35E-09	-0.837
47	4.20E+02	0.00E+00	3.00E+02	2	-7.37E-02	-1.34E-09	-0.822
48	4.40E+02	0.00E+00	3.00E+02	2	-6.96E-02	-1.33E-09	-0.808
49	4.60E+02	0.00E+00	3.00E+02	2	-6.52E-02	-1.31E-09	-0.795
50	4.80E+02	0.00E+00	3.00E+02	2	-6.08E-02	-1.30E-09	-0.782
51	5.00E+02	0.00E+00	3.00E+02	2	-5.65E-02	-1.28E-09	-0.771
52	5.20E+02	0.00E+00	3.00E+02	2	-5.23E-02	-1.26E-09	-0.76
53	5.40E+02	0.00E+00	3.00E+02	2	-4.82E-02	-1.24E-09	-0.75
54	5.60E+02	0.00E+00	3.00E+02	2	-4.44E-02	-1.21E-09	-0.742
55	5.80E+02	0.00E+00	3.00E+02	2	-4.08E-02	-1.19E-09	-0.733
56	6.00E+02	0.00E+00	3.00E+02	2	-3.73E-02	-1.16E-09	-0.726
57	6.20E+02	0.00E+00	3.00E+02	2	-3.40E-02	-1.14E-09	-0.719
58	6.40E+02	0.00E+00	3.00E+02	2	-3.09E-02	-1.11E-09	-0.712
59	6.60E+02	0.00E+00	3.00E+02	2	-2.79E-02	-1.08E-09	-0.706
60	6.80E+02	0.00E+00	3.00E+02	2	-2.50E-02	-1.05E-09	-0.701
61	7.00E+02	0.00E+00	3.00E+02	2	-2.23E-02	-1.02E-09	-0.697
62	7.20E+02	0.00E+00	3.00E+02	2	-1.96E-02	-9.76E-10	-0.692
63	7.40E+02	0.00E+00	3.00E+02	2	-1.71E-02	-9.32E-10	-0.689
64	7.60E+02	0.00E+00	3.00E+02	2	-1.47E-02	-8.83E-10	-0.685
65	7.80E+02	0.00E+00	3.00E+02	2	-1.24E-02	-8.28E-10	-0.683
66	8.00E+02	0.00E+00	3.00E+02	2	-1.01E-02	-7.68E-10	-0.68
67	8.20E+02	0.00E+00	3.00E+02	2	-7.99E-03	-7.03E-10	-0.679
68	8.40E+02	0.00E+00	3.00E+02	2	-5.92E-03	-6.33E-10	-0.677
69	8.60E+02	0.00E+00	3.00E+02	2	-3.91E-03	-5.60E-10	-0.676
70	8.80E+02	0.00E+00	3.00E+02	2	-1.95E-03	-4.82E-10	-0.676

71	9.00E+02	0.00E+00	3.00E+02	2	0.00E+00	-3.99E-10	-0.675
72	9.20E+02	0.00E+00	3.00E+02	2	1.95E-03	-3.11E-10	-0.676
73	9.40E+02	0.00E+00	3.00E+02	2	3.91E-03	-2.17E-10	-0.676
74	9.60E+02	0.00E+00	3.00E+02	2	5.92E-03	-1.16E-10	-0.677
75	9.80E+02	0.00E+00	3.00E+02	2	7.99E-03	-4.60E-12	-0.679
76	1.00E+03	0.00E+00	3.00E+02	2	1.01E-02	1.18E-10	-0.68
77	-5.00E+02	0.00E+00	8.00E+02	3	1.03E-01	9.04E-09	-0.592
78	-4.80E+02	0.00E+00	8.00E+02	3	1.03E-01	8.99E-09	-0.6
79	-4.60E+02	0.00E+00	8.00E+02	3	1.02E-01	8.91E-09	-0.608
80	-4.40E+02	0.00E+00	8.00E+02	3	1.01E-01	8.82E-09	-0.615
81	-4.20E+02	0.00E+00	8.00E+02	3	9.96E-02	8.70E-09	-0.623
82	-4.00E+02	0.00E+00	8.00E+02	3	9.80E-02	8.57E-09	-0.63
83	-3.80E+02	0.00E+00	8.00E+02	3	9.63E-02	8.42E-09	-0.638
84	-3.60E+02	0.00E+00	8.00E+02	3	9.43E-02	8.25E-09	-0.645
85	-3.40E+02	0.00E+00	8.00E+02	3	9.21E-02	8.05E-09	-0.652
86	-3.20E+02	0.00E+00	8.00E+02	3	8.97E-02	7.84E-09	-0.659
87	-3.00E+02	0.00E+00	8.00E+02	3	8.70E-02	7.61E-09	-0.665
88	-2.80E+02	0.00E+00	8.00E+02	3	8.42E-02	7.36E-09	-0.672
89	-2.60E+02	0.00E+00	8.00E+02	3	8.11E-02	7.09E-09	-0.678
90	-2.40E+02	0.00E+00	8.00E+02	3	7.78E-02	6.80E-09	-0.684
91	-2.20E+02	0.00E+00	8.00E+02	3	7.43E-02	6.50E-09	-0.69
92	-2.00E+02	0.00E+00	8.00E+02	3	7.07E-02	6.18E-09	-0.696
93	-1.80E+02	0.00E+00	8.00E+02	3	6.69E-02	5.85E-09	-0.701
94	-1.60E+02	0.00E+00	8.00E+02	3	6.29E-02	5.57E-09	-0.706
95	-1.40E+02	0.00E+00	8.00E+02	3	5.88E-02	5.48E-09	-0.71

96	-1.20E+02	0.00E+00	8.00E+02	3	5.45E-02	5.39E-09	-0.715
97	-1.00E+02	0.00E+00	8.00E+02	3	5.02E-02	5.28E-09	-0.719
98	-8.00E+01	0.00E+00	8.00E+02	3	4.57E-02	5.16E-09	-0.722
99	-6.00E+01	0.00E+00	8.00E+02	3	4.12E-02	5.02E-09	-0.725
100	-4.00E+01	0.00E+00	8.00E+02	3	3.67E-02	4.88E-09	-0.728
101	-2.00E+01	0.00E+00	8.00E+02	3	3.21E-02	4.73E-09	-0.731
102	0.00E+00	0.00E+00	8.00E+02	3	2.75E-02	4.56E-09	-0.733
103	2.00E+01	0.00E+00	8.00E+02	3	2.29E-02	4.39E-09	-0.735
104	4.00E+01	0.00E+00	8.00E+02	3	1.84E-02	4.21E-09	-0.737
105	6.00E+01	0.00E+00	8.00E+02	3	1.39E-02	4.02E-09	-0.738
106	8.00E+01	0.00E+00	8.00E+02	3	9.50E-03	3.83E-09	-0.739
107	1.00E+02	0.00E+00	8.00E+02	3	5.20E-03	3.64E-09	-0.739
108	1.20E+02	0.00E+00	8.00E+02	3	1.03E-03	3.44E-09	-0.739
109	1.40E+02	0.00E+00	8.00E+02	3	-3.00E-03	3.24E-09	-0.739
110	1.60E+02	0.00E+00	8.00E+02	3	-6.88E-03	3.04E-09	-0.739
111	1.80E+02	0.00E+00	8.00E+02	3	-1.06E-02	3.04E-09	-0.738
112	2.00E+02	0.00E+00	8.00E+02	3	-1.41E-02	3.12E-09	-0.737
113	2.20E+02	0.00E+00	8.00E+02	3	-1.74E-02	3.21E-09	-0.735
114	2.40E+02	0.00E+00	8.00E+02	3	-2.05E-02	3.29E-09	-0.734
115	2.60E+02	0.00E+00	8.00E+02	3	-2.34E-02	3.37E-09	-0.732
116	2.80E+02	0.00E+00	8.00E+02	3	-2.60E-02	3.46E-09	-0.73
117	3.00E+02	0.00E+00	8.00E+02	3	-2.84E-02	3.55E-09	-0.728
118	3.20E+02	0.00E+00	8.00E+02	3	-3.05E-02	3.64E-09	-0.726
119	3.40E+02	0.00E+00	8.00E+02	3	-3.24E-02	3.73E-09	-0.723
120	3.60E+02	0.00E+00	8.00E+02	3	-3.40E-02	3.82E-09	-0.72

121	3.80E+02	0.00E+00	8.00E+02	3	-3.54E-02	3.92E-09	-0.718
122	4.00E+02	0.00E+00	8.00E+02	3	-3.65E-02	4.02E-09	-0.715
123	4.20E+02	0.00E+00	8.00E+02	3	-3.73E-02	4.12E-09	-0.712
124	4.40E+02	0.00E+00	8.00E+02	3	-3.79E-02	4.22E-09	-0.709
125	4.60E+02	0.00E+00	8.00E+02	3	-3.83E-02	4.32E-09	-0.706
126	4.80E+02	0.00E+00	8.00E+02	3	-3.84E-02	4.43E-09	-0.703
127	5.00E+02	0.00E+00	8.00E+02	3	-3.82E-02	4.53E-09	-0.7
128	5.20E+02	0.00E+00	8.00E+02	3	-3.78E-02	4.64E-09	-0.697
129	5.40E+02	0.00E+00	8.00E+02	3	-3.72E-02	4.75E-09	-0.694
130	5.60E+02	0.00E+00	8.00E+02	3	-3.64E-02	4.86E-09	-0.691
131	5.80E+02	0.00E+00	8.00E+02	3	-3.53E-02	4.98E-09	-0.688
132	6.00E+02	0.00E+00	8.00E+02	3	-3.41E-02	5.09E-09	-0.685
133	6.20E+02	0.00E+00	8.00E+02	3	-3.26E-02	5.21E-09	-0.682
134	6.40E+02	0.00E+00	8.00E+02	3	-3.10E-02	5.33E-09	-0.68
135	6.60E+02	0.00E+00	8.00E+02	3	-2.93E-02	5.45E-09	-0.677
136	6.80E+02	0.00E+00	8.00E+02	3	-2.73E-02	5.57E-09	-0.675
137	7.00E+02	0.00E+00	8.00E+02	3	-2.53E-02	5.69E-09	-0.673
138	7.20E+02	0.00E+00	8.00E+02	3	-2.31E-02	5.82E-09	-0.671
139	7.40E+02	0.00E+00	8.00E+02	3	-2.08E-02	5.94E-09	-0.669
140	7.60E+02	0.00E+00	8.00E+02	3	-1.84E-02	6.07E-09	-0.668
141	7.80E+02	0.00E+00	8.00E+02	3	-1.60E-02	6.19E-09	-0.666
142	8.00E+02	0.00E+00	8.00E+02	3	-1.34E-02	6.32E-09	-0.665
143	8.20E+02	0.00E+00	8.00E+02	3	-1.08E-02	6.44E-09	-0.664
144	8.40E+02	0.00E+00	8.00E+02	3	-8.14E-03	6.57E-09	-0.663
145	8.60E+02	0.00E+00	8.00E+02	3	-5.45E-03	6.69E-09	-0.663

146	8.80E+02	0.00E+00	8.00E+02	3	-2.73E-03	6.81E-09	-0.663
147	9.00E+02	0.00E+00	8.00E+02	3	0.00E+00	6.94E-09	-0.662
148	9.20E+02	0.00E+00	8.00E+02	3	2.73E-03	7.05E-09	-0.663
149	9.40E+02	0.00E+00	8.00E+02	3	5.45E-03	7.17E-09	-0.663
150	9.60E+02	0.00E+00	8.00E+02	3	8.14E-03	7.28E-09	-0.663
151	9.80E+02	0.00E+00	8.00E+02	3	1.08E-02	7.39E-09	-0.664
152	1.00E+03	0.00E+00	8.00E+02	3	1.34E-02	7.49E-09	-0.665

Table B-2: Displacement of Pavement of Layered Elastic System

No.	Coordinates				Normal Strain			Shear Strain		
	X	Y	Z	L	XX	YY	ZZ	XZ	YZ	XY
1	-5.00E+02	0.00E+00	3.00E+02	2	2.00E-04	-1.12E-04	5.88E-05	-2.65E-04	-2.32E-11	2.73E-11
2	-4.80E+02	0.00E+00	3.00E+02	2	2.06E-04	-1.30E-04	8.15E-05	-2.93E-04	-2.56E-11	2.94E-11
3	-4.60E+02	0.00E+00	3.00E+02	2	2.08E-04	-1.51E-04	1.10E-04	-3.24E-04	-2.83E-11	3.14E-11
4	-4.40E+02	0.00E+00	3.00E+02	2	2.04E-04	-1.75E-04	1.47E-04	-3.56E-04	-3.11E-11	3.31E-11
5	-4.20E+02	0.00E+00	3.00E+02	2	1.91E-04	-2.01E-04	1.91E-04	-3.90E-04	-3.41E-11	3.43E-11
6	-4.00E+02	0.00E+00	3.00E+02	2	1.70E-04	-2.30E-04	2.45E-04	-4.22E-04	-3.69E-11	3.50E-11
7	-3.80E+02	0.00E+00	3.00E+02	2	1.39E-04	-2.61E-04	3.08E-04	-4.51E-04	-3.94E-11	3.50E-11
8	-3.60E+02	0.00E+00	3.00E+02	2	9.89E-05	-2.94E-04	3.79E-04	-4.75E-04	-4.15E-11	3.43E-11
9	-3.40E+02	0.00E+00	3.00E+02	2	4.98E-05	-3.28E-04	4.58E-04	-4.92E-04	-4.30E-11	3.30E-11
10	-3.20E+02	0.00E+00	3.00E+02	2	-5.86E-06	-3.62E-04	5.41E-04	-4.99E-04	-4.36E-11	3.12E-11
11	-3.00E+02	0.00E+00	3.00E+02	2	-6.55E-05	-3.97E-04	6.27E-04	-4.95E-04	-4.33E-11	2.90E-11
12	-2.80E+02	0.00E+00	3.00E+02	2	-1.26E-04	-4.30E-04	7.12E-04	-4.80E-04	-4.20E-11	2.66E-11
13	-2.60E+02	0.00E+00	3.00E+02	2	-1.83E-04	-4.63E-04	7.93E-04	-4.54E-04	-3.97E-11	2.45E-11
14	-2.40E+02	0.00E+00	3.00E+02	2	-2.33E-04	-4.93E-04	8.66E-04	-4.17E-04	-3.64E-11	2.27E-11
15	-2.20E+02	0.00E+00	3.00E+02	2	-2.74E-04	-5.20E-04	9.30E-04	-3.71E-04	-3.25E-11	2.15E-11
16	-2.00E+02	0.00E+00	3.00E+02	2	-3.02E-04	-5.44E-04	9.81E-04	-3.20E-04	-2.80E-11	2.11E-11
17	-1.80E+02	0.00E+00	3.00E+02	2	-3.17E-04	-5.64E-04	1.02E-03	-2.65E-04	-2.32E-11	2.16E-11
18	-1.60E+02	0.00E+00	3.00E+02	2	-3.18E-04	-5.81E-04	1.04E-03	-2.11E-04	-2.01E-11	2.30E-11
19	-1.40E+02	0.00E+00	3.00E+02	2	-3.06E-04	-5.95E-04	1.06E-03	-1.60E-04	-2.24E-11	2.45E-11
20	-1.20E+02	0.00E+00	3.00E+02	2	-2.85E-04	-6.06E-04	1.06E-03	-1.14E-04	-2.48E-11	2.57E-11
21	-1.00E+02	0.00E+00	3.00E+02	2	-2.57E-04	-6.13E-04	1.05E-03	-7.68E-05	-2.73E-11	2.64E-11
22	-8.00E+01	0.00E+00	3.00E+02	2	-2.26E-04	-6.19E-04	1.04E-03	-4.81E-05	-2.96E-11	2.65E-11
23	-6.00E+01	0.00E+00	3.00E+02	2	-1.97E-04	-6.22E-04	1.03E-03	-2.80E-05	-3.18E-11	2.60E-11
24	-4.00E+01	0.00E+00	3.00E+02	2	-1.73E-04	-6.25E-04	1.02E-03	-1.54E-05	-3.35E-11	2.48E-11

25	-2.00E+01	0.00E+00	3.00E+02	2	-1.58E-04	-6.26E-04	1.01E-03	-8.33E-06	-3.46E-11	2.29E-11
26	0.00E+00	0.00E+00	3.00E+02	2	-1.53E-04	-6.26E-04	1.01E-03	-4.15E-06	-3.49E-11	2.03E-11
27	2.00E+01	0.00E+00	3.00E+02	2	-1.58E-04	-6.26E-04	1.01E-03	1.41E-07	-3.43E-11	1.72E-11
28	4.00E+01	0.00E+00	3.00E+02	2	-1.74E-04	-6.24E-04	1.02E-03	7.48E-06	-3.26E-11	1.38E-11
29	6.00E+01	0.00E+00	3.00E+02	2	-1.98E-04	-6.22E-04	1.03E-03	2.05E-05	-2.98E-11	1.03E-11
30	8.00E+01	0.00E+00	3.00E+02	2	-2.27E-04	-6.18E-04	1.04E-03	4.10E-05	-2.59E-11	6.89E-12
31	1.00E+02	0.00E+00	3.00E+02	2	-2.57E-04	-6.12E-04	1.05E-03	7.01E-05	-2.10E-11	3.90E-12
32	1.20E+02	0.00E+00	3.00E+02	2	-2.84E-04	-6.04E-04	1.06E-03	1.08E-04	-1.52E-11	1.52E-12
33	1.40E+02	0.00E+00	3.00E+02	2	-3.04E-04	-5.94E-04	1.06E-03	1.53E-04	-8.86E-12	-6.92E-14
34	1.60E+02	0.00E+00	3.00E+02	2	-3.15E-04	-5.80E-04	1.04E-03	2.04E-04	-2.16E-12	-7.37E-13
35	1.80E+02	0.00E+00	3.00E+02	2	-3.12E-04	-5.62E-04	1.02E-03	2.58E-04	-4.89E-13	-7.10E-13
36	2.00E+02	0.00E+00	3.00E+02	2	-2.97E-04	-5.42E-04	9.78E-04	3.12E-04	-5.40E-13	-6.57E-13
37	2.20E+02	0.00E+00	3.00E+02	2	-2.68E-04	-5.17E-04	9.27E-04	3.63E-04	-6.03E-13	-6.15E-13
38	2.40E+02	0.00E+00	3.00E+02	2	-2.27E-04	-4.90E-04	8.63E-04	4.07E-04	-6.72E-13	-5.88E-13
39	2.60E+02	0.00E+00	3.00E+02	2	-1.77E-04	-4.60E-04	7.90E-04	4.43E-04	-7.41E-13	-5.78E-13
40	2.80E+02	0.00E+00	3.00E+02	2	-1.20E-04	-4.28E-04	7.09E-04	4.69E-04	-8.07E-13	-5.84E-13
41	3.00E+02	0.00E+00	3.00E+02	2	-6.01E-05	-3.94E-04	6.25E-04	4.84E-04	-8.63E-13	-5.99E-13
42	3.20E+02	0.00E+00	3.00E+02	2	-7.74E-07	-3.59E-04	5.39E-04	4.87E-04	-9.08E-13	-6.17E-13
43	3.40E+02	0.00E+00	3.00E+02	2	5.49E-05	-3.24E-04	4.56E-04	4.80E-04	-9.42E-13	-6.26E-13
44	3.60E+02	0.00E+00	3.00E+02	2	1.04E-04	-2.90E-04	3.78E-04	4.63E-04	-9.68E-13	-6.20E-13
45	3.80E+02	0.00E+00	3.00E+02	2	1.45E-04	-2.57E-04	3.06E-04	4.39E-04	-9.91E-13	-5.90E-13
46	4.00E+02	0.00E+00	3.00E+02	2	1.77E-04	-2.26E-04	2.43E-04	4.10E-04	-1.02E-12	-5.34E-13
47	4.20E+02	0.00E+00	3.00E+02	2	2.00E-04	-1.97E-04	1.88E-04	3.77E-04	-1.06E-12	-4.52E-13
48	4.40E+02	0.00E+00	3.00E+02	2	2.14E-04	-1.71E-04	1.43E-04	3.43E-04	-1.11E-12	-3.50E-13
49	4.60E+02	0.00E+00	3.00E+02	2	2.20E-04	-1.47E-04	1.06E-04	3.10E-04	-1.18E-12	-2.35E-13
50	4.80E+02	0.00E+00	3.00E+02	2	2.19E-04	-1.26E-04	7.59E-05	2.78E-04	-1.27E-12	-1.18E-13

51	5.00E+02	0.00E+00	3.00E+02	2	2.15E-04	-1.07E-04	5.28E-05	2.49E-04	-1.38E-12	-9.05E-15
52	5.20E+02	0.00E+00	3.00E+02	2	2.07E-04	-9.08E-05	3.48E-05	2.22E-04	-1.51E-12	8.52E-14
53	5.40E+02	0.00E+00	3.00E+02	2	1.97E-04	-7.65E-05	2.10E-05	1.99E-04	-1.64E-12	1.60E-13
54	5.60E+02	0.00E+00	3.00E+02	2	1.87E-04	-6.41E-05	1.01E-05	1.78E-04	-1.77E-12	2.18E-13
55	5.80E+02	0.00E+00	3.00E+02	2	1.77E-04	-5.33E-05	1.31E-06	1.60E-04	-1.89E-12	2.63E-13
56	6.00E+02	0.00E+00	3.00E+02	2	1.68E-04	-4.39E-05	-5.89E-06	1.44E-04	-1.99E-12	3.08E-13
57	6.20E+02	0.00E+00	3.00E+02	2	1.60E-04	-3.56E-05	-1.20E-05	1.30E-04	-2.09E-12	3.64E-13
58	6.40E+02	0.00E+00	3.00E+02	2	1.53E-04	-2.83E-05	-1.72E-05	1.16E-04	-2.17E-12	4.46E-13
59	6.60E+02	0.00E+00	3.00E+02	2	1.46E-04	-2.20E-05	-2.16E-05	1.04E-04	-2.25E-12	5.65E-13
60	6.80E+02	0.00E+00	3.00E+02	2	1.40E-04	-1.64E-05	-2.52E-05	9.19E-05	-2.34E-12	7.29E-13
61	7.00E+02	0.00E+00	3.00E+02	2	1.35E-04	-1.15E-05	-2.81E-05	8.06E-05	-2.44E-12	9.40E-13
62	7.20E+02	0.00E+00	3.00E+02	2	1.29E-04	-7.34E-06	-3.02E-05	6.99E-05	-2.56E-12	1.19E-12
63	7.40E+02	0.00E+00	3.00E+02	2	1.24E-04	-3.78E-06	-3.15E-05	5.97E-05	-2.72E-12	1.48E-12
64	7.60E+02	0.00E+00	3.00E+02	2	1.19E-04	-8.06E-07	-3.22E-05	5.02E-05	-2.91E-12	1.79E-12
65	7.80E+02	0.00E+00	3.00E+02	2	1.14E-04	1.63E-06	-3.23E-05	4.13E-05	-3.13E-12	2.10E-12
66	8.00E+02	0.00E+00	3.00E+02	2	1.09E-04	3.56E-06	-3.20E-05	3.31E-05	-3.39E-12	2.41E-12
67	8.20E+02	0.00E+00	3.00E+02	2	1.05E-04	5.05E-06	-3.14E-05	2.56E-05	-3.66E-12	2.71E-12
68	8.40E+02	0.00E+00	3.00E+02	2	1.02E-04	6.14E-06	-3.08E-05	1.86E-05	-3.94E-12	3.00E-12
69	8.60E+02	0.00E+00	3.00E+02	2	9.92E-05	6.88E-06	-3.02E-05	1.21E-05	-4.22E-12	3.29E-12
70	8.80E+02	0.00E+00	3.00E+02	2	9.77E-05	7.31E-06	-2.99E-05	5.97E-06	-4.49E-12	3.59E-12
71	9.00E+02	0.00E+00	3.00E+02	2	9.71E-05	7.45E-06	-2.97E-05	-9.10E-13	-4.75E-12	3.92E-12
72	9.20E+02	0.00E+00	3.00E+02	2	9.77E-05	7.31E-06	-2.99E-05	-5.97E-06	-5.01E-12	4.31E-12
73	9.40E+02	0.00E+00	3.00E+02	2	9.92E-05	6.88E-06	-3.02E-05	-1.21E-05	-5.27E-12	4.79E-12
74	9.60E+02	0.00E+00	3.00E+02	2	1.02E-04	6.14E-06	-3.08E-05	-1.86E-05	-5.56E-12	5.36E-12
75	9.80E+02	0.00E+00	3.00E+02	2	1.05E-04	5.05E-06	-3.14E-05	-2.56E-05	-5.89E-12	6.03E-12
76	1.00E+03	0.00E+00	3.00E+02	2	1.09E-04	3.56E-06	-3.20E-05	-3.31E-05	-6.28E-12	6.82E-12

77	-5.00E+02	0.00E+00	8.00E+02	3	-2.71E-05	-2.04E-04	2.92E-04	-2.24E-04	-1.96E-11	1.55E-11
78	-4.80E+02	0.00E+00	8.00E+02	3	-3.75E-05	-2.11E-04	3.07E-04	-2.24E-04	-1.96E-11	1.51E-11
79	-4.60E+02	0.00E+00	8.00E+02	3	-4.82E-05	-2.17E-04	3.22E-04	-2.24E-04	-1.96E-11	1.47E-11
80	-4.40E+02	0.00E+00	8.00E+02	3	-5.92E-05	-2.23E-04	3.38E-04	-2.23E-04	-1.95E-11	1.43E-11
81	-4.20E+02	0.00E+00	8.00E+02	3	-7.04E-05	-2.30E-04	3.53E-04	-2.21E-04	-1.93E-11	1.39E-11
82	-4.00E+02	0.00E+00	8.00E+02	3	-8.17E-05	-2.36E-04	3.68E-04	-2.18E-04	-1.91E-11	1.35E-11
83	-3.80E+02	0.00E+00	8.00E+02	3	-9.31E-05	-2.42E-04	3.83E-04	-2.15E-04	-1.88E-11	1.30E-11
84	-3.60E+02	0.00E+00	8.00E+02	3	-1.05E-04	-2.48E-04	3.98E-04	-2.11E-04	-1.85E-11	1.26E-11
85	-3.40E+02	0.00E+00	8.00E+02	3	-1.16E-04	-2.54E-04	4.13E-04	-2.06E-04	-1.81E-11	1.21E-11
86	-3.20E+02	0.00E+00	8.00E+02	3	-1.27E-04	-2.60E-04	4.28E-04	-2.01E-04	-1.76E-11	1.16E-11
87	-3.00E+02	0.00E+00	8.00E+02	3	-1.38E-04	-2.65E-04	4.42E-04	-1.95E-04	-1.70E-11	1.11E-11
88	-2.80E+02	0.00E+00	8.00E+02	3	-1.49E-04	-2.71E-04	4.55E-04	-1.88E-04	-1.64E-11	1.07E-11
89	-2.60E+02	0.00E+00	8.00E+02	3	-1.59E-04	-2.76E-04	4.69E-04	-1.80E-04	-1.57E-11	1.02E-11
90	-2.40E+02	0.00E+00	8.00E+02	3	-1.69E-04	-2.81E-04	4.81E-04	-1.72E-04	-1.50E-11	9.79E-12
91	-2.20E+02	0.00E+00	8.00E+02	3	-1.78E-04	-2.86E-04	4.93E-04	-1.62E-04	-1.42E-11	9.38E-12
92	-2.00E+02	0.00E+00	8.00E+02	3	-1.87E-04	-2.90E-04	5.04E-04	-1.53E-04	-1.33E-11	8.99E-12
93	-1.80E+02	0.00E+00	8.00E+02	3	-1.95E-04	-2.94E-04	5.15E-04	-1.42E-04	-1.24E-11	8.64E-12
94	-1.60E+02	0.00E+00	8.00E+02	3	-2.03E-04	-2.98E-04	5.24E-04	-1.31E-04	-1.17E-11	8.32E-12
95	-1.40E+02	0.00E+00	8.00E+02	3	-2.09E-04	-3.01E-04	5.33E-04	-1.20E-04	-1.14E-11	8.00E-12
96	-1.20E+02	0.00E+00	8.00E+02	3	-2.15E-04	-3.04E-04	5.41E-04	-1.07E-04	-1.12E-11	7.69E-12
97	-1.00E+02	0.00E+00	8.00E+02	3	-2.20E-04	-3.07E-04	5.47E-04	-9.50E-05	-1.09E-11	7.38E-12
98	-8.00E+01	0.00E+00	8.00E+02	3	-2.24E-04	-3.10E-04	5.53E-04	-8.21E-05	-1.05E-11	7.07E-12
99	-6.00E+01	0.00E+00	8.00E+02	3	-2.27E-04	-3.12E-04	5.57E-04	-6.90E-05	-1.01E-11	6.78E-12
100	-4.00E+01	0.00E+00	8.00E+02	3	-2.29E-04	-3.13E-04	5.61E-04	-5.57E-05	-9.64E-12	6.51E-12
101	-2.00E+01	0.00E+00	8.00E+02	3	-2.30E-04	-3.14E-04	5.63E-04	-4.22E-05	-9.14E-12	6.27E-12
102	0.00E+00	0.00E+00	8.00E+02	3	-2.29E-04	-3.15E-04	5.64E-04	-2.87E-05	-8.61E-12	6.05E-12

103	2.00E+01	0.00E+00	8.00E+02	3	-2.28E-04	-3.16E-04	5.63E-04	-1.52E-05	-8.04E-12	5.86E-12
104	4.00E+01	0.00E+00	8.00E+02	3	-2.26E-04	-3.16E-04	5.62E-04	-1.79E-06	-7.44E-12	5.71E-12
105	6.00E+01	0.00E+00	8.00E+02	3	-2.22E-04	-3.15E-04	5.59E-04	1.14E-05	-6.82E-12	5.60E-12
106	8.00E+01	0.00E+00	8.00E+02	3	-2.17E-04	-3.14E-04	5.55E-04	2.43E-05	-6.17E-12	5.53E-12
107	1.00E+02	0.00E+00	8.00E+02	3	-2.12E-04	-3.13E-04	5.50E-04	3.68E-05	-5.51E-12	5.50E-12
108	1.20E+02	0.00E+00	8.00E+02	3	-2.05E-04	-3.12E-04	5.44E-04	4.89E-05	-4.83E-12	5.53E-12
109	1.40E+02	0.00E+00	8.00E+02	3	-1.98E-04	-3.10E-04	5.37E-04	6.05E-05	-4.15E-12	5.60E-12
110	1.60E+02	0.00E+00	8.00E+02	3	-1.90E-04	-3.08E-04	5.29E-04	7.16E-05	-3.46E-12	5.71E-12
111	1.80E+02	0.00E+00	8.00E+02	3	-1.80E-04	-3.05E-04	5.20E-04	8.20E-05	-3.37E-12	5.87E-12
112	2.00E+02	0.00E+00	8.00E+02	3	-1.71E-04	-3.02E-04	5.11E-04	9.18E-05	-3.49E-12	6.03E-12
113	2.20E+02	0.00E+00	8.00E+02	3	-1.60E-04	-2.99E-04	5.00E-04	1.01E-04	-3.61E-12	6.20E-12
114	2.40E+02	0.00E+00	8.00E+02	3	-1.49E-04	-2.96E-04	4.89E-04	1.09E-04	-3.73E-12	6.37E-12
115	2.60E+02	0.00E+00	8.00E+02	3	-1.38E-04	-2.92E-04	4.77E-04	1.17E-04	-3.86E-12	6.54E-12
116	2.80E+02	0.00E+00	8.00E+02	3	-1.26E-04	-2.89E-04	4.65E-04	1.24E-04	-3.99E-12	6.72E-12
117	3.00E+02	0.00E+00	8.00E+02	3	-1.13E-04	-2.85E-04	4.52E-04	1.30E-04	-4.13E-12	6.91E-12
118	3.20E+02	0.00E+00	8.00E+02	3	-1.01E-04	-2.80E-04	4.39E-04	1.35E-04	-4.28E-12	7.09E-12
119	3.40E+02	0.00E+00	8.00E+02	3	-8.78E-05	-2.76E-04	4.25E-04	1.39E-04	-4.43E-12	7.29E-12
120	3.60E+02	0.00E+00	8.00E+02	3	-7.48E-05	-2.72E-04	4.12E-04	1.43E-04	-4.59E-12	7.49E-12
121	3.80E+02	0.00E+00	8.00E+02	3	-6.18E-05	-2.67E-04	3.98E-04	1.45E-04	-4.75E-12	7.69E-12
122	4.00E+02	0.00E+00	8.00E+02	3	-4.88E-05	-2.63E-04	3.84E-04	1.47E-04	-4.92E-12	7.90E-12
123	4.20E+02	0.00E+00	8.00E+02	3	-3.59E-05	-2.58E-04	3.69E-04	1.48E-04	-5.09E-12	8.12E-12
124	4.40E+02	0.00E+00	8.00E+02	3	-2.31E-05	-2.53E-04	3.55E-04	1.48E-04	-5.27E-12	8.34E-12
125	4.60E+02	0.00E+00	8.00E+02	3	-1.05E-05	-2.49E-04	3.42E-04	1.47E-04	-5.46E-12	8.56E-12
126	4.80E+02	0.00E+00	8.00E+02	3	1.79E-06	-2.44E-04	3.28E-04	1.46E-04	-5.66E-12	8.79E-12
127	5.00E+02	0.00E+00	8.00E+02	3	1.38E-05	-2.40E-04	3.14E-04	1.44E-04	-5.87E-12	9.02E-12
128	5.20E+02	0.00E+00	8.00E+02	3	2.54E-05	-2.35E-04	3.01E-04	1.41E-04	-6.08E-12	9.26E-12

129	5.40E+02	0.00E+00	8.00E+02	3	3.65E-05	-2.31E-04	2.89E-04	1.37E-04	-6.30E-12	9.51E-12
130	5.60E+02	0.00E+00	8.00E+02	3	4.72E-05	-2.27E-04	2.76E-04	1.33E-04	-6.53E-12	9.76E-12
131	5.80E+02	0.00E+00	8.00E+02	3	5.73E-05	-2.23E-04	2.64E-04	1.28E-04	-6.77E-12	1.00E-11
132	6.00E+02	0.00E+00	8.00E+02	3	6.69E-05	-2.19E-04	2.53E-04	1.23E-04	-7.02E-12	1.03E-11
133	6.20E+02	0.00E+00	8.00E+02	3	7.60E-05	-2.15E-04	2.42E-04	1.17E-04	-7.28E-12	1.05E-11
134	6.40E+02	0.00E+00	8.00E+02	3	8.44E-05	-2.11E-04	2.32E-04	1.10E-04	-7.55E-12	1.08E-11
135	6.60E+02	0.00E+00	8.00E+02	3	9.22E-05	-2.08E-04	2.23E-04	1.03E-04	-7.83E-12	1.11E-11
136	6.80E+02	0.00E+00	8.00E+02	3	9.94E-05	-2.05E-04	2.14E-04	9.60E-05	-8.12E-12	1.13E-11
137	7.00E+02	0.00E+00	8.00E+02	3	1.06E-04	-2.02E-04	2.06E-04	8.83E-05	-8.42E-12	1.16E-11
138	7.20E+02	0.00E+00	8.00E+02	3	1.12E-04	-1.99E-04	1.99E-04	8.03E-05	-8.73E-12	1.19E-11
139	7.40E+02	0.00E+00	8.00E+02	3	1.17E-04	-1.97E-04	1.92E-04	7.20E-05	-9.05E-12	1.21E-11
140	7.60E+02	0.00E+00	8.00E+02	3	1.22E-04	-1.95E-04	1.86E-04	6.35E-05	-9.39E-12	1.24E-11
141	7.80E+02	0.00E+00	8.00E+02	3	1.26E-04	-1.93E-04	1.81E-04	5.48E-05	-9.73E-12	1.27E-11
142	8.00E+02	0.00E+00	8.00E+02	3	1.29E-04	-1.91E-04	1.77E-04	4.59E-05	-1.01E-11	1.30E-11
143	8.20E+02	0.00E+00	8.00E+02	3	1.32E-04	-1.90E-04	1.74E-04	3.69E-05	-1.05E-11	1.32E-11
144	8.40E+02	0.00E+00	8.00E+02	3	1.34E-04	-1.89E-04	1.71E-04	2.78E-05	-1.08E-11	1.35E-11
145	8.60E+02	0.00E+00	8.00E+02	3	1.35E-04	-1.88E-04	1.69E-04	1.86E-05	-1.12E-11	1.37E-11
146	8.80E+02	0.00E+00	8.00E+02	3	1.36E-04	-1.88E-04	1.68E-04	9.29E-06	-1.16E-11	1.40E-11
147	9.00E+02	0.00E+00	8.00E+02	3	1.37E-04	-1.88E-04	1.67E-04	-7.28E-12	-1.20E-11	1.42E-11
148	9.20E+02	0.00E+00	8.00E+02	3	1.36E-04	-1.88E-04	1.68E-04	-9.29E-06	-1.24E-11	1.44E-11
149	9.40E+02	0.00E+00	8.00E+02	3	1.35E-04	-1.88E-04	1.69E-04	-1.86E-05	-1.28E-11	1.46E-11
150	9.60E+02	0.00E+00	8.00E+02	3	1.34E-04	-1.89E-04	1.71E-04	-2.78E-05	-1.33E-11	1.48E-11
151	9.80E+02	0.00E+00	8.00E+02	3	1.32E-04	-1.90E-04	1.74E-04	-3.69E-05	-1.37E-11	1.49E-11
152	1.00E+03	0.00E+00	8.00E+02	3	1.29E-04	-1.91E-04	1.77E-04	-4.59E-05	-1.41E-11	1.51E-11

Table B-3: The Normal and Shear Stress Output of layered elastic system

No.	Coordinates				Normal Strain			Shear Strain		
	X	Y	Z	L	XX	YY	ZZ	XZ	YZ	XY
1	-5.00E+02	0.00E+00	3.00E+02	2	2.00E-04	-1.12E-04	5.88E-05	-2.65E-04	-2.32E-11	2.73E-11
2	-4.80E+02	0.00E+00	3.00E+02	2	2.06E-04	-1.30E-04	8.15E-05	-2.93E-04	-2.56E-11	2.94E-11
3	-4.60E+02	0.00E+00	3.00E+02	2	2.08E-04	-1.51E-04	1.10E-04	-3.24E-04	-2.83E-11	3.14E-11
4	-4.40E+02	0.00E+00	3.00E+02	2	2.04E-04	-1.75E-04	1.47E-04	-3.56E-04	-3.11E-11	3.31E-11
5	-4.20E+02	0.00E+00	3.00E+02	2	1.91E-04	-2.01E-04	1.91E-04	-3.90E-04	-3.41E-11	3.43E-11
6	-4.00E+02	0.00E+00	3.00E+02	2	1.70E-04	-2.30E-04	2.45E-04	-4.22E-04	-3.69E-11	3.50E-11
7	-3.80E+02	0.00E+00	3.00E+02	2	1.39E-04	-2.61E-04	3.08E-04	-4.51E-04	-3.94E-11	3.50E-11
8	-3.60E+02	0.00E+00	3.00E+02	2	9.89E-05	-2.94E-04	3.79E-04	-4.75E-04	-4.15E-11	3.43E-11
9	-3.40E+02	0.00E+00	3.00E+02	2	4.98E-05	-3.28E-04	4.58E-04	-4.92E-04	-4.30E-11	3.30E-11
10	-3.20E+02	0.00E+00	3.00E+02	2	-5.86E-06	-3.62E-04	5.41E-04	-4.99E-04	-4.36E-11	3.12E-11
11	-3.00E+02	0.00E+00	3.00E+02	2	-6.55E-05	-3.97E-04	6.27E-04	-4.95E-04	-4.33E-11	2.90E-11
12	-2.80E+02	0.00E+00	3.00E+02	2	-1.26E-04	-4.30E-04	7.12E-04	-4.80E-04	-4.20E-11	2.66E-11
13	-2.60E+02	0.00E+00	3.00E+02	2	-1.83E-04	-4.63E-04	7.93E-04	-4.54E-04	-3.97E-11	2.45E-11
14	-2.40E+02	0.00E+00	3.00E+02	2	-2.33E-04	-4.93E-04	8.66E-04	-4.17E-04	-3.64E-11	2.27E-11
15	-2.20E+02	0.00E+00	3.00E+02	2	-2.74E-04	-5.20E-04	9.30E-04	-3.71E-04	-3.25E-11	2.15E-11
16	-2.00E+02	0.00E+00	3.00E+02	2	-3.02E-04	-5.44E-04	9.81E-04	-3.20E-04	-2.80E-11	2.11E-11
17	-1.80E+02	0.00E+00	3.00E+02	2	-3.17E-04	-5.64E-04	1.02E-03	-2.65E-04	-2.32E-11	2.16E-11
18	-1.60E+02	0.00E+00	3.00E+02	2	-3.18E-04	-5.81E-04	1.04E-03	-2.11E-04	-2.01E-11	2.30E-11
19	-1.40E+02	0.00E+00	3.00E+02	2	-3.06E-04	-5.95E-04	1.06E-03	-1.60E-04	-2.24E-11	2.45E-11
20	-1.20E+02	0.00E+00	3.00E+02	2	-2.85E-04	-6.06E-04	1.06E-03	-1.14E-04	-2.48E-11	2.57E-11
21	-1.00E+02	0.00E+00	3.00E+02	2	-2.57E-04	-6.13E-04	1.05E-03	-7.68E-05	-2.73E-11	2.64E-11
22	-8.00E+01	0.00E+00	3.00E+02	2	-2.26E-04	-6.19E-04	1.04E-03	-4.81E-05	-2.96E-11	2.65E-11
23	-6.00E+01	0.00E+00	3.00E+02	2	-1.97E-04	-6.22E-04	1.03E-03	-2.80E-05	-3.18E-11	2.60E-11
24	-4.00E+01	0.00E+00	3.00E+02	2	-1.73E-04	-6.25E-04	1.02E-03	-1.54E-05	-3.35E-11	2.48E-11
25	-2.00E+01	0.00E+00	3.00E+02	2	-1.58E-04	-6.26E-04	1.01E-03	-8.33E-06	-3.46E-11	2.29E-11
26	0.00E+00	0.00E+00	3.00E+02	2	-1.53E-04	-6.26E-04	1.01E-03	-4.15E-06	-3.49E-11	2.03E-11
27	2.00E+01	0.00E+00	3.00E+02	2	-1.58E-04	-6.26E-04	1.01E-03	1.41E-07	-3.43E-11	1.72E-11
28	4.00E+01	0.00E+00	3.00E+02	2	-1.74E-04	-6.24E-04	1.02E-03	7.48E-06	-3.26E-11	1.38E-11

29	6.00E+01	0.00E+00	3.00E+02	2	-1.98E-04	-6.22E-04	1.03E-03	2.05E-05	-2.98E-11	1.03E-11
30	8.00E+01	0.00E+00	3.00E+02	2	-2.27E-04	-6.18E-04	1.04E-03	4.10E-05	-2.59E-11	6.89E-12
31	1.00E+02	0.00E+00	3.00E+02	2	-2.57E-04	-6.12E-04	1.05E-03	7.01E-05	-2.10E-11	3.90E-12
32	1.20E+02	0.00E+00	3.00E+02	2	-2.84E-04	-6.04E-04	1.06E-03	1.08E-04	-1.52E-11	1.52E-12
33	1.40E+02	0.00E+00	3.00E+02	2	-3.04E-04	-5.94E-04	1.06E-03	1.53E-04	-8.86E-12	-6.92E-14
34	1.60E+02	0.00E+00	3.00E+02	2	-3.15E-04	-5.80E-04	1.04E-03	2.04E-04	-2.16E-12	-7.37E-13
35	1.80E+02	0.00E+00	3.00E+02	2	-3.12E-04	-5.62E-04	1.02E-03	2.58E-04	-4.89E-13	-7.10E-13
36	2.00E+02	0.00E+00	3.00E+02	2	-2.97E-04	-5.42E-04	9.78E-04	3.12E-04	-5.40E-13	-6.57E-13
37	2.20E+02	0.00E+00	3.00E+02	2	-2.68E-04	-5.17E-04	9.27E-04	3.63E-04	-6.03E-13	-6.15E-13
38	2.40E+02	0.00E+00	3.00E+02	2	-2.27E-04	-4.90E-04	8.63E-04	4.07E-04	-6.72E-13	-5.88E-13
39	2.60E+02	0.00E+00	3.00E+02	2	-1.77E-04	-4.60E-04	7.90E-04	4.43E-04	-7.41E-13	-5.78E-13
40	2.80E+02	0.00E+00	3.00E+02	2	-1.20E-04	-4.28E-04	7.09E-04	4.69E-04	-8.07E-13	-5.84E-13
41	3.00E+02	0.00E+00	3.00E+02	2	-6.01E-05	-3.94E-04	6.25E-04	4.84E-04	-8.63E-13	-5.99E-13
42	3.20E+02	0.00E+00	3.00E+02	2	-7.74E-07	-3.59E-04	5.39E-04	4.87E-04	-9.08E-13	-6.17E-13
43	3.40E+02	0.00E+00	3.00E+02	2	5.49E-05	-3.24E-04	4.56E-04	4.80E-04	-9.42E-13	-6.26E-13
44	3.60E+02	0.00E+00	3.00E+02	2	1.04E-04	-2.90E-04	3.78E-04	4.63E-04	-9.68E-13	-6.20E-13
45	3.80E+02	0.00E+00	3.00E+02	2	1.45E-04	-2.57E-04	3.06E-04	4.39E-04	-9.91E-13	-5.90E-13
46	4.00E+02	0.00E+00	3.00E+02	2	1.77E-04	-2.26E-04	2.43E-04	4.10E-04	-1.02E-12	-5.34E-13
47	4.20E+02	0.00E+00	3.00E+02	2	2.00E-04	-1.97E-04	1.88E-04	3.77E-04	-1.06E-12	-4.52E-13
48	4.40E+02	0.00E+00	3.00E+02	2	2.14E-04	-1.71E-04	1.43E-04	3.43E-04	-1.11E-12	-3.50E-13
49	4.60E+02	0.00E+00	3.00E+02	2	2.20E-04	-1.47E-04	1.06E-04	3.10E-04	-1.18E-12	-2.35E-13
50	4.80E+02	0.00E+00	3.00E+02	2	2.19E-04	-1.26E-04	7.59E-05	2.78E-04	-1.27E-12	-1.18E-13
51	5.00E+02	0.00E+00	3.00E+02	2	2.15E-04	-1.07E-04	5.28E-05	2.49E-04	-1.38E-12	-9.05E-15
52	5.20E+02	0.00E+00	3.00E+02	2	2.07E-04	-9.08E-05	3.48E-05	2.22E-04	-1.51E-12	8.52E-14
53	5.40E+02	0.00E+00	3.00E+02	2	1.97E-04	-7.65E-05	2.10E-05	1.99E-04	-1.64E-12	1.60E-13
54	5.60E+02	0.00E+00	3.00E+02	2	1.87E-04	-6.41E-05	1.01E-05	1.78E-04	-1.77E-12	2.18E-13
55	5.80E+02	0.00E+00	3.00E+02	2	1.77E-04	-5.33E-05	1.31E-06	1.60E-04	-1.89E-12	2.63E-13
56	6.00E+02	0.00E+00	3.00E+02	2	1.68E-04	-4.39E-05	-5.89E-06	1.44E-04	-1.99E-12	3.08E-13
57	6.20E+02	0.00E+00	3.00E+02	2	1.60E-04	-3.56E-05	-1.20E-05	1.30E-04	-2.09E-12	3.64E-13
58	6.40E+02	0.00E+00	3.00E+02	2	1.53E-04	-2.83E-05	-1.72E-05	1.16E-04	-2.17E-12	4.46E-13

59	6.60E+02	0.00E+00	3.00E+02	2	1.46E-04	-2.20E-05	-2.16E-05	1.04E-04	-2.25E-12	5.65E-13
60	6.80E+02	0.00E+00	3.00E+02	2	1.40E-04	-1.64E-05	-2.52E-05	9.19E-05	-2.34E-12	7.29E-13
61	7.00E+02	0.00E+00	3.00E+02	2	1.35E-04	-1.15E-05	-2.81E-05	8.06E-05	-2.44E-12	9.40E-13
62	7.20E+02	0.00E+00	3.00E+02	2	1.29E-04	-7.34E-06	-3.02E-05	6.99E-05	-2.56E-12	1.19E-12
63	7.40E+02	0.00E+00	3.00E+02	2	1.24E-04	-3.78E-06	-3.15E-05	5.97E-05	-2.72E-12	1.48E-12
64	7.60E+02	0.00E+00	3.00E+02	2	1.19E-04	-8.06E-07	-3.22E-05	5.02E-05	-2.91E-12	1.79E-12
65	7.80E+02	0.00E+00	3.00E+02	2	1.14E-04	1.63E-06	-3.23E-05	4.13E-05	-3.13E-12	2.10E-12
66	8.00E+02	0.00E+00	3.00E+02	2	1.09E-04	3.56E-06	-3.20E-05	3.31E-05	-3.39E-12	2.41E-12
67	8.20E+02	0.00E+00	3.00E+02	2	1.05E-04	5.05E-06	-3.14E-05	2.56E-05	-3.66E-12	2.71E-12
68	8.40E+02	0.00E+00	3.00E+02	2	1.02E-04	6.14E-06	-3.08E-05	1.86E-05	-3.94E-12	3.00E-12
69	8.60E+02	0.00E+00	3.00E+02	2	9.92E-05	6.88E-06	-3.02E-05	1.21E-05	-4.22E-12	3.29E-12
70	8.80E+02	0.00E+00	3.00E+02	2	9.77E-05	7.31E-06	-2.99E-05	5.97E-06	-4.49E-12	3.59E-12
71	9.00E+02	0.00E+00	3.00E+02	2	9.71E-05	7.45E-06	-2.97E-05	-9.10E-13	-4.75E-12	3.92E-12
72	9.20E+02	0.00E+00	3.00E+02	2	9.77E-05	7.31E-06	-2.99E-05	-5.97E-06	-5.01E-12	4.31E-12
73	9.40E+02	0.00E+00	3.00E+02	2	9.92E-05	6.88E-06	-3.02E-05	-1.21E-05	-5.27E-12	4.79E-12
74	9.60E+02	0.00E+00	3.00E+02	2	1.02E-04	6.14E-06	-3.08E-05	-1.86E-05	-5.56E-12	5.36E-12
75	9.80E+02	0.00E+00	3.00E+02	2	1.05E-04	5.05E-06	-3.14E-05	-2.56E-05	-5.89E-12	6.03E-12
76	1.00E+03	0.00E+00	3.00E+02	2	1.09E-04	3.56E-06	-3.20E-05	-3.31E-05	-6.28E-12	6.82E-12
77	-5.00E+02	0.00E+00	8.00E+02	3	-2.71E-05	-2.04E-04	2.92E-04	-2.24E-04	-1.96E-11	1.55E-11
78	-4.80E+02	0.00E+00	8.00E+02	3	-3.75E-05	-2.11E-04	3.07E-04	-2.24E-04	-1.96E-11	1.51E-11
79	-4.60E+02	0.00E+00	8.00E+02	3	-4.82E-05	-2.17E-04	3.22E-04	-2.24E-04	-1.96E-11	1.47E-11
80	-4.40E+02	0.00E+00	8.00E+02	3	-5.92E-05	-2.23E-04	3.38E-04	-2.23E-04	-1.95E-11	1.43E-11
81	-4.20E+02	0.00E+00	8.00E+02	3	-7.04E-05	-2.30E-04	3.53E-04	-2.21E-04	-1.93E-11	1.39E-11
82	-4.00E+02	0.00E+00	8.00E+02	3	-8.17E-05	-2.36E-04	3.68E-04	-2.18E-04	-1.91E-11	1.35E-11
83	-3.80E+02	0.00E+00	8.00E+02	3	-9.31E-05	-2.42E-04	3.83E-04	-2.15E-04	-1.88E-11	1.30E-11
84	-3.60E+02	0.00E+00	8.00E+02	3	-1.05E-04	-2.48E-04	3.98E-04	-2.11E-04	-1.85E-11	1.26E-11
85	-3.40E+02	0.00E+00	8.00E+02	3	-1.16E-04	-2.54E-04	4.13E-04	-2.06E-04	-1.81E-11	1.21E-11
86	-3.20E+02	0.00E+00	8.00E+02	3	-1.27E-04	-2.60E-04	4.28E-04	-2.01E-04	-1.76E-11	1.16E-11
87	-3.00E+02	0.00E+00	8.00E+02	3	-1.38E-04	-2.65E-04	4.42E-04	-1.95E-04	-1.70E-11	1.11E-11
88	-2.80E+02	0.00E+00	8.00E+02	3	-1.49E-04	-2.71E-04	4.55E-04	-1.88E-04	-1.64E-11	1.07E-11

89	-2.60E+02	0.00E+00	8.00E+02	3	-1.59E-04	-2.76E-04	4.69E-04	-1.80E-04	-1.57E-11	1.02E-11
90	-2.40E+02	0.00E+00	8.00E+02	3	-1.69E-04	-2.81E-04	4.81E-04	-1.72E-04	-1.50E-11	9.79E-12
91	-2.20E+02	0.00E+00	8.00E+02	3	-1.78E-04	-2.86E-04	4.93E-04	-1.62E-04	-1.42E-11	9.38E-12
92	-2.00E+02	0.00E+00	8.00E+02	3	-1.87E-04	-2.90E-04	5.04E-04	-1.53E-04	-1.33E-11	8.99E-12
93	-1.80E+02	0.00E+00	8.00E+02	3	-1.95E-04	-2.94E-04	5.15E-04	-1.42E-04	-1.24E-11	8.64E-12
94	-1.60E+02	0.00E+00	8.00E+02	3	-2.03E-04	-2.98E-04	5.24E-04	-1.31E-04	-1.17E-11	8.32E-12
95	-1.40E+02	0.00E+00	8.00E+02	3	-2.09E-04	-3.01E-04	5.33E-04	-1.20E-04	-1.14E-11	8.00E-12
96	-1.20E+02	0.00E+00	8.00E+02	3	-2.15E-04	-3.04E-04	5.41E-04	-1.07E-04	-1.12E-11	7.69E-12
97	-1.00E+02	0.00E+00	8.00E+02	3	-2.20E-04	-3.07E-04	5.47E-04	-9.50E-05	-1.09E-11	7.38E-12
98	-8.00E+01	0.00E+00	8.00E+02	3	-2.24E-04	-3.10E-04	5.53E-04	-8.21E-05	-1.05E-11	7.07E-12
99	-6.00E+01	0.00E+00	8.00E+02	3	-2.27E-04	-3.12E-04	5.57E-04	-6.90E-05	-1.01E-11	6.78E-12
100	-4.00E+01	0.00E+00	8.00E+02	3	-2.29E-04	-3.13E-04	5.61E-04	-5.57E-05	-9.64E-12	6.51E-12
101	-2.00E+01	0.00E+00	8.00E+02	3	-2.30E-04	-3.14E-04	5.63E-04	-4.22E-05	-9.14E-12	6.27E-12
102	0.00E+00	0.00E+00	8.00E+02	3	-2.29E-04	-3.15E-04	5.64E-04	-2.87E-05	-8.61E-12	6.05E-12
103	2.00E+01	0.00E+00	8.00E+02	3	-2.28E-04	-3.16E-04	5.63E-04	-1.52E-05	-8.04E-12	5.86E-12
104	4.00E+01	0.00E+00	8.00E+02	3	-2.26E-04	-3.16E-04	5.62E-04	-1.79E-06	-7.44E-12	5.71E-12
105	6.00E+01	0.00E+00	8.00E+02	3	-2.22E-04	-3.15E-04	5.59E-04	1.14E-05	-6.82E-12	5.60E-12
106	8.00E+01	0.00E+00	8.00E+02	3	-2.17E-04	-3.14E-04	5.55E-04	2.43E-05	-6.17E-12	5.53E-12
107	1.00E+02	0.00E+00	8.00E+02	3	-2.12E-04	-3.13E-04	5.50E-04	3.68E-05	-5.51E-12	5.50E-12
108	1.20E+02	0.00E+00	8.00E+02	3	-2.05E-04	-3.12E-04	5.44E-04	4.89E-05	-4.83E-12	5.53E-12
109	1.40E+02	0.00E+00	8.00E+02	3	-1.98E-04	-3.10E-04	5.37E-04	6.05E-05	-4.15E-12	5.60E-12
110	1.60E+02	0.00E+00	8.00E+02	3	-1.90E-04	-3.08E-04	5.29E-04	7.16E-05	-3.46E-12	5.71E-12
111	1.80E+02	0.00E+00	8.00E+02	3	-1.80E-04	-3.05E-04	5.20E-04	8.20E-05	-3.37E-12	5.87E-12
112	2.00E+02	0.00E+00	8.00E+02	3	-1.71E-04	-3.02E-04	5.11E-04	9.18E-05	-3.49E-12	6.03E-12
113	2.20E+02	0.00E+00	8.00E+02	3	-1.60E-04	-2.99E-04	5.00E-04	1.01E-04	-3.61E-12	6.20E-12
114	2.40E+02	0.00E+00	8.00E+02	3	-1.49E-04	-2.96E-04	4.89E-04	1.09E-04	-3.73E-12	6.37E-12
115	2.60E+02	0.00E+00	8.00E+02	3	-1.38E-04	-2.92E-04	4.77E-04	1.17E-04	-3.86E-12	6.54E-12
116	2.80E+02	0.00E+00	8.00E+02	3	-1.26E-04	-2.89E-04	4.65E-04	1.24E-04	-3.99E-12	6.72E-12
117	3.00E+02	0.00E+00	8.00E+02	3	-1.13E-04	-2.85E-04	4.52E-04	1.30E-04	-4.13E-12	6.91E-12
118	3.20E+02	0.00E+00	8.00E+02	3	-1.01E-04	-2.80E-04	4.39E-04	1.35E-04	-4.28E-12	7.09E-12

119	3.40E+02	0.00E+00	8.00E+02	3	-8.78E-05	-2.76E-04	4.25E-04	1.39E-04	-4.43E-12	7.29E-12
120	3.60E+02	0.00E+00	8.00E+02	3	-7.48E-05	-2.72E-04	4.12E-04	1.43E-04	-4.59E-12	7.49E-12
121	3.80E+02	0.00E+00	8.00E+02	3	-6.18E-05	-2.67E-04	3.98E-04	1.45E-04	-4.75E-12	7.69E-12
122	4.00E+02	0.00E+00	8.00E+02	3	-4.88E-05	-2.63E-04	3.84E-04	1.47E-04	-4.92E-12	7.90E-12
123	4.20E+02	0.00E+00	8.00E+02	3	-3.59E-05	-2.58E-04	3.69E-04	1.48E-04	-5.09E-12	8.12E-12
124	4.40E+02	0.00E+00	8.00E+02	3	-2.31E-05	-2.53E-04	3.55E-04	1.48E-04	-5.27E-12	8.34E-12
125	4.60E+02	0.00E+00	8.00E+02	3	-1.05E-05	-2.49E-04	3.42E-04	1.47E-04	-5.46E-12	8.56E-12
126	4.80E+02	0.00E+00	8.00E+02	3	1.79E-06	-2.44E-04	3.28E-04	1.46E-04	-5.66E-12	8.79E-12
127	5.00E+02	0.00E+00	8.00E+02	3	1.38E-05	-2.40E-04	3.14E-04	1.44E-04	-5.87E-12	9.02E-12
128	5.20E+02	0.00E+00	8.00E+02	3	2.54E-05	-2.35E-04	3.01E-04	1.41E-04	-6.08E-12	9.26E-12
129	5.40E+02	0.00E+00	8.00E+02	3	3.65E-05	-2.31E-04	2.89E-04	1.37E-04	-6.30E-12	9.51E-12
130	5.60E+02	0.00E+00	8.00E+02	3	4.72E-05	-2.27E-04	2.76E-04	1.33E-04	-6.53E-12	9.76E-12
131	5.80E+02	0.00E+00	8.00E+02	3	5.73E-05	-2.23E-04	2.64E-04	1.28E-04	-6.77E-12	1.00E-11
132	6.00E+02	0.00E+00	8.00E+02	3	6.69E-05	-2.19E-04	2.53E-04	1.23E-04	-7.02E-12	1.03E-11
133	6.20E+02	0.00E+00	8.00E+02	3	7.60E-05	-2.15E-04	2.42E-04	1.17E-04	-7.28E-12	1.05E-11
134	6.40E+02	0.00E+00	8.00E+02	3	8.44E-05	-2.11E-04	2.32E-04	1.10E-04	-7.55E-12	1.08E-11
135	6.60E+02	0.00E+00	8.00E+02	3	9.22E-05	-2.08E-04	2.23E-04	1.03E-04	-7.83E-12	1.11E-11
136	6.80E+02	0.00E+00	8.00E+02	3	9.94E-05	-2.05E-04	2.14E-04	9.60E-05	-8.12E-12	1.13E-11
137	7.00E+02	0.00E+00	8.00E+02	3	1.06E-04	-2.02E-04	2.06E-04	8.83E-05	-8.42E-12	1.16E-11
138	7.20E+02	0.00E+00	8.00E+02	3	1.12E-04	-1.99E-04	1.99E-04	8.03E-05	-8.73E-12	1.19E-11
139	7.40E+02	0.00E+00	8.00E+02	3	1.17E-04	-1.97E-04	1.92E-04	7.20E-05	-9.05E-12	1.21E-11
140	7.60E+02	0.00E+00	8.00E+02	3	1.22E-04	-1.95E-04	1.86E-04	6.35E-05	-9.39E-12	1.24E-11
141	7.80E+02	0.00E+00	8.00E+02	3	1.26E-04	-1.93E-04	1.81E-04	5.48E-05	-9.73E-12	1.27E-11
142	8.00E+02	0.00E+00	8.00E+02	3	1.29E-04	-1.91E-04	1.77E-04	4.59E-05	-1.01E-11	1.30E-11
143	8.20E+02	0.00E+00	8.00E+02	3	1.32E-04	-1.90E-04	1.74E-04	3.69E-05	-1.05E-11	1.32E-11
144	8.40E+02	0.00E+00	8.00E+02	3	1.34E-04	-1.89E-04	1.71E-04	2.78E-05	-1.08E-11	1.35E-11
145	8.60E+02	0.00E+00	8.00E+02	3	1.35E-04	-1.88E-04	1.69E-04	1.86E-05	-1.12E-11	1.37E-11
146	8.80E+02	0.00E+00	8.00E+02	3	1.36E-04	-1.88E-04	1.68E-04	9.29E-06	-1.16E-11	1.40E-11
147	9.00E+02	0.00E+00	8.00E+02	3	1.37E-04	-1.88E-04	1.67E-04	-7.28E-12	-1.20E-11	1.42E-11

148	9.20E+02	0.00E+00	8.00E+02	3	1.36E-04	-1.88E-04	1.68E-04	-9.29E-06	-1.24E-11	1.44E-11
149	9.40E+02	0.00E+00	8.00E+02	3	1.35E-04	-1.88E-04	1.69E-04	-1.86E-05	-1.28E-11	1.46E-11
150	9.60E+02	0.00E+00	8.00E+02	3	1.34E-04	-1.89E-04	1.71E-04	-2.78E-05	-1.33E-11	1.48E-11
151	9.80E+02	0.00E+00	8.00E+02	3	1.32E-04	-1.90E-04	1.74E-04	-3.69E-05	-1.37E-11	1.49E-11
152	1.00E+03	0.00E+00	8.00E+02	3	1.29E-04	-1.91E-04	1.77E-04	-4.59E-05	-1.41E-11	1.51E-11

Table B-4: Normal and Shear Strain output of layered elastic system

Appendix C: Material Specification and Gravel Road

General Classification	Granular materials (35 % or less passing No. 200)							Silt-Clay materials (more than 35% passing No 200)				
Group Classification	A-1		A-3	A-2				A-4	A-5	A-6	A-7	
	A-1-a	A-1-b		A-2-4	A-2-5	A-2-6	A-2 -7				A-7-5	A-7-6
Sieve analysis, per cent passing												
No 10 (2 mm)	50 max	-	-	-	-	-	-	-	-	-		
No 40 (0.425 mm)	30 max	50 max	51min	-	-	-	-	-	-	-		
No 200 (0.075 mm)	15 max	25 max	10 max	35 max	35 max	35 max	35 max	36 min	36 min	36 min	36 min	
Characteristics of fraction passing No 40												
LL	-		-	40 max	41 min	40 max	41 min	40 max	41 min	40 max	41 min	
PI	6 max		NP	10 max	10 max	11 min	11 min	10 max	10 max	11 min	11 min	
Usual types of constituent materials	Stone fragments, fine gravel, and sand		Fine sand	Silty or clayey gravel or sand				Silty soils		Clayey soils		
General rating as subgrade	Excellent to good					Fair to poor						

Table C-1: AASHTO Classifications of Material (AASHTO, 1993)

Soils used for improved subgrade layers shall be non-expansive, non-dispersive and free from any deleterious matter. They shall comply with the requirements shown in Table C-2.

Material Properties	G20 (Upper Layer)	G7 (Lower Layer)
CBR Dry Climatic Zones (See Note)	Minimum 20 after 4 days soaking	Minimum 7 after 4 days soaking
CBR Wet Climatic Zones (See Note)	Minimum 20 at OMC Minimum 7 after 4 days soaking	Minimum 7 at OMC Minimum 3 after 4 days soaking
PI [%]	Maximum 25	Maximum 30
Compacted Density	95% of AASHTO T180	95% of AASHTO T180
Maximum particle size	2/3 of layer thickness	2/3 of layer thickness
Compacted layer thickness	Maximum 200 mm	Maximum 250 mm

Table C-2: Subgrade material characteristics gravel wearing course design (ERA 2002)

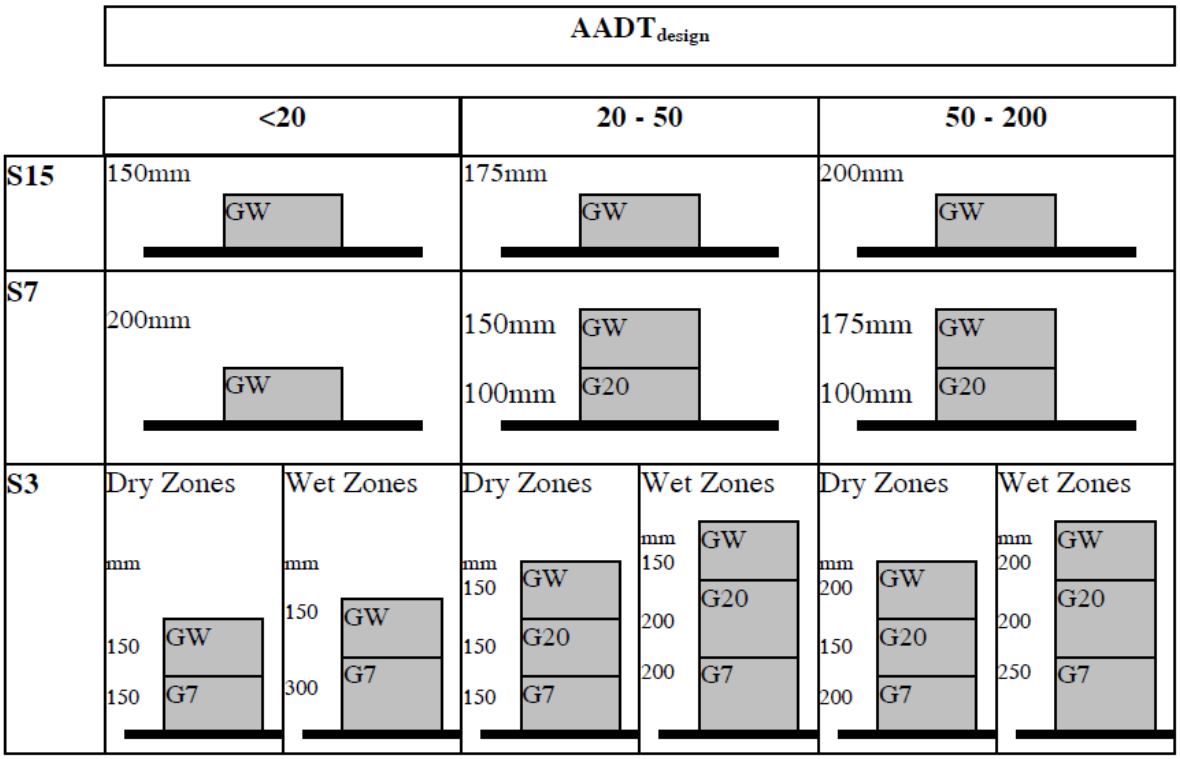

Figure C-1: Pavement and Improved Subgrade for Gravel Roads (ERA, 2002)

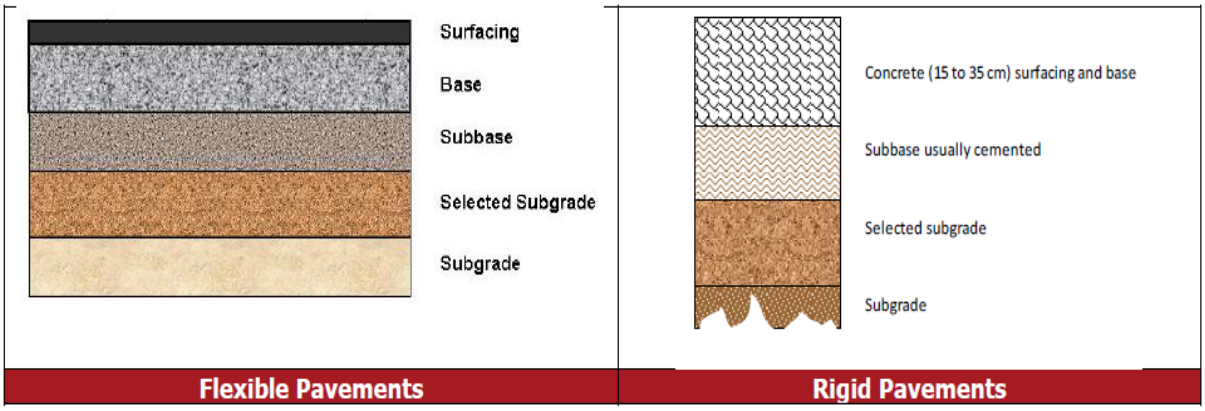

Figure C-2: Typical Pavement Structures (SA P E Manual, 2013)

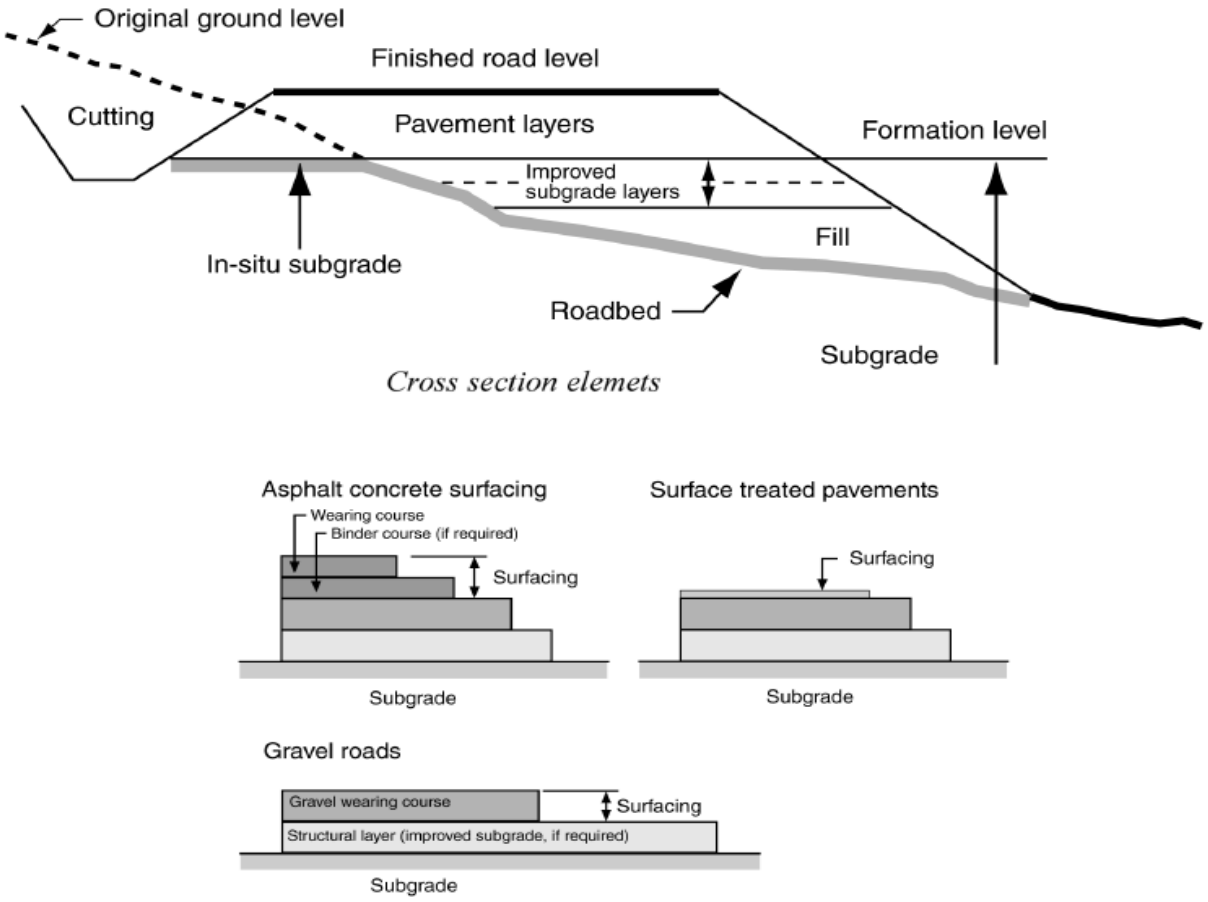

Figure C-3: Pavement Typical Detail (Tanzanian Pavement Manual, 2000)

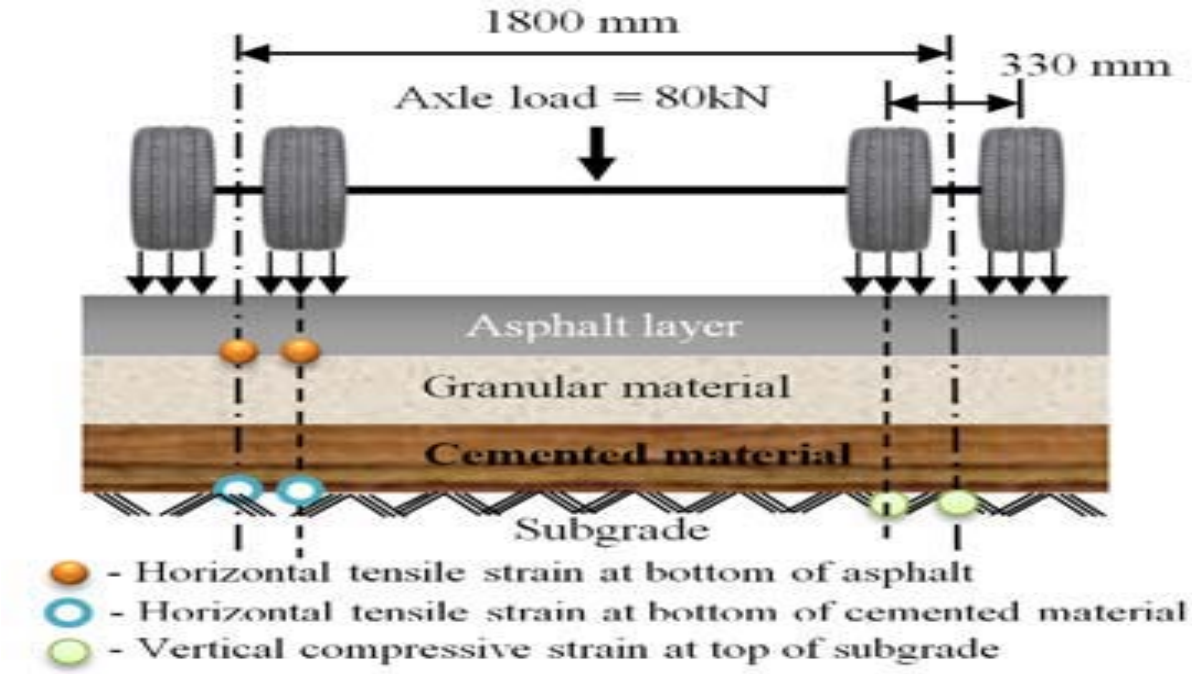

Figure C-4: Standard Axle Loading (Austroads 2004)

Appendix D: Numerical Simulation

A numerical simulation is a calculation that is run on a computer, following a program that implements a mathematical model for a physical system. Numerical simulations are required to study the behaviour of systems whose mathematical models are too complex to provide analytical solutions, as in most nonlinear systems. In the study of behavioral condition of granular material, the discreteness of the particles and the force of transmission between the particles at contact points make complex the constitutive relationship of the granular material. Additionally, the stress existing inside the sample was difficult to measure in a traditional laboratory test. These behavioral constraints of granular material were determined through an alternative boundary condition.

Simulation Software

After a rock related behavioral analysis, the computer program was introduced for DEM. This computer program was further developed to analysis the behavior of rock and unbound granular materials in discretely in current time and became a commercial DEM Code. These software's are namely 3DEC and PFC2D or PFC3D were first developed by Itasca. And there are many other open source DEM programs available, specially, LMMPS, SDEC, and YADE. In recent time, DEM and its software had proved to be better instruments of behavioral for discrete particles (discontinuous media) than any other simulation tools.

In this research recommendation for future research, the open source DEM program namely YADE (Yet another Dynamic Engine) was used to model the repeated triaxial test of unbound pavement material as indicated in figure 3.3. Basically, this software is important to analysis the behaviour of sampled materials as any other DEM program, additionally, it is easily available, easy in setup and less in cost as compare to the commercial software. And this program is available on www.yade-dem.org/packages.

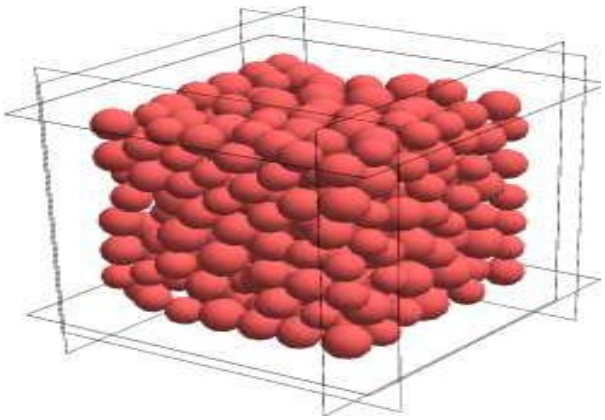

Figure D-1: A three dimensional DEM sample subject to triaxial compression (J. Kozicki, 2008)

Numerical Simulation Input Data

Particle Size and Shape

The characterizations of aggregate in physical tests in the laboratory were the main input parameters of this research. Variety of tests was carried out in laboratory to ensure that the aggregate performs as intended for this research work. One of these tests was the gradation test that used to determine the distribution of aggregate particles by size within a given sample. In this research, aggregate size analysis was conducted according to AASHTO sieve size distribution that common used for test of crushed stone aggregate. The series of these sieve sizes used for this research work are: 37.5mm, 25mm, 19mm, 16mm, 12.5mm 9.5mm 4,75mm and 2.36mm. Mostly of a sampled aggregate retained on these sieves had selected as input parameters of DEM. The apparatus used for this sample preparation and test procedure of particle size analysis had done according to AASHTO materials test specification in the laboratory.

In this research recommendation for future research, the shape of aggregate estimated in three approaches. These approaches are based on the international standards, Discrete Element Modeling and visuals or statically. The international standard classified aggregate particles as flaky when they have a thickness of less than 0.6 of their mean sieve size as a British standard. The ASTM classified the shape of coarse aggregate into three, namely flat particles, elongate particle and flat and elongate particles. In DEM the shape of the aggregate particle can be classified in to three; pyramids, elongate and spherical shapes as seen in figure 4.2. The DEM

replication of the particle shapes were done by means of the clump logic in this research. The clump representations of the particle shapes can be seen in Figures 3.7and 3.8.The elongated particles were represented by two spheres clumped together, while the pyramid shaped particles were represented by four spheres clumped together as shown in Figure 3.8. In this research, shape of the aggregate particles is considered as a sphere due to the equivalency of representation or clump logic where the particle shape was largely spherical, representation by means of a perfect sphere in YADE was deemed appropriate.

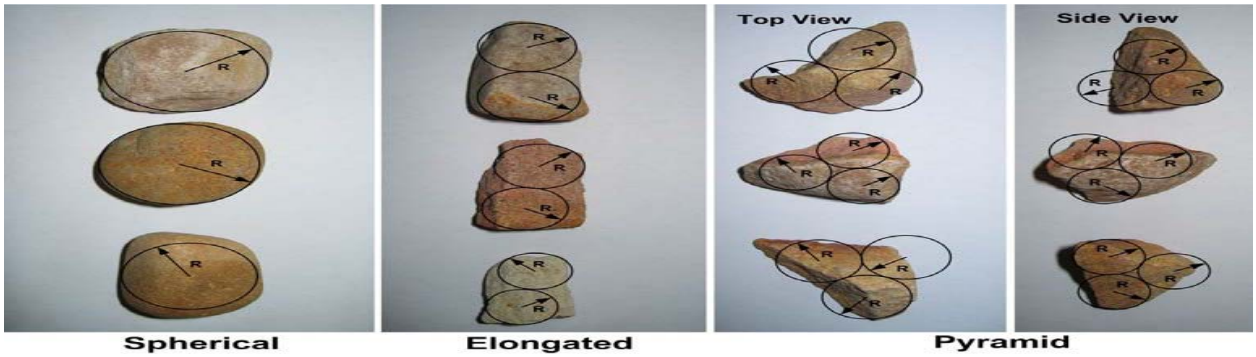

Figure D-2: Particle Shapes with Superimposed Clump Equivalents

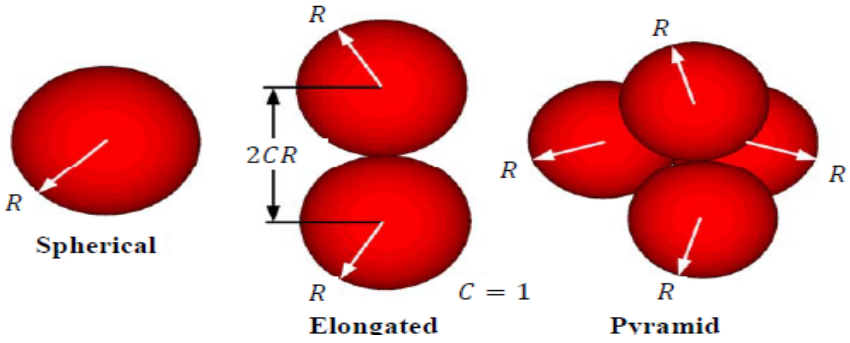

Figure D-3: Clumps Logic in Discrete Element Modeling

Particle Density, Bulk Density, Porosity and Voids Ratio

The Bulk Density, Porosity and Void Ration of the sampled aggregate were used to determine in the laboratory as well as the density of particles under study. These parameters were used to as an input data for the numerical simulation software, basically in YADE and ensure consistent of initial compaction characteristics prior to test of other, namely the CCT and DST for determination of particle stiffness and coefficient of friction. The apparatus used for a sample

preparation and a test procedure for densities determination method were done according to British Standard materials test specification. The experimental data obtained in the laboratory for numerical input parameters was indicated in table 3.1.

Particle Stiffness

It is the ability of the particles to resist deformation in response to applied load. The particle stiffness of sampled aggregate was determined as a confined young's modulus through confined compression test (CCT) in the laboratory. The bulk parameter that indicates the stiffness characteristics of a packing is the bulk stiffness and directly related to the confined young's modulus. In this research, the confined compression test was performed using the compression test machine indicated in figure 3.4 and procedure as well. The availability of confined compression test equipment, namely the large scale box shown in figure 3.7 did not find the laboratories of the country that used to determine the stiffness or confined young modulus of coarse aggregate; this makes to look other a pre-selected option. This pre-selected option is adopted by an international manual like AASHTO and ASTM. This is used for numerical simulation software, namely YADE, a type of DEM software which had a predetermined particle stiffness or normal stiffness of aggregate. The test result obtained from compression test machine in laboratory for normal particle stiffness was used as an input parameter of in this research recommendation for future research.

Inter-particle Friction Coefficient

Inter particle friction coefficient is the input parameters of Discrete Element Modeling; in this research, it was determined in the laboratory by a direct shear test. A direct shear test contains a shear box. This shear box has two parts namely a top and a bottom, with a cylindrically shape. The crushed granular material in a shear box was sheared laterally by applying a vertical load. Basically, the shear displacement occurs at a constant velocity and it creates a thin shear zone in crushed granular materials at a half of the two parts as shown in Figure 3.8. Whereas, Stresses (Normal and Shear) acting on the normal plane were obtained from measured normal and shear loads afterward used to determine bulk properties of this material, mainly the internal friction angle.

The availability equipment, namely the Direct Shear test in the laboratories of the country that used to determine the internal friction angle of coarse aggregate makes to look other a pre-

selected option. This pre-selected option is adopted by international recognized manuals such as AASHTO and ASTM. This selected alternative of internal friction angle was used as an input parameter of in this research recommendation for future research.

Particle-Wall Friction Coefficient

The coefficient friction is used to describe frictional behaviour between the individual particles and the interaction between the particles and the interface during simulation process of this research work. The experimental procedures were planned to value this coefficient of friction. The friction coefficient was determined for boundary material. The determined frictional coefficient from experimental result was applicable in DEM simulation of In this research recommendation for future research. This is obtained in the numerical simulation software, namely YADE, a type of DEM software which had a predetermined the interaction friction angle. This per selected potion of the interaction friction angle was used as an input parameter of this research.

Damping

In this research recommendation for future research, damping can be classified as local non viscous damping and viscous damping. The simulation recommended for this research require the moving wall boundaries, however, the local non viscous damping is not used for systems where large numbers of particles are driven by specified velocity boundary conditions, so, the local damping coefficients were set to zero while viscous damping was used . This is essential way for energy dissipation.

In general, viscous damping is characterized by the critical damping ratio, (Itasca, 2003). This critical damping ratio or ξ is specified in YADE, in both the normal and shear directions. When $\xi = 1$, the system is said to be critically damped. For $\xi < 1$ the system is under damped, while for $\xi > 1$ the system is over damped. When handling the crushed aggregate samples, it was clearly observed that the particles exhibit a fairly high degree of damping. It was therefore assumed that the particles are slightly under damped, and the critical damping ratio was chosen to be 0.8 and implemented directly in YADE.

Wall Stiffness

It was assumed that the wall stiffness does not have a significant influence on the results for this research. A wall stiffness value was used that is larger than the anticipated particle stiffness values, with at most one order of magnitude, to ensure largely rigid interface walls. The value that was chosen for the wall stiffness is 150 KN/m and was implemented directly in YADE for all of the simulations (in both the normal and shear directions).

Appendix E: Equation and Correlations

Stress path

A result of triaxial test was represented by diagram. This diagram is stress path. It is a line that connects a series of points, each of which represented a successive stress state of specimen during progress of a test. There are several ways in which stress path can be drawn. This research covers one of them. Lambe suggested a type of stress path representation that plots q against p (where p and q are the coordinates of top of the Mohr's circle). Thus, relationships between p and q are as follows:

$$q = \frac{\sigma_1 - \sigma_3}{2}$$

$$p = \frac{\sigma_1 + \sigma_3}{2}$$

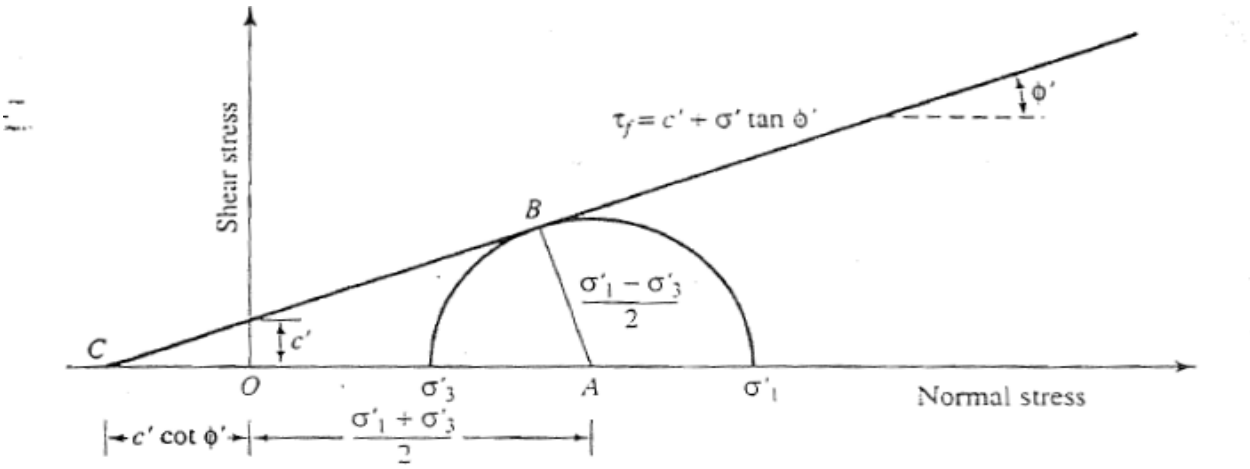

Figure E-1: Stress path (Principle Geotechnical Engineering, Fifth Edition, 2006)

$$\frac{\sigma_1 - \sigma_3}{2} = \left(\frac{\sigma_1 + \sigma_3}{2}\right) * \sin\emptyset + c(\cos\emptyset)$$

The symbols used in equations and indicate on stress path diagram, c= c', $\sigma_1 = \sigma_1'$ and $\sigma_3=\sigma_3'$, $\varphi=\varphi'$ are similar.

Unbound pavement material Californian Bearing Ratio (CBR (%)) correlation to Modulus (M_R) value indicated at row two of this table used for this research.

Strength/Index Property	Model[a]	Comments	Test Standard
California Bearing Ratio[b]	M_R (psi) = $2555(CBR)^{0.64}$ M_R (MPa) = $17.6(CBR)^{0.64}$	CBR = California Bearing Ratio (%)	AASHTO T193—The California Bearing Ratio
Stabilometer R-value	M_R (psi) = $1155 + 555R$ M_R (MPa) = $8.0 + 3.8R$	R = R-value	AASHTO T190—Resistance R-Value and Expansion Pressure of Compacted Soils
AASHTO layer coefficient	M_R (psi) = $30{,}000\ (a_i/0.14)^3$ M_R (MPa) = $207\ (a_i/0.14)^3$	a_i = AASHTO layer coefficient	AASHTO Guide for the Design of Pavement Structures (1993)
Plasticity index and gradation	$CBR = \frac{75}{1+0.728(wPI)}$	$wPI = P200*PI$ $P200$ = % passing No. 200 sieve size PI = plasticity index (%)	AASHTO T27—Sieve Analysis of Coarse and Fine Aggregates AASHTO T90—Determining the Plastic Limit and Plasticity Index of Soils
Dynamic Cone Penetration[c]	$CBR = 292/(DCP^{1.12})$	CBR = California Bearing Ratio (%) DCP =Penetration index, in./blow	ASTM D6951—Standard Test Method for Use of the Dynamic Cone Penetrometer in Shallow Pavement Applications

Table E-1: Correlations between resilient modulus and CBR value (NCHRP 1-37A)

Stresses State

The stresses applied to a specimen when running a triaxial compression test are displayed in Figure 3.6. The confining stress σ_c is applied by pressurizing the cell fluid surrounding the specimen – it is equal to the radial stress σ_r, or minor principal stress σ_3. The deviator stress q is generated by applying an axial strain ε_a to the specimen – the deviator stress acts in addition to the confining stress in the axial direction, with these combined stresses equal to the axial stress σ_a, or major principal stress σ_1. The stress state is said to be isotropic when $\sigma_1 = \sigma_3$, and anisotropic when $\sigma_1 \neq \sigma_3$.

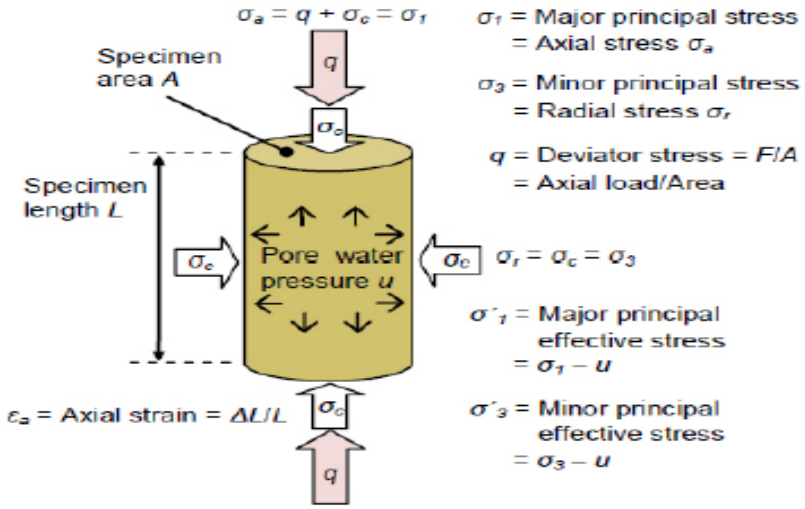

Figure E-2: Specimen stress state during triaxial compression (http://www.gdsinstruments.com/)

Appendix F: Research Photo Report

Materials Sampled

Standard Compaction Apparatus

Compaction process

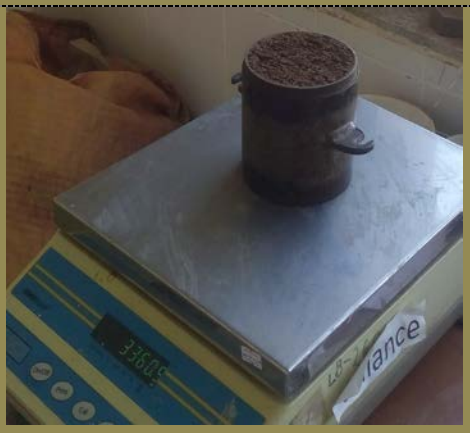

Compacted sample

Figure F-1: Standard Compaction Determine OMC and MDD at Laboratory

Sample after 24 hours in oven

Sample retained on 25mm sieve size

Sieve used in grain size determination, AASHTO

Sample prepared for triaxial specimen

Figure F-2: Grain Size Analysis of Material for Specimen Preparation

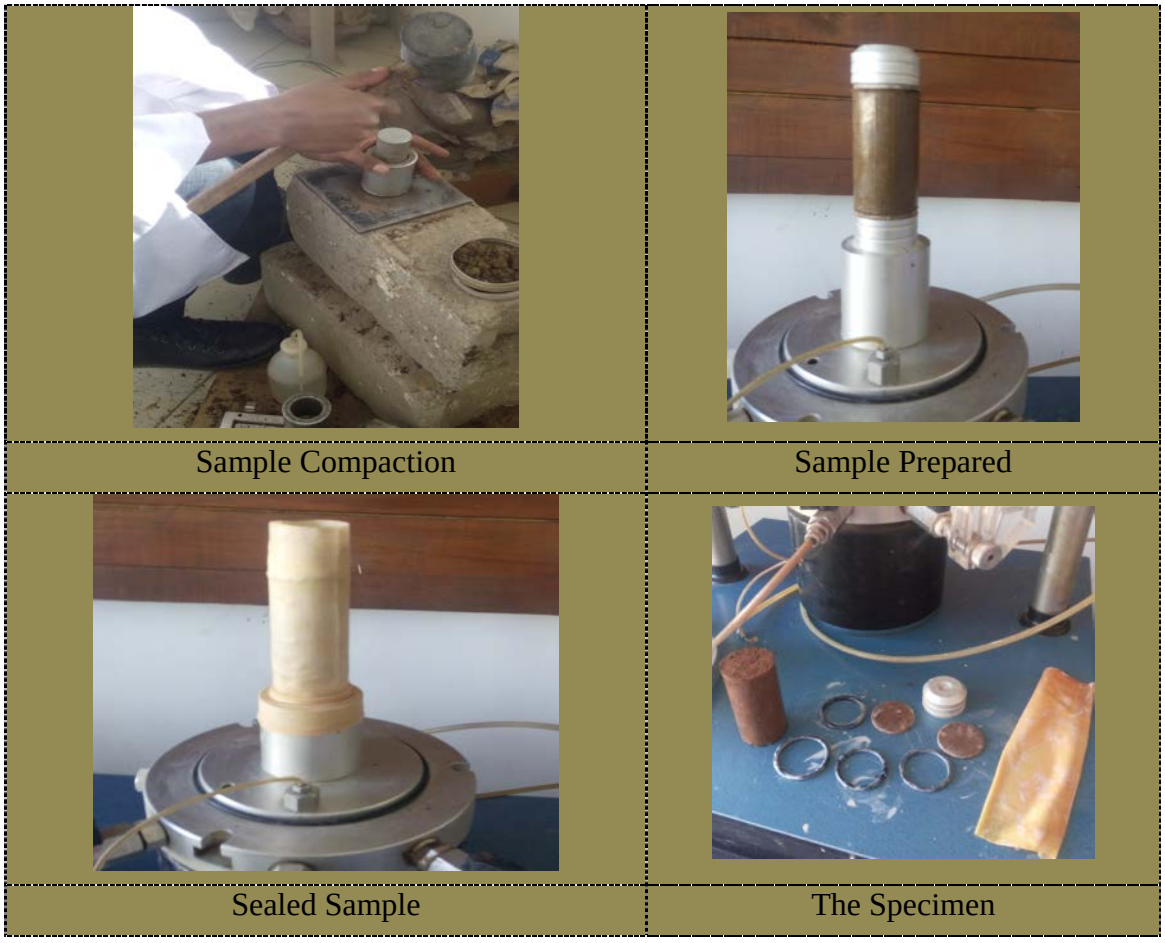

Figure F-3: Procedures of Triaxial Sample Preparation at laboratory

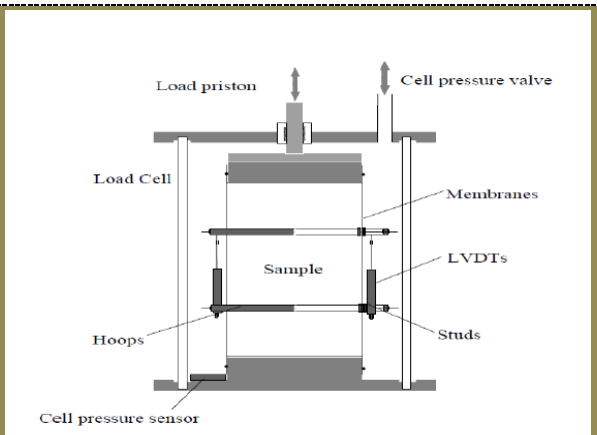

Figure 3.2 RLT apparatus at University of Nottingham

a. Repeated load apparatus

b. Triaxial cell

C. Triaxial test Installation

D. Dial and Ring Gauge

E. Air pressure cell

Pressure gauge

Figure F-4: Repeated Load Triaxial Test Equipments used in laboratory

ECDSWC Building Office

Taking the test result

Triaxial Test Equipment

Conducting the triaxial test

Figure F-5: Ethiopian Construction Design and Supervision Work Corporation laboratory

	
Existing Borrow pit	Taking Sample
	
Sampled material and used equipment	Vehicle used for sampling

Figure F-6: Sampling of Material from existing borrows pit